Kemotaksonomska i morfološka analiza fitoplanktona u trofičkom gradijentu sjevernog Tihog oceana

Višić, Hrvoje

University of Zagreb

Faculty of Natural Sciences

Department of Biology

Hrvoje Višić

Chemotaxonomic and Morphological Approach to Phytoplankton Analyses in Contrasting Trophic Systems of North Pacific

Graduation thesis

Zagreb, 2018.

Sveučilište u Zagrebu

Prirodoslovno-matematički fakultet

Biološki odsjek

Hrvoje Višić

Kemotaksonomska i morfološka analiza fitoplanktona u trofičkom gradijentu sjevernog Tihog oceana

Diplomski rad

Zagreb, 2018.

This master thesis was made at the Botanical Institute of the Department of Biology of the Faculty of Natural Sciences and Mathematics in Zagreb under the guidance of Dr. Zrinka Ljubešić, Assoc. Prof. The paper is submitted to the Department of Biology at the Faculty of Natural Sciences and Mathematics of the University of Zagreb for the purpose of acquiring a degree of Master of Environmental Sciences.

Acknowledgments

Firstly, I am very grateful to my mentor Zrinka Ljubešić who entrusted me this thesis. I am thankful for her help in all kinds of situations, for enormous patience and numerous advice, for encouraging and support, for challenging and correcting me to accomplish more.

I would also like to thank Sunčica Bosak for giving me the cell counting data, great help with identification of species and the guidance with statistics and data handling.

Also, I would like to thank Luka Šupraha for all the SEM photos and coccolithophorid taxonomy, and to Maja Mucko for the help with writing and advices.

Thank you all for a good time in the lab!

I am thankful to Schmidt Ocean Institution, whole science party of the Sea to Space Particle Investigation and the crew of the R/V Falkor for providing great samples and data for this work.

A very special thanks to Ivona Cetinić without whom none of this would be possible, and for all the advice and help with the thesis writing.

I am grateful for all my friends that were there for me, and who made the time studying more fun and fulfilled. It wouldn't be the same without you.

I am especially thankful to my beloved girlfriend Veronika Buršić for introducing me to Zrinka and this master thesis. Thank you for all the love, help, technical and emotional support through funny and stressful moments of writing this work and for being for me there at any time.

Finally, I am thankful to my family – parents Tomislav and Ivana, sister Nina, grandparents Josip and Ivanka, Živko and Nevenka – for all their emotional and financial support, patience, care and love for me and my work through all my years of study.

I also very thankful to all my extended family which helped me in any way possible – family Kalauz, Vukelja, Bujas, Jaram and Višić.

Special thanks to family Jablan who welcomed and helped me in the new city.

Thanks to everyone who believed in me when I have doubted!

TEMELJNA DOKUMENTACIJASKA KARTICA

Sveučilište u Zagrebu

Prirodoslovno matematički fakultet

Biološki odsjek Diplomski rad

Kemotaksonomska i morfološka analiza fitoplanktona u trofičkom gradijentu sjevernog Tihog oceana

Hrvoje Višić

Rooseveltov trg 6, 10000 Zagreb, Hrvatska

U sklopu Schmidt Ocean Institute ekspedicije *Sea to Space Particle Investigation* na sjevernom Tihom oceanu sakupljeni su uzorci za analizu fitoplanktona i pigmenta. Cilj ovog rada je detaljna kvantitativna, kvalitativna i kemotaksonomska analiza fitoplanktonske zajednice sjevernog Tihog oceana u svrhu određivanja stupnja trofije tog područja. Pojedine fitoplanktonske skupine mogu biti identificirane po svojim jedinstvenim optičkim svojstvima koje proizlaze iz strukturne građe samih stanica ili fluorescencije pigmenata koje proizvode. Na tome se bazira program PACE (eng. *Plankton, Aerosol, Cloud, ocean Ecosystem*) američke Nacionalne aeronautičke i svemirske administracije (NASA) za koju je napravljena analiza fitoplanktona i pigmenata. Fitoplanktonska zajednica sjevernog Tihog oceana uglavnom se sastojala od kokolitoforida (35,5%), dijatomeja (25,2%) i dinoflagelata (19,5%), dok su kriptofiti, zeleni bičaši, silikoflagelati i ostali doprinijeli fitoplanktonskoj zajednici s 19,8%. Kokolitoforidi dominiraju u nanofitoplanktonskoj frakciji na svim postajama, dok dijatomeje dominiraju u zajednici mikrofitoplanktona. Na osnovi taksonomskog sastava fitoplanktona, određenog morfološki i kemotaksonomski, istraživano je područje podijeljeno na četiri različita trofička sustava. Zabilježeno je ukupno 106 taksona dijatomeja, 48 kokolitoforida i 41 dinoflagelat, dok je 12 taksona pripadalo ostalim skupinama. Rezultati ovog istraživanja koristiti će se u svrhu razvijanja algoritama i kalibracije senzorske tehnologije orbitalnih satelita pomoću kojih će bit moguće promatrati suptilne razlike u boji oceana.

(72 stranice, 30 slika, 8 tablica, 108 bibliografskih referenci, izvornik na engleskom jeziku)

Rad je pohranjen u Središnjoj biološkoj knjižnici.

Ključne riječi: pigmenti, eutrofikacija, brojnost čestica, boja oceana, NASA PACE

Voditelj: izv. prof. dr. sc. Zrinka Ljubešić
Neposredni voditelj:

Ocjenitelji: 1. Zrinka Ljubešić, izv. prof. dr. sc.

2. Petar Kružić; izv. prof. dr. sc.

3. Mladen Juračić, prof. dr. sc.

4. Danijel Orešić, izv. prof. dr. sc.

Rad je prihvaćen: 01/02/2018

BASIC DOCUMENTATION CARD

University of Zagreb

Faculty of Science

Division of Biology Graduation thesis

Chemotaxonomic and morphological approach to phytoplankton analyses in contrasting trophic systems of North Pacific

Hrvoje Višić

Rooseveltov trg 6, 10000 Zagreb, Croatia

Sea to Space Particle Investigation Expedition (funded by Schmidt Ocean Institute) was conducted in the North Pacific Ocean, and samples were collected for phytoplankton and pigment analysis. The research aim of this study is to give detailed quantitative, qualitative and chemotaxonomic analysis of the phytoplankton community in the North Pacific to determine the trophic state of this area. Certain phytoplankton groups can be identified by their unique optical properties resulting from the structure of the cells themselves or the fluorescence of the pigments they produce. PACE (Plankton, Aerosol, Cloud, Ocean Ecosystem) program of the US National Aeronautics and Space Administration (NASA) is based on this premise for which these phytoplankton and pigment analyses have been made. The phytoplankton community of the North Pacific Ocean is mainly comprised of coccolithophores (35.5%), diatoms (25.2%) and dinoflagellate (19.5%), while cryptophytes, phytoflagellates, silicoflagellates and others contributed with 19.8%. Coccolithophorids dominate nanophytoplankton fraction at all stations, while diatoms dominate the microphytoplankton community. Based on the composition of phytoplankton and pigment concentrations, the investigated area was divided into four different trophic systems. A total of 106 taxa of diatoms, 48 coccolithophores, and 41 dinoflagellates have been recorded, while 12 taxa belonged to the other groups. The results of this research will be used to develop algorithms and calibration of sensor technology of orbital satellites by which it will be possible to observe the subtle color differences of the ocean.

(72 pages, 30 figures, 8 tables, 108 references, original in English)

Thesis deposited in the Central Biological Library

Keywords: pigments, eutrophication, particle abundance, ocean color, NASA PACE

Supervisors: izv. prof. dr. sc. Zrinka Ljubešić
Assistant supervisor:

Reviewers: 1. Dr. Zrinka Ljubešić, Assoc. Prof.

2. Dr. Petar Kružić; Assoc. Prof.

3. Dr. Mladen Juračić, Prof.

4. Dr. Danijel Orešić, Assoc. Prof.

Thesis accepted: 01/02/2018

TABLE OF CONTENTS

List of abbreviations

19BF	19'-butanoyloxyfucoxanthin
19HF	19'-hexanoyloxyfucoxanthin
BMLD	bellow mixing layer depth
CCS	California current system
Chl	Chlorophyll
CRP	Columbia River plume
CTD	conductivity-temperature-depth
CZCS	Coastal Zone Color Scanner
DCM	deep chlorophyll maximum
DMS	dimethyl sulfide
DMSO	dimethyl sulfoxide
DMSP	dimethyl sulfoniopropionate
DVChl	divinyl chlorophyll
ENSO	El Niño–Southern Oscillation
EOS PM-1	Earth Observing System Aqua
ESD	equivalent spherical diameter
HCA	hierarchical cluster analysis
HNLC	high-nutrient, low-chlorophyll
HPLC	high-performance liquid chromatography
LM	light microscopy
MGDVP	Mg-2,4-divinyl pheoporphyrin a_5 monomethyl ester
MLD	mixing layer depth
MODIS	Moderate Resolution Imaging Spectroradiometer
MVChl	monovinyl chlorophyll
N.D.	non-determined
nMDS	non-metric multi-dimensional scaling
NPP	net primary production
NPSG	North Pacific Subtropical Gyre
OCI	Ocean Color Instrument
OTUs	operational taxonomic units
PACE	Plankton, Aerosol, Cloud, ocean Ecosystem
PAPs	photosynthetic accessory pigments
PAR	photosynthetic active radiation
PCA	principal component analysis
PPPs	photoprotective pigments
rDNA	ribosomal DNA
S	surface
SeaWiFS	Sea-Viewing Wide Field-of-View Sensor
SEM	scanning electron microscope
SIMPER	similarity percentages
SOI	Schmidt Ocean Institute
ST 1–4	station 1–4
UW	underway system
VIIRS	Visible and Infrared Imager/Radiometer Suite
δ/σ	average contribution/standard deviation
$\Sigma\delta\%$	species contribution percentage

1. INTRODUCTION

1.1. The Pacific Ocean and the circulation systems

Covering the Earth with a share of 70.9%, and a volume of 1.34 billion cubic kilometers, the World Ocean represents 99% of the living space on the planet. The Pacific Ocean partakes with 44.7% of total area, and 49.4% of total volume making it the biggest ocean on Earth. It is divided by the Equator on North Pacific (21.3% area, 24.8% volume) and South Pacific (23.4% area, 24.6% volume) (Eakins and Sharman, 2010). Climate, current systems and ecological factors of North Pacific are mostly influenced and defined by the Trade Winds, North Pacific Subtropical Gyre (NPSG), and the Subarctic Gyre which, in extension, defines the Pacific Coast of North America. The anticyclonic (clockwise) NPSG and cyclonic (counterclockwise) Subarctic Gyre flowing towards the west coast of North America bifurcate into two current systems: (i) subtropical branch that forms California Current and (ii) subpolar branch that forms the Alaska Current (Fig. 1). The strength of both current systems varies on seasonal and El Niño–Southern Oscillation (ENSO) timescales.

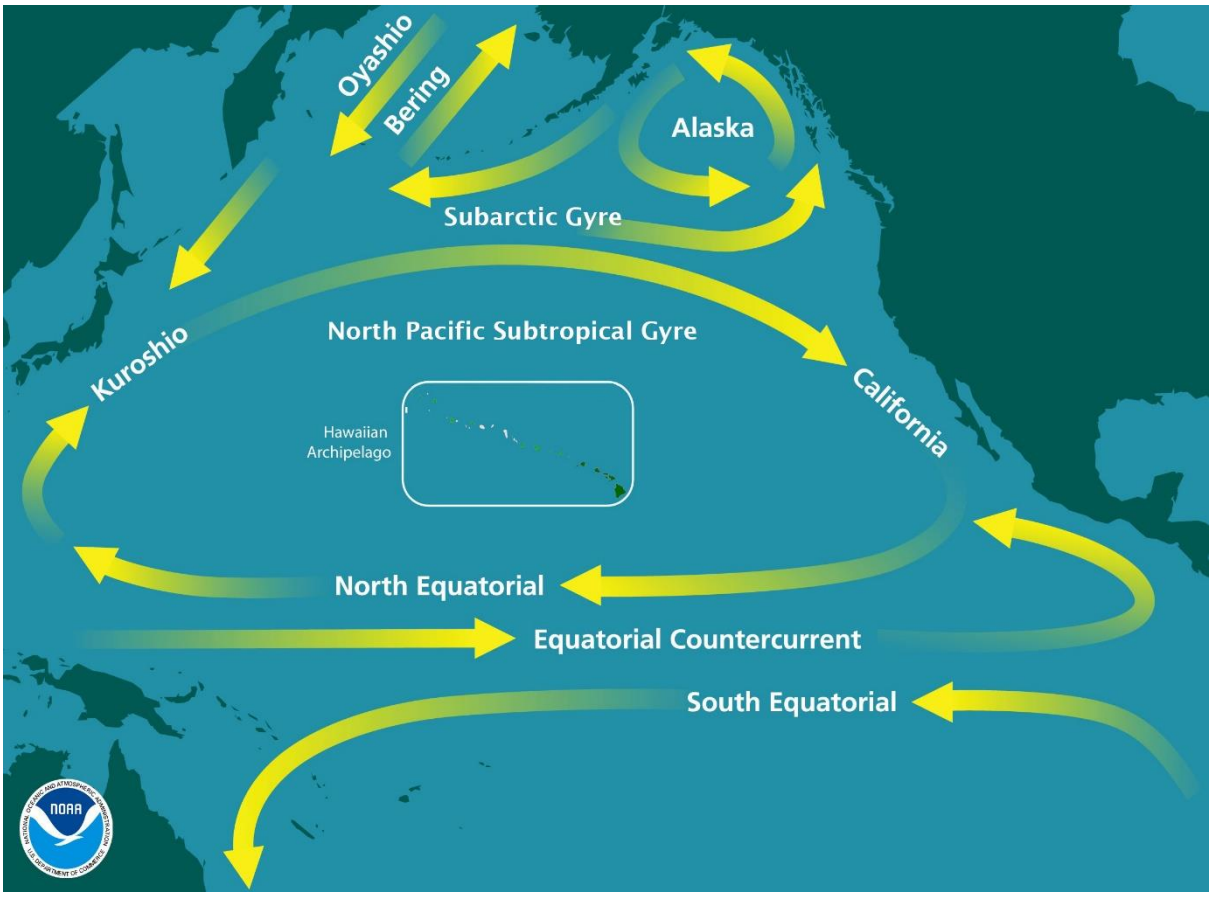

Fig. 1. Current systems of the Pacific Ocean (Edited from NOAA).

The California Current System (CCS) is comprised of the southward California Current, northward California Undercurrent, the Southern California Countercurrent (″Eddy″) and northward Davidson Current which is present only during wintertime. The California Current is strongest at the sea surface extending over the upper 500 m of the water column and carries colder and fresher water southward along the coast. The California Undercurrent is flowing northward over the continental slope of the CCS at depths of about 100–400 m transporting warmer and saltier water northward along the coast. The CCS is a transitional ecosystem between subtropical and subarctic water bodies, making it one of the most biologically important regions in the Pacific. Also, the CCS includes Columbia River, several smaller estuaries and numerous submarine canyons (Steele *et al*., 2009). Being the largest river in the Pacific Northwest, the Columbia River provides a substantial fraction of fresh water to both the CCS and Alaska Gyre with the 6th largest volume of runoff in North America. It is an important contributor of terrigenous sediments and total organic matter (nutrients) to the Pacific which in turn stimulates the growth of phytoplankton and zooplankton and raises the trophic state of the region (Fig. 2). Because of that input, especially that of iron, the plume fronts were characterized by distinct plankton community and color discontinuities. Chase *et al*. (2005) report that iron does not limit the phytoplankton, and that its productivity is impacted by iron along the CCS. Advection of cold-nutrient rich waters into the photic zone is called upwelling and the maximum that can be seen at the surface occurs off northern California in spring or summer (Kammerer, 1987; Morgan *et al*., 2005; Kudela *et al*., 2010).

Fig. 2. The stratified boundary between fresher, sediment-rich water from Columbia River and the higher-salinity Pacific Ocean (photo credit Adriana Zamudio, SOI).

The North Pacific is a region of oligotrophic waters first classified as high nutrient and low chlorophyll (HNLC) concentrations. HNLC is characterized by consistently high near-surface concentrations of macronutrients, low phytoplankton pigment biomass, limited levels of micronutrients (specifically iron) and the dominance of small producer species (Martin *et al*., 1989; Latasa *et al*., 1997). As a part of North Pacific, the NPSG is largest of the gyres with a surface area of ~20 million km^2 with a mean depth of ~5 km. It is also largest contiguous biome on Earth which includes a wide range of habitats and ecosystems ranging from warm and light-saturated but nutrient-starved surface waters to the cold and nutrient-rich deep waters. This thermal stratification makes the euphotic zone of the NPSG a two-layer system: (i) the upper, nutrient-limited layer where most of the primary production occurs and (ii) the lower layer richer in nutrients but light-limited with a lower occurrence of the photosynthesis. Different phytoplankton assemblages are found throughout the water column and are vertically stratified (Dore *et al*., 2008; Steele *et al*., 2009; Karl and Church, 2017).

1.2. Role of the phytoplankton and its pigments

At the base of marine food webs, lies the whole world unseen to the naked eye of unicellular organisms adrift in the currents that carry out photosynthesis in the euphotic zone of the water column - the phytoplankton. The name came from the Greek words φυτόν πλαγκτός (phyton planktos), which means ″plant wanderer″. By sequestering almost half of the world's carbon stock, phytoplankton plays a very important role in the Earth's biogeochemical cycle. Half of the primary production, biologically mediated fixation of carbon is done by marine phytoplankton (50 ± 28 GtC/year, Fahey *et al*., 2017). Marine phytoplankton is a highly diverse group of organisms, with a high phylogenetic, biochemical, metabolic and ecological variability (Richardson and Jackson, 2007; Zeidner *et al*., 2003; Thomas, 2013; Flombaum *et al*., 2013, De Vargas *et al*., 2015).

Phytoplankton is comprised of a phylogenetically diverse group of both prokaryotic and eukaryotic organism. Phytoplankton taxonomy can be determined using different characteristics like morphology, ecophysiology, ultrastructures of chloroplast and flagella, cellular biochemistry, molecular genetics and pigment composition. Because of that, classification is much debated with different systematic grouping. Highly diverse morphotypes can belong to the same phylogenetic lineage while for some green algae genera with spherical ball-type thallus molecular data showed that they evolved independently in different lineages (Thomas, 1997; Roy *et al*. 2011; Pal and Choudhury, 2014). Therefore, a simpler approach for classification will be presented in this thesis with focus only on morphological characteristics of most abundant forms: cyanobacteria, diatoms, dinoflagellates, coccolithophores, cryptophytes and “others” – including phytoflagellates, silicoflagellates, ciliates and other genera.

Phytoplankton can also be classified on size variation using the equivalent spherical diameter (ESD) of cells in three classes: picophytoplankton (ESD 0.2–2 μm), nanophytoplankton (ESD 2–20 μm) and microphytoplankton (ESD 20–200 μm). Picophytoplankton fraction is prevalent in most open oceanic ecosystems with oligotrophic waters. Coastal areas and large rivers mouths are usually eutrophic with a prevalence of bigger phytoplankton fractions. At times, the nanophytoplankton can account for up to 90% of the total phytoplanktonic chlorophyll in both open ocean and coastal waters. Phytoplankton and its products largely determine the trophic state of a water body (Jeffrey and Hallegraeff, 1990; Steele *et al*., 2009). Spatial and temporal distributions of phytoplankton reflect their ecological preferences, their dependence on nutrient availability, specific temperature ranges, light levels and water circulation (Kirchman, 2000, Cushman-Roisin *et al*., 2001, Mousing *et al*., 2016).

The differences between community composition are determined by the β diversity of the marine phytoplankton. β diversity is described as the shift in taxa composition between regions which is strongly influenced by environmental heterogeneity and oceanographic features, such as sharp environmental gradients and spatial distances, which may act as a physical barrier and influence the distributional patterns and the scale of planktonic dispersal along ocean currents (Whitaker, 1960; Longhurst, 2007; Watson *et al*., 2011). Planktonic dispersal rate varies across marine planktonic taxa (Finlay, 2002; Martiny *et al*., 2006; Jenkins *et al*., 2007), and Villarino *et al*. (2018) found that β diversity declines logarithmically with surface ocean transit times, which makes the dispersal limitation more important determinant of community structure than the niche segregation, at least for the tropical and subtropical open ocean. This represents a negative relationship between dispersal scale and body size where less abundant and larger-fraction plankton shows (in near-surface, epipelagic waters) shorter dispersal scales and larger spatial species-turnover rates than the more abundant, smaller-fraction plankton. The larger phytoplankton will be more similar at geographically proximate locations, and dissimilar between distant locations while it would allow smaller, more abundant phytoplankton (body size <2 mm) to travel greater distances (Villarino *et al*., 2018).

Distribution patterns of net primary production (NPP) are hence tightly connected to a combination of physical (e.g. light availability, ocean circulation, and water column stratification) and biological processes (e.g. microbial activity, zooplankton pressure; Field *et al*., 1998). Such heterogeneity in NPP is very much alike to one seen on land, where large regions of low productivity are contrasting small areas of high NPP (Field *et al*., 1998). Even minor changes in plankton composition, spatial distribution and seasonality can have far-reaching implications for the productivity of oceanic ecosystem, food web dynamics, biogeochemical cycling and ultimately, human livelihood (Falkowski *et al*., 1998; Boyd and Newton, 1999; Karl *et al*., 2012). Hence, in order to understand the oceans of today, and predict the oceans of tomorrow, it is an imperative to understand the interconnectivity between the phytoplankton and its surrounding.

Because algae are photosynthetic organisms, they possess chlorophyll in their chloroplasts which is a primary photosynthetic pigment and a light receptor in photosystem I of light reaction. Chlorophyll *a* (Chl *a*) has been valuable biomass and productivity indicator of oceanic phytoplankton for decades. (Wright *et al*., 2005). Chlorophylls are composed of a porphyrin ring system similar to that of haemoglobin but, instead of an iron atom at the center, it has that of a magnesium. Types of chlorophylls like Chl *a*, *b*, c_1, c_2, *d* and *e* present in algal cells with Chl *a* being universal in all members of autotrophic algae while other (secondary and tertiary pigments) act as accessory photosynthetic pigments. One of these accessory pigments are yellow, orange or red hydrocarbons called carotenoids and occur either inside or outside the plastid. Carotenoids can be divided into (i) the carotenoids (oxygen-free hydrocarbons) and (ii) the xanthophylls (their oxygenated derivatives). The most common algal carotene and xanthophyll is the ß-carotene and fucoxanthin, respectively. Other major pigments include red or blue phycobiliproteins (the phycoerythrobilin and phycocyanobilin, respectively), usually aligned in rows along the flattened vesicles, the thylakoids. Method of using pigments as proxies for analyzing the composition and distribution of oceanic phytoplankton is regarded as chemotaxonomy. Specifically, the taxon-specific photosynthetic accessory pigments (PAPs) and photoprotective pigments (PPPs) are estimated through HPLC. Along with classical taxonomic identification and cell count estimates, the pigment-based chemotaxonomy is very powerful and relatively cost-effective tool advantageous for the use in monitoring and research of large-scale ecosystems and biomes like the North Pacific (Wright *et al*., 2005; Pal and Kumar, 2014). Detection of cyanobacterial picophytoplankton fraction is problematic because they can't be filtered and analyzed like bigger phytoplankton. Guillard *et al*. (1985) and Morel *et al*. (1993) observed that the divinyl chlorophyll *a* (DVChl *a*) and zeaxanthin (among chlorophylls and carotenoids, respectively) were the most predominant in cyanobacterial cultures, and concluded they are very specific and characteristic to cyanobacteria. This means that the DVChl *a* and zeaxanthin can be used as a signature marker of picoplanktonic cyanobacteria for the marine environment and their abundance can be observed indirectly through the pigments' concentrations (Stockner and Antia, 1986). Studies that used chemotaxonomic approach including all the primary, secondary and tertiary pigments for detection of phytoplankton community and validation of ocean color remote sensing of the Pacific Ocean are very scarce. They usually only deal with Chl *a* and/or another accessory pigment for specific taxon for community and pigment distributions (Everitt *et al*., 1990), Chl *a*-only remote viewing (Alvain *et al*., 2005), nutrients-blooms interactions and biogeochemical responses (DiTullio *et al*., 1993; Coale *et al*., 1996). The absorption spectra of some of the major pigments are shown at Fig. 3.

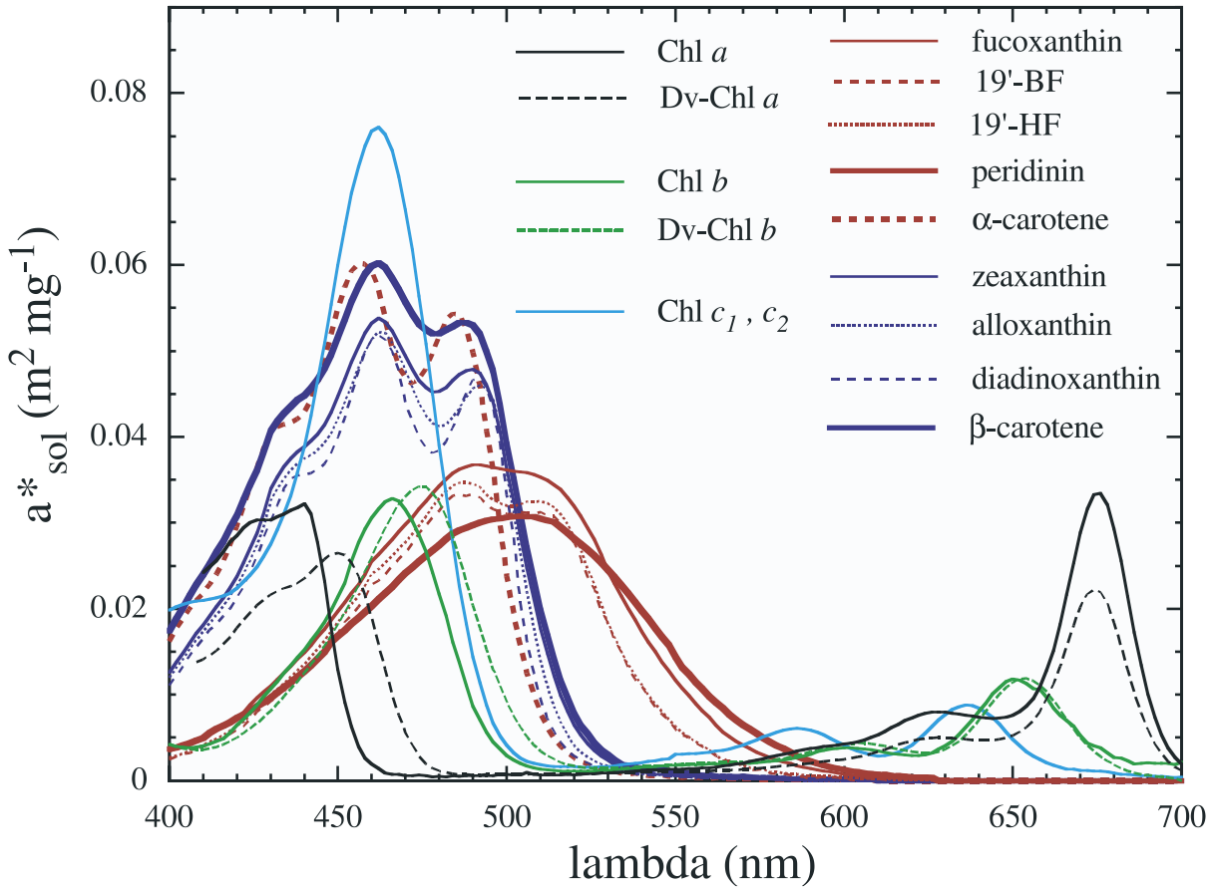

Fig. 3. Absorption spectra of the pigments (Bricaud *et al*., 2004).

1.3. Phytoplankton taxonomy

It is often said that we know more about the space than of the oceans even though the oceans are more accessible to us than space. The previous statement holds true regarding our knowledge about phytoplankton species and its interactions with the environment. There have been few more thorough expeditions in the Pacific Ocean set to find more about its composition of both the autotrophic and heterotrophic plankton community. Chavez *et al*. (1990) studied composition and spatial variability of phytoplankton taxa in relation to primary production in the Equatorial Pacific and found that most that most of the primary production, chlorophyll concentrations, and the phytoplankton abundances reached maxima at around the equator. Booth *et al*. (1993) analyzed the temporal variation of autotrophic and heterotrophic communities in the subarctic Pacific, and they observed that the general structure of the autotrophic community was similar to that in the North Atlantic (with certain variations). *Synechococcus* spp. dominated the picoplankton but the coccolithophores, such as *Emiliania huxleyi*, had minor contributions to biomass. Other important contributors to the community composition were centric (*Chaetoceros* spp.) and pennate (*Nitzschia* sp.) diatoms, cyanobacteria *Synechococcus* spp., the prymnesiophytes, red fluorescing picoplankton and athecate dinoflagellates. Cryptophytes,

prasinophytes, silicoflagellates (*Dictyocha* sp.), *Chrysochromulina* spp., *Phaeocystis pouchetii* and *Micromonas pusilla* contributed to a lesser degree.

Most impactful circumglobal research expeditions happened under the multinational Tara Oceans consortium from 2009 to 2013 (Karsenti *et al*., 2011). All taxonomic levels from prokaryotic and eukaryotic plankton have been encompassed along with the viruses. Around 11,200 morphospecies have been cataloged, while analysis of 18S ribosomal DNA sequences showed around 150,000 operational taxonomic units (OTUs) for eukaryotic diversity (De Vargas *et al*., 2015). Heterotrophic protistan groups had the highest biodiversity of eukaryotic plankton, while phytoplankton species were fewer (around 4350 morphospecies). General information and identification characteristics used for determination of five major phytoplankton groups are shown in Table 1. Various pigment compositions and types of aforementioned taxa are shown in Table 2.

Cyanobacteria, named by their cyan color, are the oldest organism on Earth that helped pay the way for the more complex organism by oxygenating Earth's early atmosphere around 2 billion years ago, during the Proterozoic eon ('the Great Oxygenation Event'). They are prokaryotes, so the cyanobacterial cells do not contain membrane-bound organelles like chloroplasts, but instead, they have thylakoids peripherally in the cytoplasm. Furthermore, the phototrophic eukaryotes that photosynthesize using plastids have evolved because of endosymbiosis with the ancient cyanobacteria. Even today, the cyanobacteria are the only photosynthetic prokaryotes able to produce oxygen. Two of cosmopolitan cyanobacteria species that are usually observed together, the *Prochlorococcus* and *Synechococcus*, play a significant role in the global carbon cycle and contribute up to 50% of fixed carbon in marine systems (Partensky *et al*., 1999b; Hamilton *et al*., 2015). Signature pigment for the *Prochlorococcus* is DVChl *a* and for the *Synechococcus* is zeaxanthin. Because most of the cyanobacteria are part of picophytoplankton fraction, they can't be filtered and analyzed like bigger phytoplankton (Roy *et al*., 2011).

Diatoms (Greek διά τέμνειν/diá témnein, "cut in half") are unicellular or colonial cell chains covered by characteristic siliceous frustules with two overlapping valves, a smaller valve called hypotheca and larger epitheca. Valves have a variety of shapes (boat-like, circular, oblong, square, triangular, elliptical or polygonal) and are usually ornamented. A cell wall is mainly composed of silica and partly of pectic substances. Each valve is composed of two or more pieces which are usually ornamented. Diatoms have two forms based on symmetry: (i) *Centrales* (radially symmetrical) and (ii) *Pennales* (bilaterally symmetrical). They produce a special type of spore – the auxospore. Diatoms are very widely distributed in the sea and in all kinds of freshwaters, as well as in the soil and in other terrestrial habitats. The signature pigment is fucoxanthin (Roy *et al*., 2011).

Dinoflagellates (Greek δῖνος/dînos, Latin flagellum – 'whirling whip') are mostly unicellular with two halves, epicone and hypocone, made up of unarmoured or armored thecal plates with cellulose

with a transverse girdle groove into an upper epicingulum and a lower hypocingulum. Plastids are present in around half of the species. Ejectile organelles, the trichocysts, are present peripherally. They have two flagella, one longitudinal and one transverse. Also, they can have various morphological shapes (spines, horn, and wings). Some species have bioluminescent properties. Widely distributed in tropical, subtropical and temperate oceans. They can be or can have endosymbionts. Some species have bioluminescent properties. The signature pigment is peridinin (Roy *et al*., 2011).

Coccolithophores (Greek κόκκος λίθος φόρος/kókkos líthos phóros – to carry stone seed) are biflagellate or coccoid unicells with the outer covering of organic scales or small regular calcareous plates – the coccoliths. The coccoliths consist of calcium carbonate, in the crystalline form of calcite which may be replaced by aragonite and vaterite in nitrogen-limited cultures. The coccoliths are assembled in the Golgi cisternae. Some species have a heteromorphic life cycle. Coccolithophores play an important role with the Greenhouse effect and carbon cycling by transporting calcium carbonate into depths. They may influence weather and climate patterns by producing volatile Sulphur compounds (dimethyl sulfide, 'DMS'; dimethylsulfoniopropionate, 'DMSP'; dimethylsulfoxide 'DMSO') that act as cloud seeding nuclei. The signature pigment is 19'-hexanoyloxyfucoxanthin (19HF; Roy *et al*., 2011).

Cryptophytes are ovoid, asymmetrical, flagellate unicells, often flattened. They have unique cell covering, the pellicle, that is made up of a ridged periplast superimposed on an inner layer of thin proteinaceous plates. Also, vestigial nucleomorph and the complex vacuolar system are present but microtubular cytoskeleton is absent. Flagella comes out of apical gullet or furrow with ejectile organelles, the trichocysts, present peripherally or in the furrow-gullet system. Cryptophytes may be endosymbiotic in ciliates and dinoflagellates. Two large parietal chromatophores are often present in the cells, giving them very diverse pigmentation, which can vary even more depending on the endosymbiont color: gold for haptophyte/diatom, green for prasinophyte, red for cryptophytes. The signature pigment is alloxanthin (Roy *et al*., 2011).

Other common types of marine plankton include a variety of unicellular, nonmotile algae and bacteria, motile flagellates, and ciliates. Size varies from less than 1 μm to bigger than 1 mm. Recent observations have shown a great abundance of eukaryotic picoplankton. By their trophic mode of nutrition, they can be phototrophic (using photosynthesis), heterotrophic (uptake of organic material) or mixotrophic (combination of photo-, litho-, chemo- and organotrophy). Different phytoflagellates, silicoflagellates and others have been included in this group. Most prominent are prasinophytes which are small, green unicells that can be either flagellate, coccoid, colonial or filamentous. They are morphologically diverse but with simple cellular structures with only a single chloroplast and a single mitochondrion. Notable member *Micromonas* is found in marine waters worldwide. Generally, signature pigment for all green algae is Chl *b* but, specifically for prasinophytes, the signature pigment is prasinoxanthin (Roy *et al*., 2011).

Table 1. General information and identification characteristics for major taxon groups modified from Roy *et al*. (2011).

Taxon	Cyanobacteria	Diatoms	Dinoflagellates	Coccolithophores	Cryptophytes
Organization	Unicellular or colonies	Unicellular or colonies	Unicellular	Unicellular	Unicellular
Size	1 µm - 2 mm colonies	2 µm - 200 µm, some 2 mm	2 µm- 200 µm, some 2 mm	5 µm–30 µm	6–20 µm
Form	Coccoid, filamentous (unbranched, pseudobranched or branched).	*Centrales* (radial symmetry) or *Pinales* (bilateral symmetry); boat-like, circular, square, triangular, elliptical or polygonal.	Various shapes (spines, horns, and wings).	*Heterococcoliths* (diverse CaCO3 elements) or *Holococcoliths* (one type of calcite crystals); spherical, ovoid or coccoid.	Ovoid, asymmetrical, often flattened with gullet or furrow.
Cell covering	Rigid murein peptidoglycan layer surrounded by outer double-layered lipopolysaccharide and mucilaginous sheath.	Siliceous frustules and organic layer arranged in two overlapping valves (smaller hypotheca and larger epitheca), usually ornamented.	Multilayer theca, unarmored and armored forms with cellulose plates inside thecal vesicles, girdle divides the cell into epicone and hypocone.	The coccoliths ($CaCO_3$ scales) lying over uncalcified scales formed in the Golgi cisternae, organic scales made from cellulose matrix and pectic polysaccharides.	Proteinaceous pellicle - ridged periplast superimposed on an inner layer of proteinaceous plates.
Flagella	Absent.	Absent, except in male gametes.	Two dimorphic, transverse in girdle, longitudinal in sulcus.	Motile forms - two smooth equal or subequal flagella.	Two equal or subequal flagella with tubular hairs.
Storage reserves	Polyglucan, cyanophycin, polyphosphate granules (Jeffrey, 2006).	Chrysolaminarin and oil.	Starch and oil (Thomas, 2006).	Chrysolaminarin.	Starch.
Internal structure	No membrane-bound organelles; inclusions, granules, crystalloids, membranous structures, akinetes, heterocysts and carboxysomes present.	Large vacuole, internal pyrenoid, DNA in ring nucleoid.	Large nucleus, permanently condensed chromosomes, ejectile trichocysts, various pyrenoids (Jeffrey, 2006).	Internal pyrenoid, haptonema present.	Thylakoids in pairs filled with electron-dense material, proteinaceus pyrenoid, complex vacuolar system, trichocysts ejectosome and vestigial nucleomorph.
Chloroplasts	None, thylakoids with phycobilisomes on the surface.	One to many, with four membranes, girdle lamellae with three thylakoids.	Present in half of species, three membranes with thylakoids in bands of three.	One or two discoid.	One or two.
Culture color	Pale green, blue-green, grey-green or red	Yellow, orange to golden-brown	Reddish-brown or color of endosymbiont.	Gold to golden-brown.	Red or blue-green.
Biotopes	Cosmopolite, almost all of the biotopes, endosymbionts.	Ubiquitous in marine and freshwater, sea-ice and air; epibiotic, endobiotic.	Tropical, subtropical, temperate and polar oceans, terrestrial freshwaters.	Cosmopolite, abundant in tropical and subtropical oceans, few in polar waters.	Ubiquitous in freshwater, estuarine and marine environments, soil and snow.
Geological age	Paleoarchaean-paleoproterozoic (Hamilton, 2014).	Centrics: Jurassic and early Cretaceous (Gersonde and Harwood, 1990). Araphid pennates: late Cretaceous. Raphid pennates: middle Eocene (Medlin *et al*., 1993).	Dinocysts in Silurian (Thomas, 1997), Triassic (Macrae R.A., *et al*., 1996).	Rare occurrence in Paleozoic and Triassic, abundant in Jurassic (Tappan, 1980; Thomas, 1997).	Cryptospores from Ordovician (Edwards *et al*., 2014).

Table 2. Different pigment compositions of major taxon groups of algae

TAXON	PIGMENTS
CYANOBACTERIA	Five Types (Jeffrey & Wright, 2006): **CYANO-1**; typical of *Trichodesmium* spp. and *Oscillatoria* sp. (Hertzberg *et al*., 1971; Aakermann *et al*., 1992; Carpenter *et al*., 1993); **Chlorophylls**: Chl *a*, MGDVP (trace); **Carotenoids**: zeaxanthin, ß, ß-carotene, myxoxanthophyll, echinone, canthaxanthin, oscillaxanthin, nostoxanthine, aphanizophyll, and 4-keto-myxoxanthophyll; **CYANO-2**; typical of *Synechococcus* spp. **Chlorophylls**: Chl *a*, MGDVP (trace); **Carotenoids**: zeaxanthin, ß, ß-carotene (Jeffrey & Wright, 1997); **Phycobiliproteins**: phycocyanin, allophycocyanin, phycoerythrocyanin and phycoerythrin (Rowan, 1989); **CYANO-3:** typical of *Prochloron* and *Prochlorothrix*; **Chlorophylls**: Chl *a*, Chl *b*, MGDVP; **Carotenoids**: ß, ß-carotene, zeaxanthin, cryptoxanthin, traces of ß, ß-carotene monoepoxide, echinenone (Burger-Wiersma *et al*., 1986; Foss *et al*., 1987; Goericke *et al*., 2000); **CYANO-4:** typical of *Prochlorococcus*; **Chlorophylls**: DVChl *a*, DVChl *b*, MGDVP (Goericke and Repeta, 1992); **Carotenoids**: ß, ε-carotene, zeaxanthin; **CYANO-5:** typical of *Acaryochloris*; **Chlorophylls**: Chl *d*, traces of Chl *a* and MGDVP; **Carotenoids**: ß, ε-carotene and zeaxanthin; **Phycobiliproteins:** traces of phycocyanin and allophycocyanin (Miyashita *et al*., 1996, 1997, 2003)
DIATOMS	**DIATOM-1**: Chl *a*, Chl c_1, Chl c_2, MGDVP (trace); **DIATOM-2**: Chl *a*, Chl c_2, Chl c_3, MGDVP (trace); **DIATOM-3**: Chl *a*, Chl c_1, Chl c_2, Chl c_3, MGDVP (trace); **Carotenoids**: fucoxanthin, diadinoxanthin, diatoxanthin, ß, ß-carotene, 19'-butanoyloxyfucoxanthin; minor amounts of violaxanthin, antheraxanthin, and zeaxanthin (Lohr and Wilhelm, 1999)
DINOFLAGELLATES	Five types (Jeffrey & Wright, 2006): **DINO-1:** peridinin-containing; **Chlorophylls:** Chl *a*, c_2, MGDVP; **Carotenoids:** peridinin, diadinoxanthin,diatoxanthin, dinoxanthin, peridininol, P-457 (7',8'- dihydroneoxanthin-20'-al-3'-ß-lactoside), pyrrhoxanthin and ß, ß-carotene; **DINO-2:** Haptophyte-containing: **Chlorophylls:** Chl *a*, c_2, c_3, MGDVP; Carotenoids: 19'-hexanoyloxyfucoxanthin, fucoxanthin, diadinoxanthin, 19'-butanoyloxyfucoxanthin, diatoxanthin, gyroxanthin diester, ß, ß-carotene, ß, ε-carotene. (Carreto *et al*., 2001) **DINO-3:** Diatom-containing: **Chlorophylls:** Chl *a*, c_1, c_2; **Carotenoids:** fucoxanthin, diadinoxanthin, diatoxanthin, ß, ß-carotene; zeaxanthin, canthaxanthin and b, ψ-carotene (Kempton *et al*., 2002; Takano *et al*., 2008) **DINO-4:** Cryptophyte-containing: **Chlorophylls:** Chl *a*; c_2; **Carotenoids:** alloxanthin; **Phycobiliproteins:** phycoerythrin, phycocyanin (Vesk *et al*., 1996; Hewes *et al*., 1998; Meyer-Harms and Pollehne, 1998) **DINO-5:** Prasinophyte-containing: **Chlorophylls:** Chl *a*, *b*; **Carotenoids:** ß, ß-carotene, neoxanthin, violaxanthin, zeaxanthin; rarely prasinoxanthin
COCCOLITHOPHORES	Six pigment types (Zapata *et al*., 2004): **Chlorophylls**: Chl *a*, MGDVP; variable distributions of chlorophyll c pigments: Chl c_1, c_2, c_3, Chl c_2-mgdg, MVChl c_3; **Carotenoids**: **HAPTO 3–8**, all contain fucoxanthin, diadinoxanthin, diatoxanthin and ß, ß-carotene; **HAPTO 5**, 4-ketofucoxanthin; **HAPTO 6**, 7 and 8: also contain 19'- butanoyloxyfucoxanthin, 19'-hexanoyloxyfucoxanthin and 4-keto-19'-hexanoyloxyfucoxanthin (Zapata *et al*., 2004; Jeffrey and Wright, 2006; Airs and Llewellyn, 2006)
CRYPTOPHYTES	**Chlorophylls**: Chls *a* and c_2, MGDVP; **Carotenoids**: alloxanthin, crocoxanthin, monadoxanthin; b, ε-carotene; **Phycobiliproteins**: phycoerythrins and phycocyanins

1.4. Remote viewing of oceans with satellites

With the advancements in the space industry, optical technologies have been improving over the past few decades giving us new insights for both the Earth and other planets. With a unique vantage point in space, satellites' remote sensing capabilities enabled us to gain insight into various aspects of the oceans. The spectral composition of the visible light that is reflected from the ocean determines its color. What color will the ocean be, depends on the particulate and dissolved particles in the water column, the viewing angle, current atmospheric conditions and spectrum of the sunlight. With the help of satellite oceanography, it will be possible to explore the spatial and temporal distribution and variability of phytoplankton communities and link it to higher trophic states and ocean biogeochemistry.

Historically, most of the gathered datasets were focused solely on the concentrations of Chl *a* or the determination of calcium carbonate presence from the coccolithophores (which makes them highly reflective across all visible wavelengths). All other pigments and constituents were treated as signal contamination even though it would be possible to derive much more biogeochemical properties from optical data (Coble, 2007).

NASA's first instrument devoted to the measurement of ocean color was the Coastal Zone Color Scanner (CZCS) experiment that operated from 1978 to 1986. CZCS was a multi-channel scanning radiometer aboard the Nimbatus 7 orbital satellite whose spectral bands, spatial resolution, and dynamic range were optimized for use over water. Even though it had had four spectral bands used primarily for ocean color, the data it gave was very limited. Next significant step was the Sea-Viewing Wide Field-of-View Sensor (SeaWiFS) that delivered better resolution global maps of chlorophyll pigment concentrations (Fig. 4). SeaWiFS had 8 spectral bands from 412 to 865 nm and it operated from 1997 to 2010. From 2002, more ocean color data has been made available by Moderate Resolution Imaging Spectroradiometer (MODIS) on board the Earth Observing System Aqua (EOS PM-1) satellite. Aqua MODIS acquires data in 36 spectral bands from the entire Earth's surface every 2 days. The Visible and Infrared Imager/Radiometer Suite (VIIRS), MODIS's successor launched in 2012, has 22 spectral bands ranging from 412 nm to 12 nm. NASA's Plankton, Aerosol, Cloud, ocean Ecosystem (PACE) mission aims to widen spectral coverage to 350-885 nm of wavelengths at 5 nm intervals (Fig. 5). It will extend key systematic ocean color, aerosol, and cloud data records. The primary instruments planned for PACE are: (i) Ocean Color Instrument (OCI) and Multi-angle Polarimeter (Robinson, 2010; URL 1, URL 2). The OCI is a spectrometer that will measure the intensity of the ultraviolet, visible, near infrared and several shortwave infrared bands continuously at a finer resolution than previous NASA ocean color sensors. Multi-angle Polarimeter is a radiometer that will measure how the oscillation of sunlight within a geometric plane is changed by passing through clouds, aerosols, and the ocean.

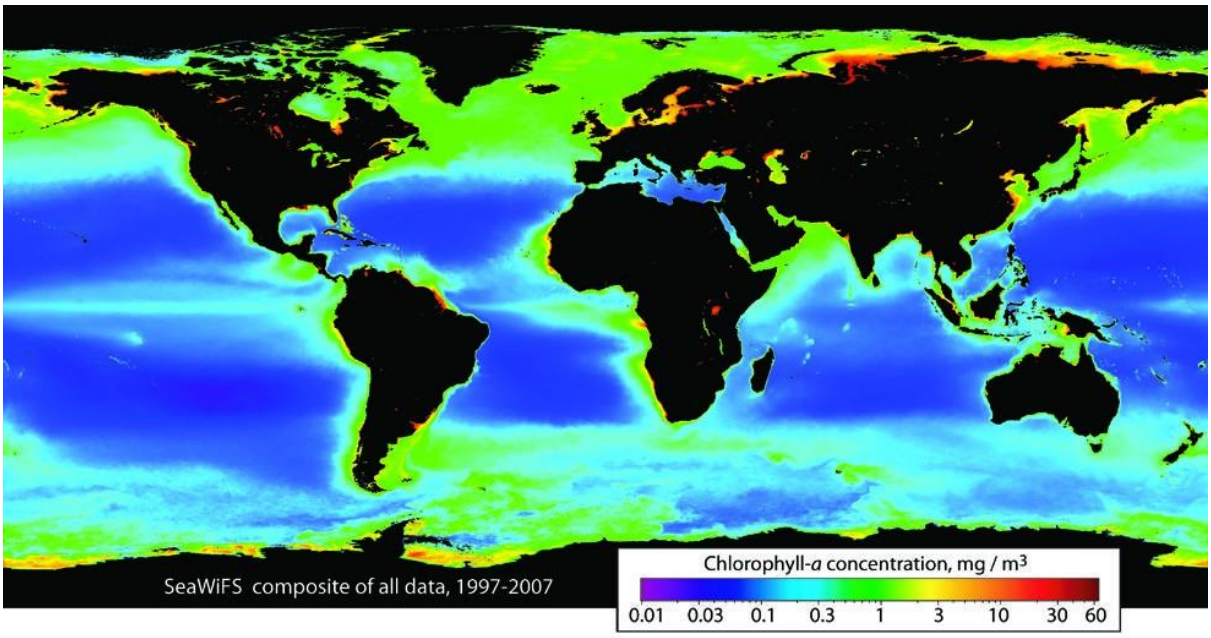

Fig. 4. Global composite image of all SeaWiFS chlorophyll *a* data acquired 1997-2007 (URL 2).

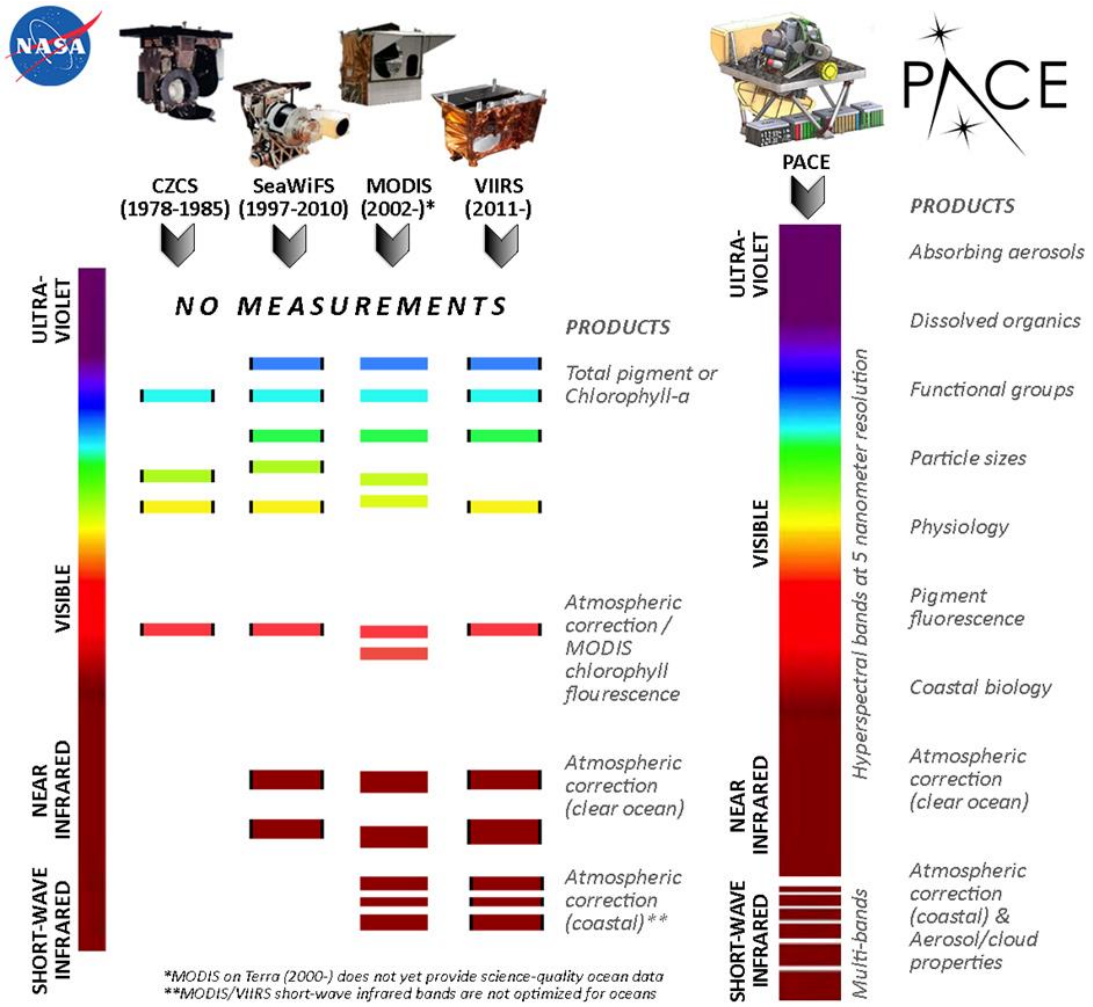

Fig. 5. Spectral coverage ocean color heritage sensors compared to PACE (edited from NASA).

When higher amounts of sediment and phytoplankton pigments are present in the ocean, due to their absorption and scattering properties, the reflectance of the blue portion of the spectra decreases, and green increases. Thus, the color of the ocean changes from blue to green and brown. Certain phytoplankton groups can be identified by their unique optical properties resulting from the morphological structure of the cells themselves, or the fluorescence of pigments they contain. By analyzing the light reflecting from the surface of the ocean, and by calibrating satellites' sensor technologies, it will be possible to observe the subtle differences in ocean color and translate them to changes in phytoplankton community found in the upper layers of the ocean. Due to the limitations of technology and large ocean dimensions, there needs to be found an alternative to classical field sampling that remote sensing of the oceans offers (Steele *et al*., 2009; Robinson, 2010).

2. THE AIM OF THE RESEARCH

Our understanding of the North Pacific phytoplankton community is limited – probably due to the scarcity of the research conducted in that important oceanic ecosystem. Due to vast expanses of Earth's biggest ocean, it is very hard to collect whole sets of data that can display meaningful relationships in such intertwined and complex systems. Considering the vast spatial scale to cover when investigating the Pacific Ocean, scientists were unable to use just basic tools such as microscopy or chemotaxonomy to produce good community composition estimations. Due to this reason, more and more studies today are leaning on Sanger and High Throughput Sequencing methods of rDNA gene markers (De Vargas *et al*., 2015) to cover the phytoplankton composition in this large ecosystem. Additionally, there is a lack of taxonomists along with equipment for good quality morphological identifications of phytoplankton species is expensive in comparison to everyday price dropping in molecular-based research. Therefore, the aims of this thesis are:

1) Detailed quantitative and qualitative analysis of phytoplankton community in the North Pacific Ocean using microscopy (LM and SEM)
2) Trophic level estimation of different parts of North Pacific Ocean based on taxonomy and chemotaxonomy

The results of this research will be used in the PACE project to develop algorithms and calibration of sensor technology of orbital satellites by which it will be possible to observe the subtle color differences of the ocean.

3. MATERIALS AND METHODS

3.1. Expedition – Location and time

Sea to Space Particle Investigation cruise (funded by Schmidt Ocean Institute (SOI)) was conducted from January 24 to February 20, 2017, in North Pacific. The aim of the cruise was to connect the color of the ocean with the trophic state of the ocean and use those data to develop algorithms and phytoplankton proxies for the NASA's PACE mission (URL 1). The satellite is currently under construction with the launch scheduled in 2022. It will monitor the state of the ocean by analyzing the distribution of phytoplankton, the color of the ocean and aerosol-cloud dynamics.

The expedition started in Honolulu, Hawaii heading to California coast near Monterey Bay, after which the ship turned north along the coastline to the mouth of Columbia River Bar and ended in Portland, Oregon (Fig. 6). The scientific crew was comprised from many collaborating teams covering wide interdisciplinary field of oceanography, both on the small and big scale (NASA Goddard Space Flight Center, Universities Space Research Association, United States Geological Survey, Skidmore College, Moss Landing Marine Laboratories, Sequoia Sciences, LabexMER, University of Western Brittany, Duke University, Brown University and University of Zagreb (Fig. 7, 8).

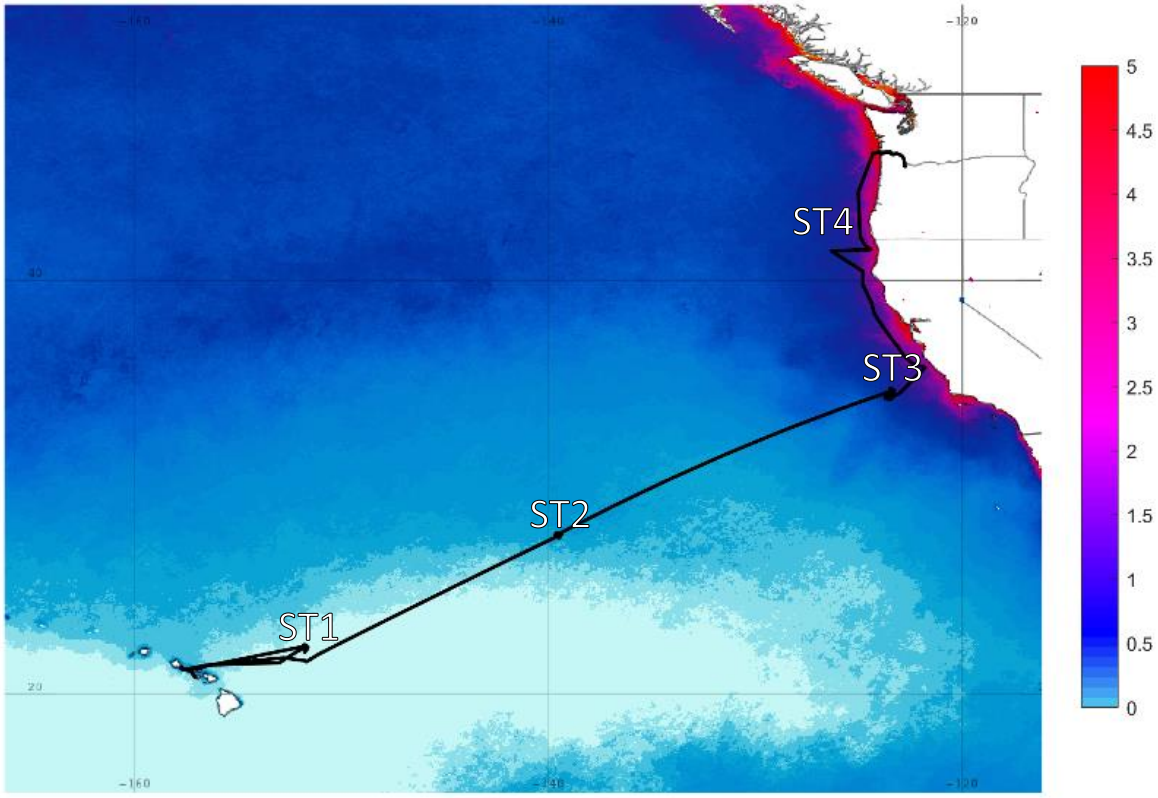

Fig. 6. Cruise track of the Sea to Space cruise (black line), superimposed onto the MODIS Aqua Chlorophyll averages for the month of February (2002-2017 average).

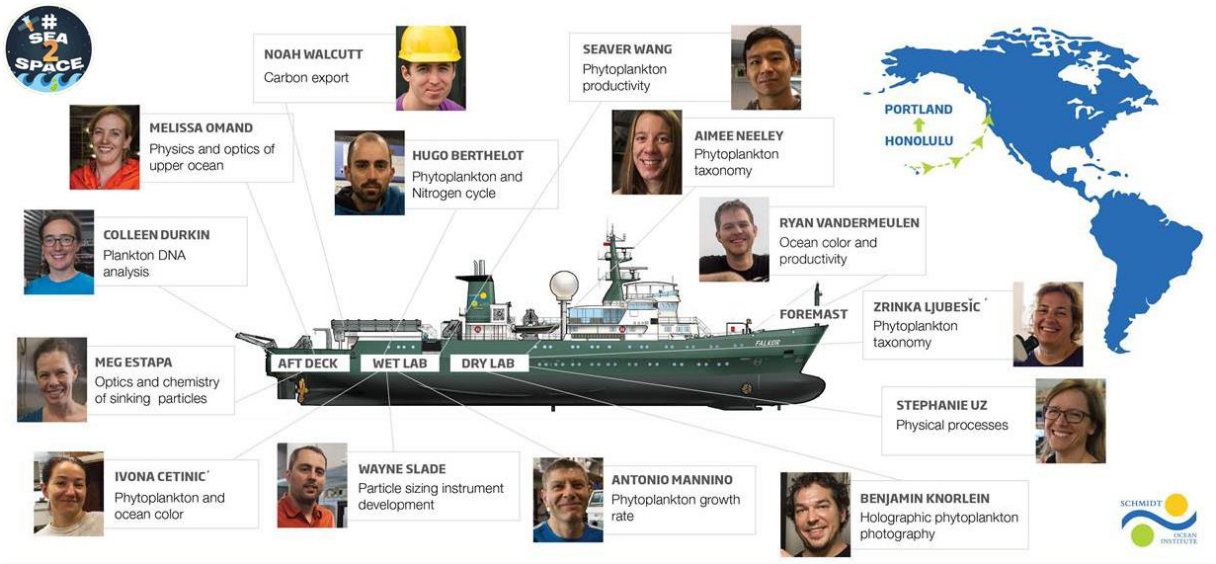

Fig. 7. Schematic of R/V Falkor with participating science crew and transect of a cruise (edited from SOI).

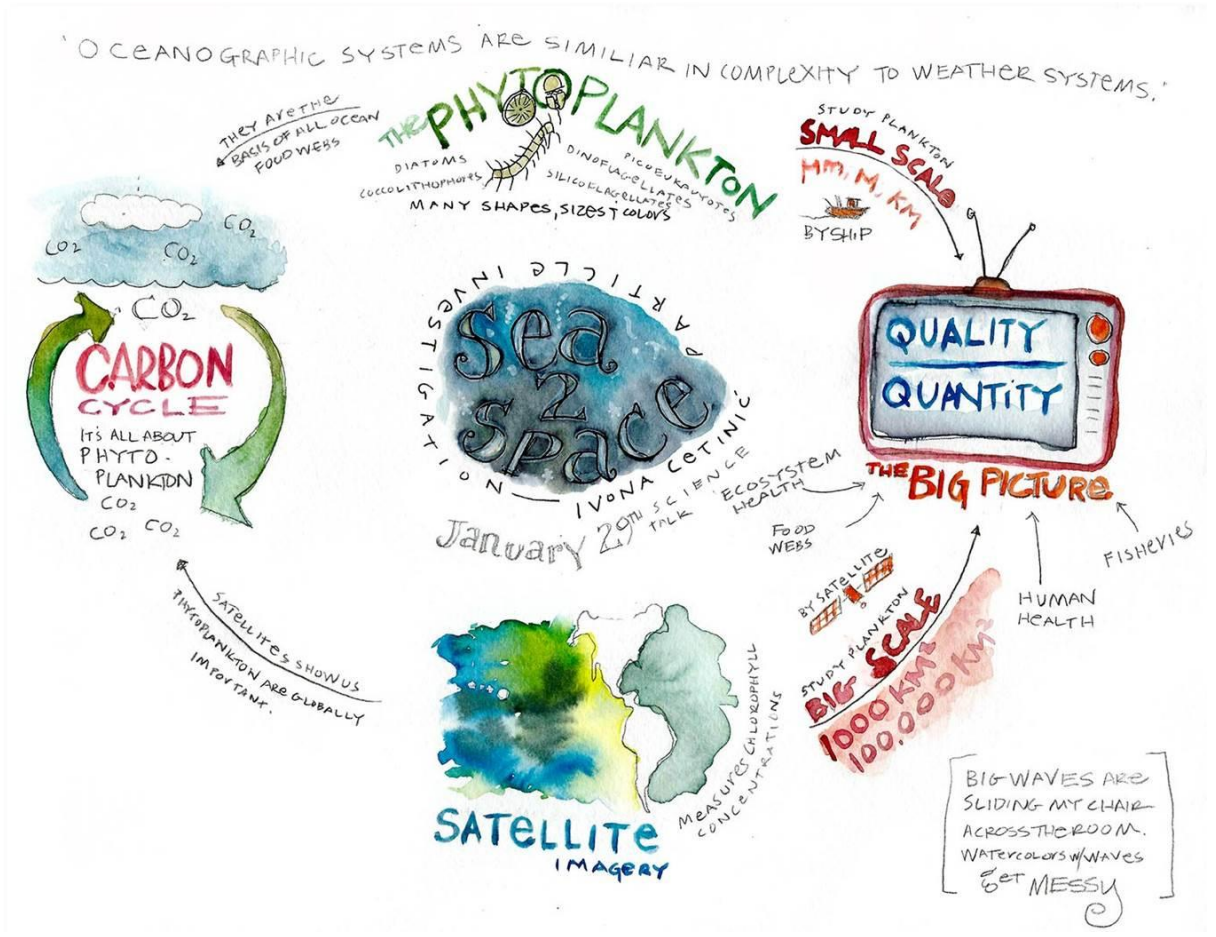

Fig. 8. Scheme of the research covered in the Sea to Space particle investigation project (illustration by Kirsten Carlson).

3.2. Sampling

Interdisciplinary research during Sea to Space particle investigation was conducted onboard of the oceanographic research vessel R/V Falkor (Fig. 7). The sampling design was highly adaptive with station positions and sampling depths defined using the distribution of specific circulation patterns derived from satellite imagery, and real-time *in situ* data (temperature, salinity, optical properties of seawater). Samples for phytoplankton and pigment analyses were taken by10 L Niskin rosette sampler (Fig. 9) equipped with Conductivity-Temperature-Depth probes (CTD) from three depths: the surface layer (S), deep chlorophyll maximum (DCM), and mixed layer depth (MLD). Additionally, at Station CTD 14, one sample was taken below the mixing layer depth (BMLD) at –180 meters. The total number of samples taken using CTD probes was 38. For qualitative plankton analysis, additional samples were taken from the Niskin bottles and filtered through 20 μm mesh. Total of 27 net samples was collected.

Surface sampling was conducted using ships' underway system (UW) and timed with the overpass of the ocean color satellites, around 13:00 h. Samples were taken at 12 locations. Underway sampling was accompanied by continues radiometry at the bow and radiometric profiles from the stern of the ship when the weather conditions allowed it. Phytoplankton samples were fixed with 2% neutralized formaldehyde and stored in 250 mL bottles until analyses in the laboratory of biological oceanography, Department of Biology, University of Zagreb.

For more detailed taxonomic analyses, a volume of 400 mL seawater was filtered using weak vacuum onto polycarbonate filters (0.8 μm Cyclopore, 25 mm diameter, Whatman) that were placed on cellulose nitrate membranes filter (0.8 μm Whatman) to ensure an even distribution of material (Fig. 7). The filters were rinsed with 2 mL of bottled drinking water (pH = 7.54) and dried in an oven at 50°C. The filters were stored in dry containers for the analysis in the laboratory at the University of Uppsala.

Four-liter triplicate seawater samples were filtered on GF/F filters for phytoplankton pigment analysis and stored in liquid nitrogen until the high-performance liquid chromatography (HPLC) analysis in the NASA's Goddard Space Flight Center (Fig. 10), following methods described in Hooker *et al*. (2012).

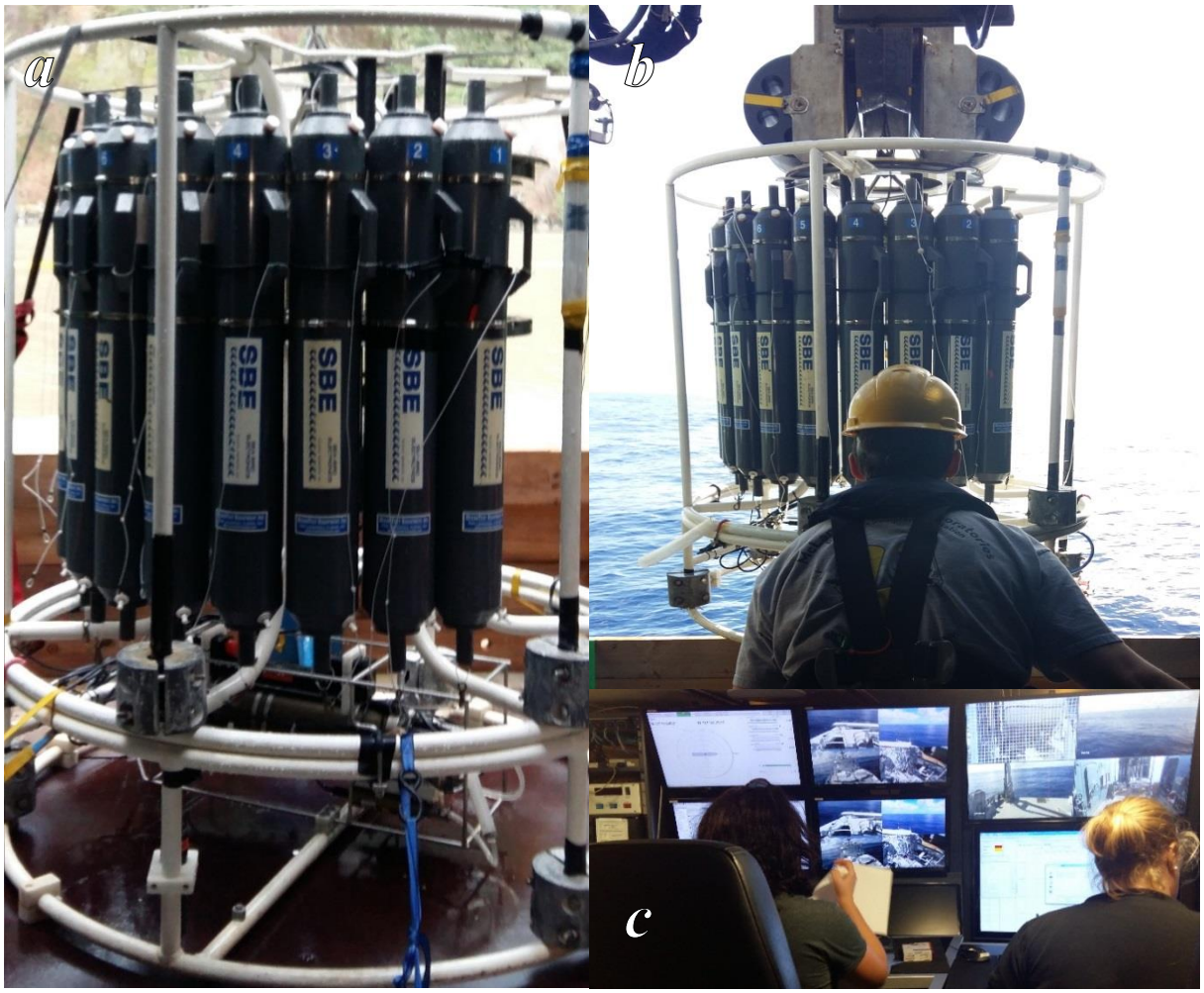

Fig. 9. a) Niskin bottles with CTD probes arranged in a rosette; b) rosette recovery from the ocean, c) CTD control room.

3.3. Phytoplankton community analysis

Light microscopy (LM) was used to determine the phytoplankton composition and abundance. Subsamples of 50 or 100 mL, depending on cell density, were settled for 24 h and 48 h respectively and analyzed under a Zeiss Axiovert 200 inverted microscope using the Utermöhl method (Utermöhl, 1958). Cells larger than 20 µm were designated as microphytoplankton, and cells between 2 and 20 µm as nanophytoplankton. Typically, one transect across the counting chamber was analyzed at ×400, and two at ×200 magnification. The total count was completed at ×100 magnification for rare taxa. The minimum cell abundance that can be detected by this method is 20 cells L^{-1}. For additional taxonomic analyses, net samples were analyzed with Zeiss Axiovert 200 inverted microscope and images of all species were taken and analyzed with Zeiss AxioVision SE64 (version 4.9.1). Scanning electron microscopy (SEM) was used for the qualitative analysis (taxonomic diversity) of the phytoplankton community. Prior to the SEM analysis, a piece of filter was mounted on an aluminium stub, sputter-coated with gold and examined under a Zeiss Supra35-VP SEM.

Fig. 10. Sampling and filtration methods: a) sample filtration for HPLC; b) subsampling from CTD probe (pigment and phytoplankton analysis); c) filtration from Niskin bottles; d) filter excitation; e) bottle preparation for phytoplankton; f) sample filtration for SEM.

3.4. Statistical analysis

The basic statistical analysis was performed using the software Microsoft Office 365 ProPlus (Microsoft Corporation, version 1705) while all the multivariate analyses were performed using the software Primer 6.0 (Primer-E Ltd, 2002) It was done to determine frequencies of dominant phytoplankton taxa and to analyze pigments. The tests based on a Bray–Curtis rank similarity matrix were calculated using log(x+1) transformed data. Similarity percentages analyses (SIMPER) (Clarke, 1993) were used to observe the percentage contribution of each taxon and pigment to the average dissimilarity between samples of different stations. Hierarchical cluster analysis (HCA) with the group averaging linking and non-metric multi-dimensional scaling (nMDS) was performed to investigate similarities among phytoplankton composition and pigments (Clarke and Warwick, 1994). This analysis was also based on the Bray–Curtis similarity measure (Bray and Curtis, 1957). Finally, principal component analysis (PCA) was performed to find correlations between phytoplankton abundance, pigment concentration through different trophic states. Data visualization and chart plotting was made using the software Grapher 12 (GoldenSoftware) and Microsoft Excel. Phytoplankton micrographs and plates were made and edited using Adobe's Photoshop CC 2015 and Illustrator CC 2017.

4. RESULTS

4.1. Phytoplankton abundance analyses

Multivariate statistical analyses (Hierarchical cluster analysis, HCA) based on the phytoplankton diversity and abundance separated the samples into four groups corresponding to four trophic levels (Fig. 11). Station 1 (ST1) and Station 2 (ST2) were oligotrophic stations, while Station 3 (ST3), and Station 4 (ST4) included highly productive areas. Positions of ST1 and ST2 were in ultraoligotrophic North Pacific Subtropical Gyre (NPSG), while ST 3 was positioned in Californian Current System (CCS) and ST4 in the Columbia River plume (CRP).

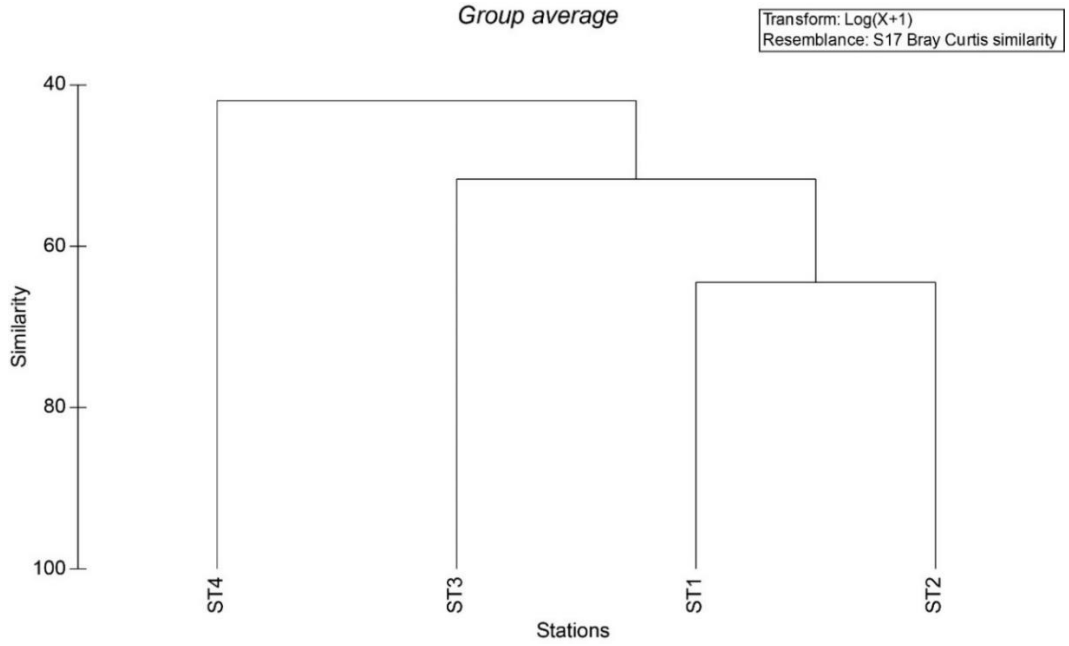

Fig. 11. Cluster analysis separation of stations according to phytoplankton community composition.

The phytoplankton community of North Pacific was mostly comprised of coccolithophores (35.5%), diatoms (25.2%) and dinoflagellates (19.5%) while cryptophytes, phytoflagellates, silicoflagellates, haptophytes, etc. were included in group "other" that makes 19.8%. Coccolithophores dominated in nanophytoplankton on all stations, with the maximal contribution of 74.3% recorded at ST2. At the same station, the least diatoms (1.7%) and other phytoplankton (4.1%) was recorded. Highest contribution of diatoms (17.3%) and "other" phytoplankton groups (29.3%) in nanophytoplankton was recorded at ST4, which also has the lowest percentage of dinoflagellates (11.7%). On the other hand, diatoms dominated microphytoplankton community, with a maximal contribution at ST1 (50.2%) and ST3 (90.7%). On other two stations, their contribution is significant, but the coccolithophores took the dominance with 51.7% at ST2 and 68.6% at ST4, respectively. Dinoflagellates contributed, both in microphytoplankton and nanophytoplankton with maximum abundances on ST1 (Fig. 12).

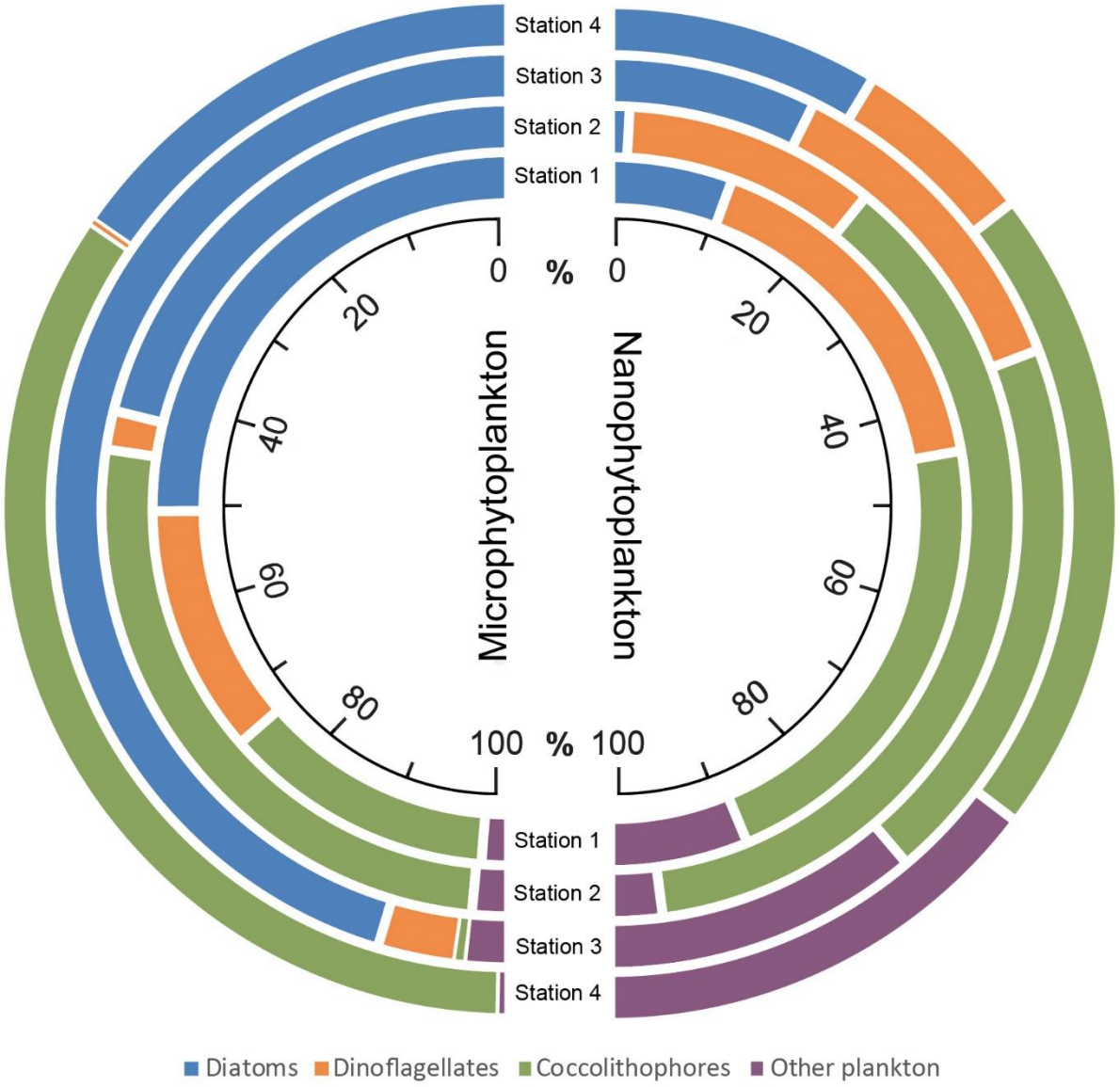

Fig. 12. Contribution (in percentage) of each major taxon group to microphytoplankton and nanophytoplankton community per stations.

A total of 207 taxa have been determined from both CTD probes and net samples of which: 106 diatoms, 48 coccolithophores, 41 dinoflagellates, 7 other autotrophs, 4 heterotrophs and 1 cyanobacteria. Cryptophytes have been observed but no taxon has been determined (Table 3). From 207 taxa, more than a half (113) taxa are found only in net samples: 42 diatoms, 40 coccolithophores, 27 dinoflagellates and 4 other heterotrophs.

Vertical profiles of phytoplankton community composition (Fig. 13), follow the same overall pattern seen above, however, within the profile, the abundances and ratio of groups seem to vary somewhat. The abundance of nanophytoplankton varied across the station, with lowest numbers found at ST2. Regardless of the station, vertical profiles of the nanophytoplankton were dominated by the coccolithophores. Nano-sized diatoms were present at all stations, with lowest contributions detected at ST2 (DCM samples had no nano-sized diatoms at all). Oddly, while the surface sample collected at ST4

had the highest number of the “other” nanophytoplankton, this group was not detected in the rest of that vertical profile.

The diatoms dominated micro-community, in all vertical profiles; even more so, they were the only group of microphytoplankton found at the ST4 in the DCM layer. The coccolithophores contributed significantly to the community of the ST1 and ST2, with highest numbers found at ST2 in the MLD (74.2%). The situation changes dramatically at eutrophic ST3 and ST4, where coccolithophorid contribution falls to 1.1% at the surface and to 0.4% at MLD of ST3. At ST4 no coccolithophores have been detected. The contribution of dinoflagellates to microphytoplankton was significant only at ST1, with the lowest numbers encountered at the surface of ST4 (0.7%, no dinoflagellates below the surface). Bellow it, none have been detected. Finally, other plankton contributed minimally to the overall microphytoplankton abundances (same to nano-fraction). Highest numbers were found within surface samples, with the highest being at station 2 (7.1%). At the MLD, the other plankton is only detected at station 3 (0.4%). The BMLD has been only sampled once at ST1, and it is not depicted in the figure.

The composition of nanophytoplankton was: 44% of coccolithophores, 39% of dinoflagellates and 17% of other phytoplankton, while nano-diatoms haven’t been detected. Microphytoplankton composition was almost reversed with 52% of diatoms, 32% of dinoflagellates and 16% of other plankton.

The change of phytoplankton community along the transect is shown in Fig. 14. In case of both size fractions, several trends are visible. The oligotrophic stations have a lower amount of phytoplankton than the eutrophic stations. The coccolithophores dominate among the nanophytoplankton, while the diatoms dominate the microphytoplankton. In microphytoplankton, diatom abundance increases for an order of a magnitude with the transition to the eutrophic ocean (ST3 and ST4), while such change is not visible in nano-fraction of the diatom community. Dinoflagellate and coccolithophores abundance is more-less constant across the stations. On the nano-side of the community, “other” cells exhibit similar behavior to micro-diatoms, increasing their abundances at coastal stations.

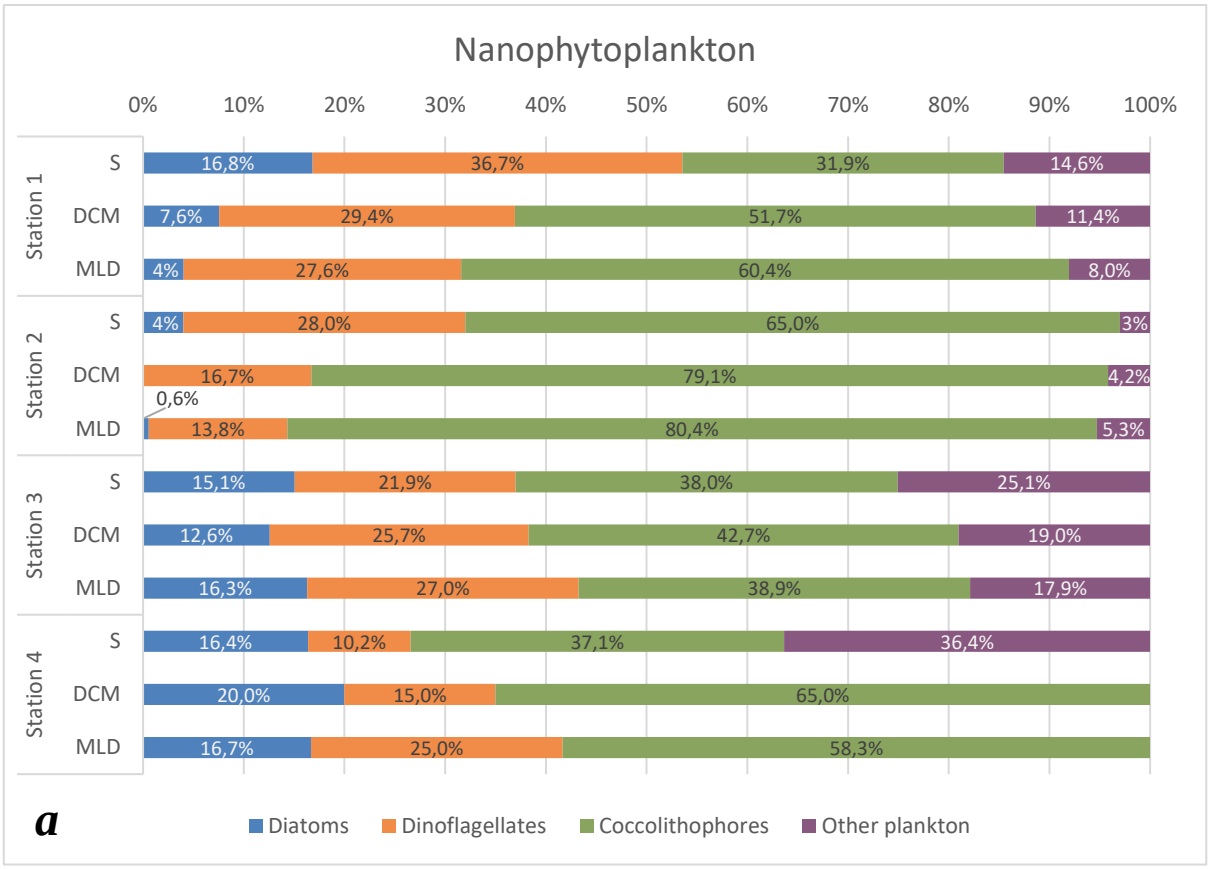

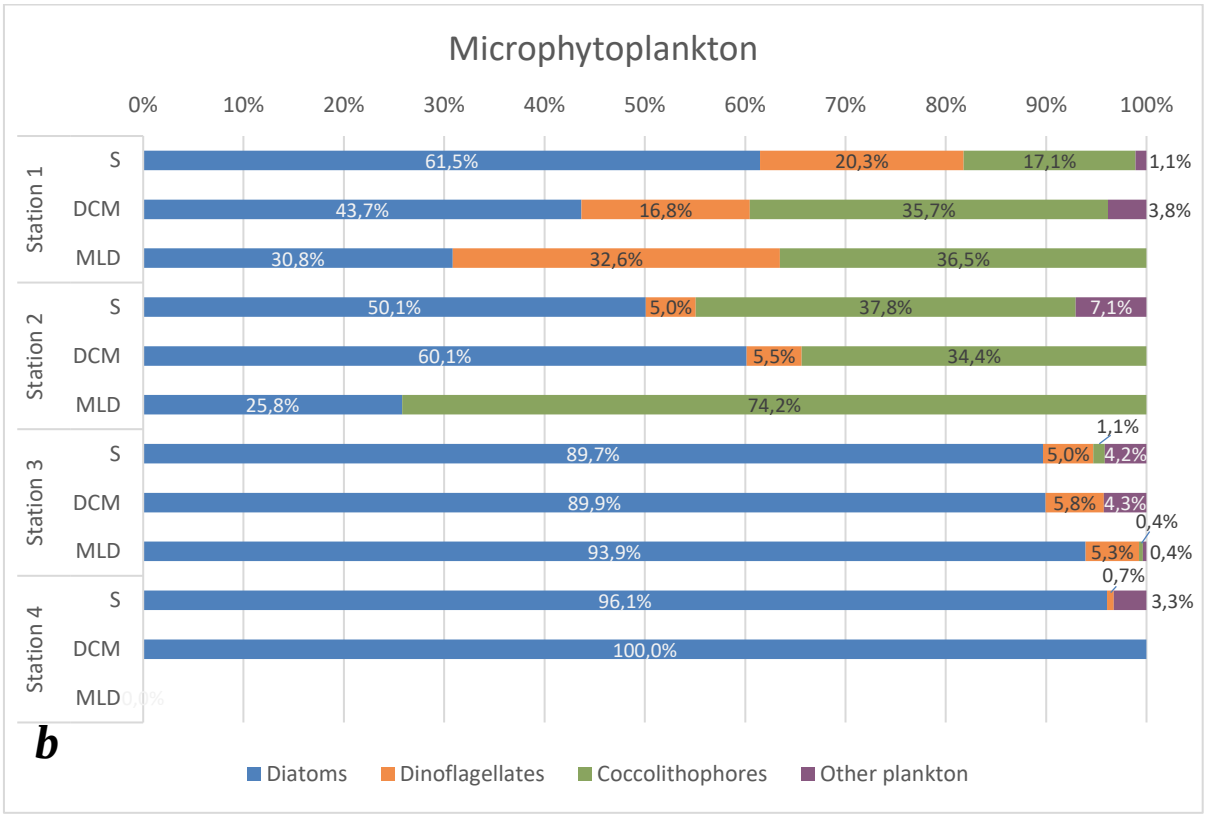

Fig. 13. Phytoplankton group abundance of a) nanophytoplankton and b) microphytoplankton at three investigated layers (surface, S; deep chlorophyll maximum, DCM; mixed layer depth, MLD) expressed as a percentage at four different trophic regions in the North Pacific, winter 2017.

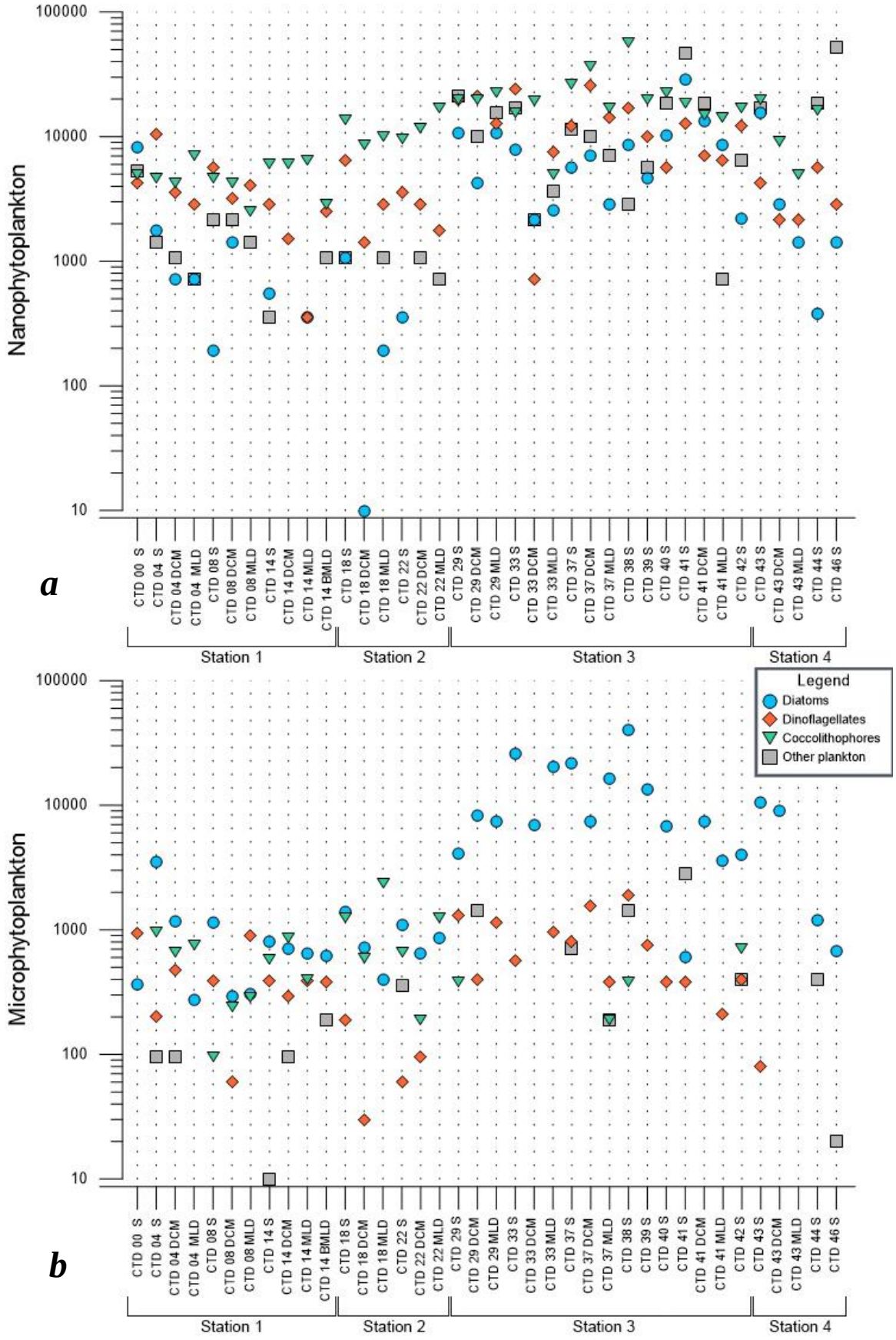

Fig. 14. Spatial phytoplankton distribution of a) nanophytoplankton and b) microphytoplankton over the investigated transect in North Pacific, winter 2017.

Table 3. List of taxa/groups determined by the Utermöhl method and recorded in net samples (20 μm). Taxa marked with an asterisk were present only in net samples.

Diatoms
Alveus marinus (Grunow) Kaczmarska & Fryxell
Amphora sp.
Asterolampra marylandica Ehrenberg *
Asteromphalus heptactis (Brébisson) Ralfs*
Asteromphalus sarcophagus Wallich
Bacteriastrum comosum Pavillard
Bacteriastrum furcatum Shadbolt
Bacteriastrum minus G.Karsten*
Bacteriastrum biconicum Pavillard*
Bacteriastrum spp.*
Caloneis robusta Cleve
Chaetoceros aequatorialis Cleve*
Chaetoceros affinis Lauder
Chaetoceros atlanticus var. neapolitanus (Schroeder) Hustedt
Chaetoceros coarctatus Lauder*
Chaetoceros concavicornis L.A.Mangin*
Chaetoceros constrictus Gran
Chaetoceros contortus F.Schütt
Chaetoceros convolutus Castracane
Chaetoceros curvisetus Cleve*
Chaetoceros dadayi Pavillard*
Chaetoceros danicus Cleve
Chaetoceros debilis Cleve
Chaetoceros decipiens Cleve
Chaetoceros didymus Ehrenberg*
Chaetoceros densus (Cleve) Cleve
Chaetoceros diversus Cleve*
Chaetoceros indicus Karsten*
Chaetoceros laciniosus F.Schütt
Chaetoceros lauderi/teres Ralfs ex Lauder/Cleve
Chaetoceros messanensis Castracane
Chaetoceros perpusillus Cleve
Chaetoceros peruvianus Brightwell
Chaetoceros pseudoaurivillii J.Ikari*
Chaetoceros pseudobrevi Pavillard
Chaetoceros pseudodichaeta J.Ikari
Chaetoceros pseudosymmetricus E.Steemann Nielsen*
Chaetoceros radicans F.Schütt
Chaetoceros simplex Ostenfeld
Chaetoceros socialis H.S.Lauder
Chaetoceros spp.*
Chaetoceros tetrastichon Cleve

(Continued on next page)

Diatoms

Climacodium biconcavum Cleve
Corethron hystrix Hensen
Coscinodiscus sp. 1*
Coscinodiscus sp. 2*
Cyclotella choctawhatcheeana Prasad
Cylindrotheca closterium (Ehrenberg) Reimann & J.C.Lewin *
Dactyliosolen fragilissimus (Bergon) Hasle
Dactyliosolen phuketensis (B.G.Sundström) G.R.Hasle
Detonula pumila (Castracane) Gran*
Ditylum brightwellii (T.West) Grunow*
Entomoneis sp.*
Eucampia cornuta (Cleve) Grunow*
Eucampia sp.
Fragilaria spp.
Fragilariopsis doliolus (Wallich) Medlin & P.A.Sims*
Gossliera tropica Schütt*
Guinardia delicatula (Cleve) Hasle
Guinardia flaccida (Castracane) H.Peragallo*
Gyrosigma sp.*
Haslea spp.*
Haslea wawrikae (Hustedt) R.Simonsen
Hemiaulus hauckii Grunow ex Van Heurck
Lennoxia faveolata H.A.Thomsen & K.R.Buck
Leptocylindrus danicus Cleve
Leptocylindrus mediterraneus (H.Peragallo) Hasle
Lioloma sp.*
Meuniera membranacea (Cleve) P.C.Silva
Navicula distans (W.Smith) Ralfs*
Navicula spp.
Neocalyptrella robusta (G.Norman ex Ralfs) Hernández-Becerril & Meave del Castillo
Neodelphineis indica (F.J.R.Taylor) Y.Tanimura
Nitzschia bicapitata Cleve
Nitzschia braarudii Hasle
Nitzschia longissima (Brébisson) Ralfs
Nitzschia sicula (Castracane) Hustedt
Nitzschia spp.
Odontella longicruris (Greville) M.A.Hoban*
Plagiotropis spp.
Planktoniella sol (G.C.Wallich) Schütt
Pleurosigma sp.
Podosira sp.*
Proboscia alata (Brightwell) Sundström
Pseudo-nitzschia delicatissima (Cleve) Heiden
Pseudo-nitzschia pseudodelicatissima (Hasle) Hasle

(Continued on next page)

Diatoms

Pseudo-nitzschia seriata (Cleve) H.Peragallo*
Pseudosolenia calcar-avis(Schultze) B.G.Sundström
Rhizosolenia castracanei H.Peragallo*
Rhizosolenia clevei Ostenfeld
Rhizosolenia clevei var. communis Sundström*
Rhizosolenia fallax B.G.Sundström*
Rhizosolenia formosa H.Peragallo*
Rhizosolenia hebetata f. semispina (Hensen) Gran
Rhizosolenia imbricata Brightwell
Rhizosolenia setigera f. pungens (A.Cleve) Brunel*
Skeletonema sp.
Striatella sp.*
Thalassionema bacillare (Heiden) Kolbe
Thalassionema frauenfeldii (Grunow) Tempère & Peragallo*
Thalassionema nitzschioides (Grunow) Mereschkowsky
Thalassionema spp.
Thalassiosira rotula Meunier*
Thalassiosira spp.
Thalassiothrix spp.
Tropidoneis sp.*
Other unidentified diatoms (<20µm)

Dinoflagellates

Ceratocorys sp.*
Chrysocromulina sp.
Dinophysis acuminata Claparède & Lachmann*
Dinophysis sp.*
Diplopsalis sp.*
Gonyaulax spp.*
Gymnodinium spp.
Gyrodinium spp.
Karenia sp.
Oxytoxum spp.*
Oxytoxum variabile Schiller
Oxytoxum sphaeroideum Stein
Oxytoxum milneri Murray & Whitting
Phalacroma rotundatum (Claparéde & Lachmann) Kofoid & Michener*
Phalacroma sp.*
Podolampas elegans Schütt*
Podolampas palmipes Stein*
Podolampas sp.*
Prorocentrum balticum (Lohmann) Loeblich*
Prorocentrum compressum (J.W.Bailey) Abé ex J.D.Dodge *
Prorocentrum micans Ehrenberg*
Prorocentrum rostratum Stein

(Continued on next page)

Dinoflagellates

Protoperidinium bipes (Paulsen) Balech*
Protoperidinium spp.
Scrippsiella sp.
Tripos arietinus (Cleve) F.Gómez*
Tripos azoricus (Cleve) F.Gómez*
Tripos carriensis (Gourret) F.Gómez*
Tripos concilians (Jørgenen) F.Gómez*
Tripos extensum (Gourret) F.Gómez*
Tripos furca (Ehrenberg) F.Gómez
Tripos fusus (Ehrenberg) F.Gómez
Tripos lineatum (Ehrenberg) F.Gómez*
Tripos macroceros (Ehrenberg) F.Gómez*
Tripos massiliensis (Gourret) F.Gómez
Tripos muelleri Bory*
Tripos pentagonum (Gourret) F.Gómez*
Tripos pulchellus (Schröder) F.Gómez*
Tripos spp.*
Tripos symmetricus (Pavillard) F.Gómez*
Tripos teres (Kofoid) F.Gómez
Other unidentified dinoflagellates (<20µm)

Coccolithophores

Acanthoica quattrospina Lohmann*
Calcidiscus leptoporus subsp. quadriperforatus (Kamptner) Geisen*
Calciosolenia brasiliensis (Lohmann) J.R.Young
Calciosolenia corsellii Malinverno*
Calciosolenia murrayi Gran
Calciosolenia spp.*
Calyptrosphaera galea Lecal-Schlauder*
Calyptrosphaera oblonga Lohmann
Calyptrosphaera sp.*
Coronosphaera mediterranea (Lohmann) Gaarder*
Discosphaera tubifera (Murray & Blackman) Ostenfeld
Emiliania huxleyi type A Young & Westbroek*
Emiliania huxleyi type B Young & Westbroek*
Florisphaera profunda Okada & Honjo*
Gephyrocapsa ericsonii McIntyre & Bé*
Gephyrocapsa ericsonii protohuxleyi type Cros & Fortuño*
Gephyrocapsa muellerae Bréhéret*
Helicosphaera carteri (Wallich) Kamptner*
Helicosphaera spp.*
Michaelsarsia adriatica (Schiller) Manton, Bremer & Oates
Michaelsarsia elegans Gran*
Ophiaster formosus Gran *
Ophiaster hydroideus (Lohmann) Lohmann*

(Continued on next page)

Coccolithophores

Ophiaster sp.
*Polycrater sp.**
Rhabdolithes claviger (G.Murray & Blackman) Voeltzkow*
Rhabdosphaera stylifera Lohmann
Rhabdosphaera xiphos (Deflandre & Fert) Norris*
Scyphosphaera apsteinii Lohmann*
Syracosphaera anthos (Lohman) Janin*
Syracosphaera bannockii (Borsetti & Cati) Cros*
Syracosphaera corolla J.Lecal*
Syracosphaera dilatata Jordan*
Syracosphaera halldalii HOL Gaarder ex R.W.Jordan & J.C.Green*
Syracosphaera hirsuta Kleijne & Cros*
Syracosphaera marginaporata M.Knappertsbusch*
Syracosphaera molischii type 2 Young*
Syracosphaera molischii Schiller HOL*
Syracosphaera nana (Kamptner) Okada & McIntyre*
Syracosphaera nodosa Kamptner*
Syracosphaera ossa type 2 Young*
Syracosphaera pulchra Lohmann
Syracosphaera rotula Okada & McIntyre*
Syracosphaera sp.*
Umbellosphaera irregularis Paasche*
Umbellosphaera tenuis (Kamptner) Paasche*
*Umbilicosphaera foliosa (Kamptner ex Kleijne) Geisen**
Umbilicosphaera hulburtiana Gaardner*
Other unidentified Coccolithophores (<20µm)

Cryptophyceae

Cyanobacteria

Richelia intracelularis J.A.Schmidt

Other autotrophs

Chrysocromulina sp.
Dictyocha fibula Ehrenberg
Eutreptia sp.
Meringosphaera mediterranea Lohmann
Micromonas sp.
Octactis speculum (Ehrenberg) F.H.Chang, J.M.Grieve & J.E.Sutherland
Phaeocystis sp.
Other unidentified phytoflagellates (<20µm)

Other heterotrophs

Ebria tripartita (J.Schumann) Lemmermann*
Globigerina spp.*
Radiolaria sp.*
Rhabdonellopsis sp.*
Other unidentified heterotrophs (<20 µm)

List of most abundant groups (abundance $>10^4$ cells L^{-1}, the frequency of occurrence >50 %) by stations are shown in Table 4. On the oligotrophic ST1 and ST2, similar abundance and phytoplankton community composition were recorded *Nitzchia bicapitata* was dominant diatom, recorded along the whole transect. Nano-scale dinoflagellate *Gyrodinium* sp. was dominant with the highest abundance at ST1, while it was absent at ST2, where the unidentified dinoflagellates dominated the dinoflagellate community. Also, nano-scale coccolithophores are abundant at both stations (ST1 and ST2). The largest taxa diversity and abundances, when compared to other station were recorded at the more eutrophic, coastal ST3, Specifically, undetermined coccolithophores and dinoflagellates reached highest numbers at this station, while the highest abundance of diatoms was recorded with *Pseudo-nitzschia pseudodelicatissima*. The CRP, represented as ST4, has the lowest phytoplankton diversity. Nevertheless, it has the largest abundance of cryptophytes than all other stations. Most abundant diatom taxon at this station is an undetermined nano-scale *Thalassiosira* species.

Table 4. Maximum abundances and frequencies for dominant species per station (frequency of appearance >50%). Blank cells are values that couldn't be determined because there were less than 40 cells in 1L.

	DOMINANT TAXA/GROUP	Station 1		Station 2		Station 3		Station 4	
		MAX	Fr	MAX	Fr	MAX	Fr	MAX	Fr
DIATOMS	*Chaetoceros affinis* (Fig. 18f)							4940	60
	Chaetoceros contortus (Fig. 17a)					2660	63		
	Chaetoceros convolutus (Fig. 17d, i)					5320	88		
	Chaetoceros debilis (Fig. 18a)					2660	50	6460	60
	Chaetoceros perpusillus (Fig. 16e)	380	60	380	75				
	Lennoxia faveolata (Fig. 17j)					14200	69		
	Leptocylindrus mediterraneus (Fig. 15i)	190	60	380	63				
	Nitzschia bicapitata (Fig. 18c, g)	710	50	1420	63	4260	56	7100	60
	Nitzschia braarudii (Fig. 15h)	190	50						
	Nitzschia longissima (Fig. 15e)	285	60			3800	94		
	Nitzschia sicula (Fig. 17b, k)					760	50		
	Nitzschia sp.	570	60						
	Nitzschia sp. 1			285	50				
	Proboscia alata (Fig. 17g)					380	50		
	Pseudo-nitzschia pseudodelicatissima (Fig. 17h)					22420	100		
	Rhizosolenia hebetata f. semispina (Fig. 17f)					1900	88		
	Rhizosolenia cleveii (Fig. 17e)					1140	75		
	Thalassionema nitzschioides (Fig. 17l, m)					1900	50		
	Thalassiosira sp. (<20 µm) (Fig. 18h, i)					8520	69	8520	60
	Unknown diatoms (<20 µm)	1420	50			10650	63		
DINOFLAGELLATES	*Gymnodinium* spp. (Fig. 15c)	380	50						
	Gyrodinium spp. (Fig. 15d)	710	60	190	63	1140	81		
	Gyrodinium spp. (<20 µm)	3550	50						
	Oxytoxum cf. variabile (<20 µm) (Fig. 17c)					2130	50		
	N.D. dinoflagellates (5-10 µm)	1420	70	2130	63	19880	50		
	N.D. dinoflagellates (10-20 µm)	2840	100	4615	100	19880	88	5680	100

(Continued on next page)

	DOMINANT TAXA/GROUP	Station 1		Station 2		Station 3		Station 4	
		MAX	Fr	MAX	Fr	MAX	Fr	MAX	Fr
COCCOLITHOPHORES	*Calciosolenia brasiliensis* (Fig. 16c)			380	63				
	Calciosolenia murrayi (Fig. 16a, b)	570	50	760	88				
	Discosphaera tubifera (Fig. 16f, g)	570	50	760	88				
	Michaelsarsia adriaticus (Fig. 15f, g)	190	60						
	Ophiaster sp. (Fig. 16d, h)			950	50				
	N.D. coccolitophorids (<5µm)	3550	90	7810	100	24140	88	7100	80
	N.D. coccolitophorids (5-10 µm) (Fig. 18d, e)	4615	100	8520	100	29820	100	12780	80
	N.D. coccolithophorids (10 - 20 µm)			3195	100				
OTHER	*Cryptophyceae* (Fig. 18b)	1065	70	1065	75	32660	100	48280	60
	Micromonas					2840	50		
	Phytoflagellates (Fig. 15a, b)	1065	80			8520	75		

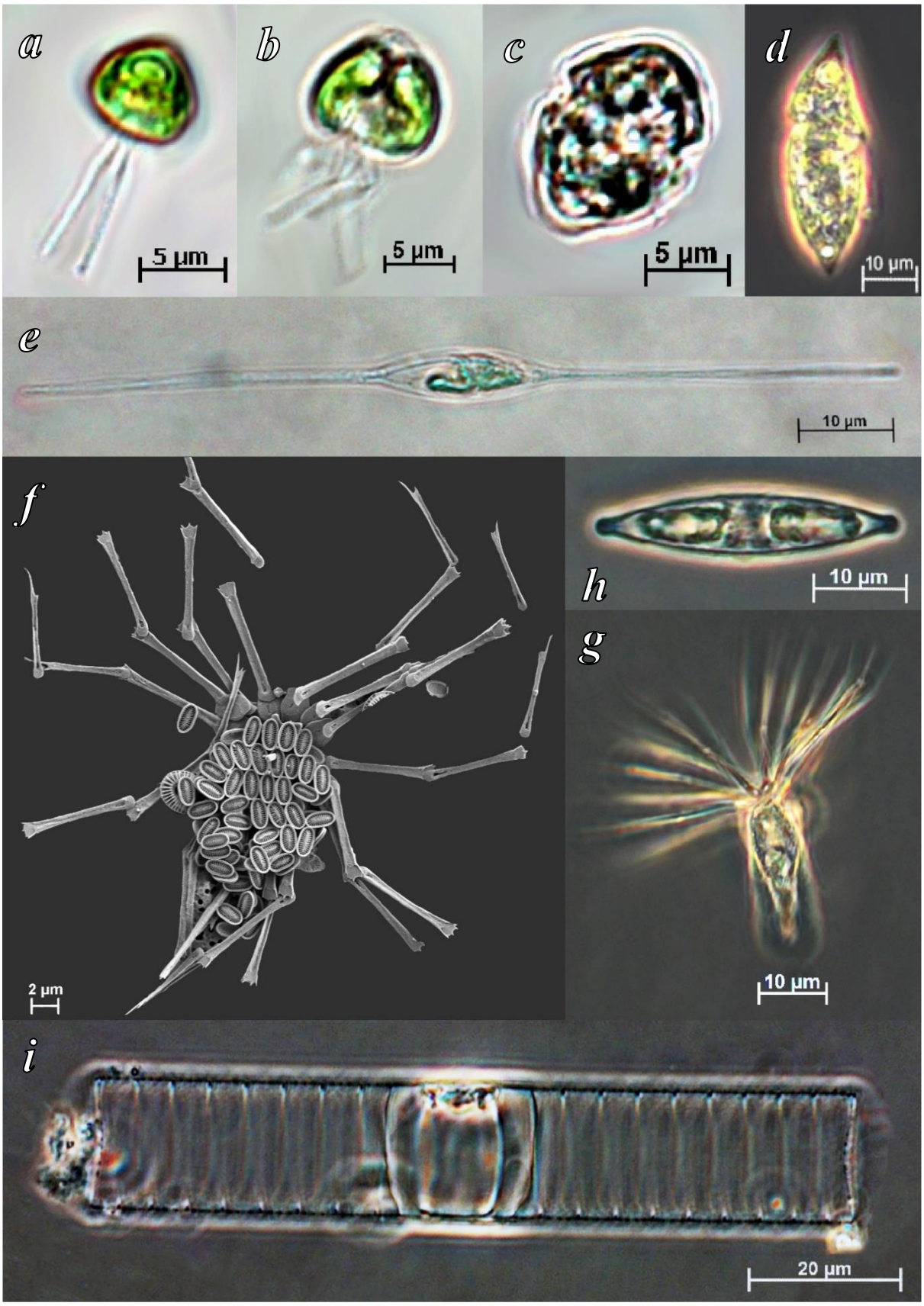

Fig. 15. Micrographs of dominant taxa found at ST1: a) & b) Phytoflagellates; c) *Gymnodinium* sp.; d) *Gyrodinium* sp.; e) *Nitzschia longissima*; f) & g) *Michaelsarsia adriaticus*; h) *Nitzschia braarudii*; i) *Leptocylindrus mediterraneus.*

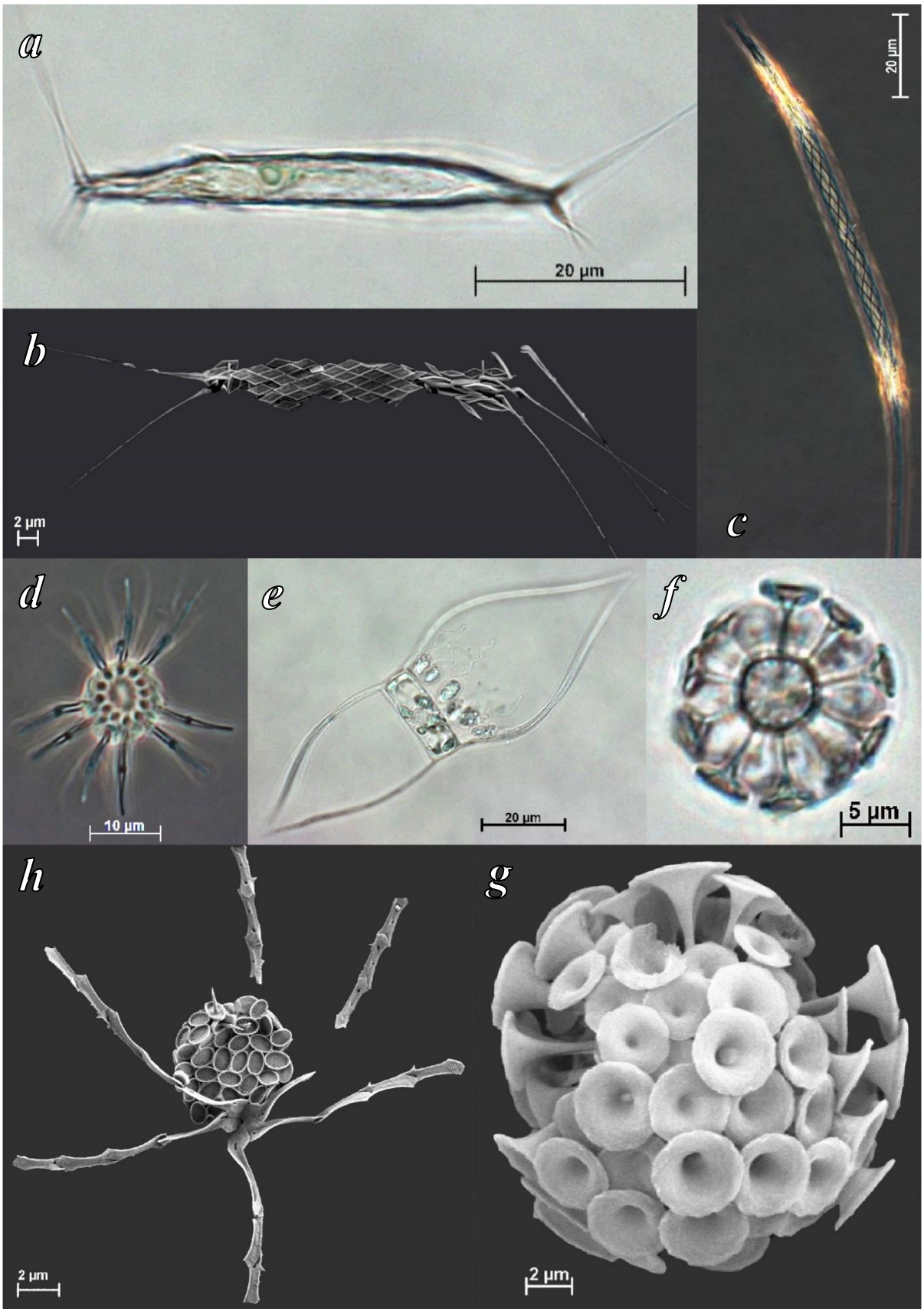

Fig. 16. Micrographs of dominant taxa found at ST2: a) & b) *Calciosolenia murrayi*; c) *Calciosolenia brasiliensis*; d) *Ophiaster* sp.; e) *Chaetoceros perpusillus*; f) & g) *Discosphaera tubifera*; h) *Ophiaster hydroideus.*

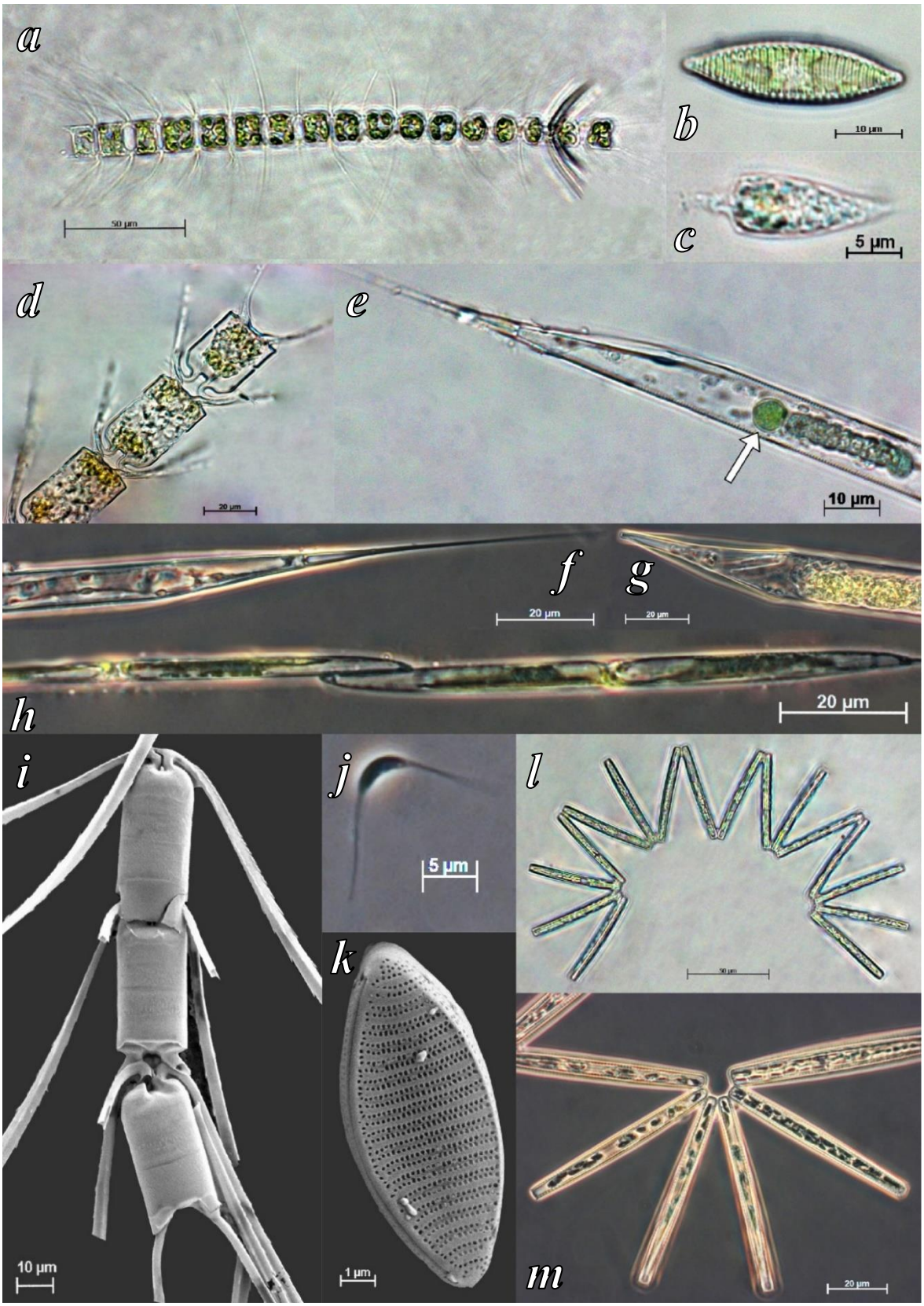

Fig. 17. Micrographs of dominant taxa found at ST3: a) *Chaetoceros contortus*; b) & k) *Nitzschia sicula*; c) *Oxytoxum variabile*; d) & i) *Chaetoceros convolutus*; e) *Rhizosolenia clevei* with *Richelia intracelularis* (arrow); f) *Rhizosolenia hebetata f. semispina* g) *Proboscia alata*; h) *Pseudo-nitzschia pseudodelicatissima;* j) *Lennoxia faveolata;* l) & m) *Thalassionema nitzschioides.*

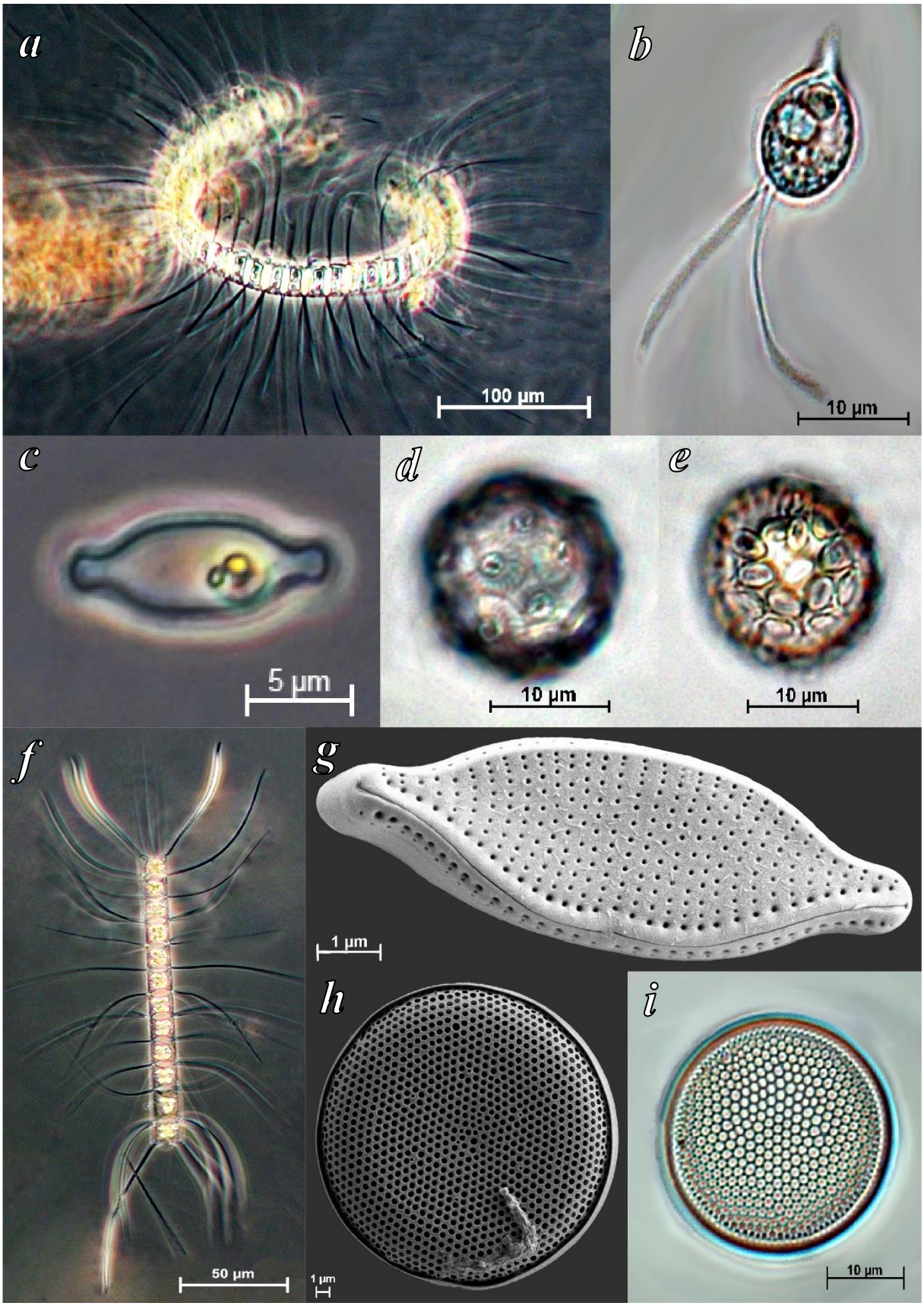

Fig. 18. Micrographs of dominant taxa found at ST4: a) *Chaetoceros debilis;* b) Cryptophyta; c) & g) *Nitzschia bicapitata*; d) & e) Coccolithophores; f) *Chaetoceros affinis*; h) & i) *Thalassiosira* sp.

SIMPER analysis was used to confirm the dominant species contributions by the station (Table 5). It shows very similar trends to one observed in Table 4, where the domination and large abundance of undetermined coccolithophores and dinoflagellates exceed at all stations. Specific taxon groups that are different between first two stations, is the major contribution of the phytoflagellates to the community at ST1, while at ST2 the *Rhizosolenia hebetata f. semispina* dominates. For the last two stations, cryptophytes are an important player at both coastal stations, while the difference between those two arises from the dominance (ST3) or absence (ST4) of *Pseudo-nitzschia pseudodelicatissima*.

Table 5. Similarities percentage (SIMPER) analysis for each taxon/group by stations. Blank cells are values that couldn't be determined because there were less than 40 cells in 1L. Taxa with similarity contribution <2 have been excluded from this table. Taxa/groups with average contribution higher than 1 are marked in bold. Abbreviations: average contribution/standard deviation (δ/σ), species contribution (Σδ%).

Station 1 taxa	**δ/σ**	**Σδ%**
Undetermined coccolithophorids (5-10 µm)	**8.47**	**15.61**
Undetermined dinoflagellates (10-20 µm)	**5.44**	**13.84**
Undetermined coccolithophorids (<5µm)	**1.79**	**12.09**
Phytoflagellates	**1.24**	**7.61**
Undetermined dinoflagellates (5-10 µm)	0.91	6.13
Cryptophyceae	0.91	5.75
Gymnodinium spp.	0.52	2.67
Gyrodinium spp. (<20 µm)	0.53	2.54
Gyrodinium spp.	0.65	2.50
Nitzschia bicapitata	0.52	2.50
Chaetoceros perpusillus	0.61	2.39
Michelsarsia adriatica	0.63	2.37
Unknown pennate diatoms (<20 µm)	0.53	2.36
Nitzschia longissima	0.67	2.33
Nitzschia sp.	0.67	2.06
Leptocylindrus mediterraneus	0.66	2.02

Station 2 taxa	**δ/σ**	**Σδ%**
Rhizosolenia hebetata f. semispina	**7.34**	**14.73**
Undetermined coccolithophorids (<5µm)	**6.72**	**14.02**
Undetermined dinoflagellates (10-20 µm)	**8.06**	**12.37**
Undetermined coccolitophorids (10-20 µm)	**7.43**	**12.20**
Discosphaera tubifera	**1.64**	**6.67**
Calciosolenia murrayi	**1.55**	**5.87**
Cryptophyceae	**1.02**	**5.60**
Undetermined dinoflagellates (5-10 µm)	0.72	4.30
Chaetoceros perpusillus	**1.03**	**3.22**
Calciosolenia brasiliensis	0.72	2.99
Nitzschia bicapitata	0.68	2.45
Gyrodinium spp.	0.70	2.05
Leptocylindrus mediterraneus	0.72	2.05

Station 3 taxa	**δ/σ**	**Σδ%**
Undetermined coccolithophorids (5-10 µm)	**6.40**	**10.06**
Cryptophyceae	**4.97**	**9.02**
Undetermined coccolithophorids (<5µm)	**1.67**	**7.81**
Pseudo-nitzschia pseudodelicatissima	**6.14**	**7.62**
Undetermined dinoflagellates (10-20 µm)	**1.64**	**7.41**
Nitzschia longissima	**2.17**	**5.41**
Chaetoceros convolutus	**1.61**	**4.93**
Phytoflagellates	**1.06**	**4.63**
***Gyrodinium* spp.**	**1.26**	**4.02**
Lennoxia faveolata	0.88	3.84
Thalassiosira (<20 µm)	0.88	3.83
Rhizosolenia hebetata f. semispina	**1.60**	**3.52**
Unknown pennate diatoms (<20 µm)	0.75	3.16
Rhizosolenia cleveii	**1.03**	**2.68**
Chateoceros contortus	0.74	2.21
Nitzschia bicapitata	0.65	2.10

Station 4 taxa	**δ/σ**	**Σδ%**
Undetermined dinoflagellates (10-20 µm)	**2.74**	**28.89**
Undetermined coccolithophorids (<5µm)	**1.03**	**17.23**
Undetermined coccolithophorids (5-10 µm)	**1.05**	**15.73**
Cryptophyceae	0.57	8.81
Thalassiosira (<20 µm)	0.58	6.23
Chaetoceros affinis	0.60	5.13
Nitzschia bicapitata	0.61	5.03
Chaetoceros debilis	0.61	4.86

Testing the similarity between samples of phytoplankton abundance was performed using hierarchical clustering which showed gradual separation of oligotrophic stations from the coastal station and the CRP (Fig. 18). ST1 and ST2 exhibit expected similarity at around 40% for the oligotrophic region, while the CTD 08 S and CTD 14 BMLD stand out more, having greater similarity ST3 and ST4 samples, respectively. Majority of the ST3 samples have clustered together with similarity around 50%. The ST4 samples have clustered between ST2 and ST3, with similarity being closer to ST2, with the exception of sample CTD 46. The surface sample of CTD 46 stands out the most with the smallest similarity of 20% between all other samples.

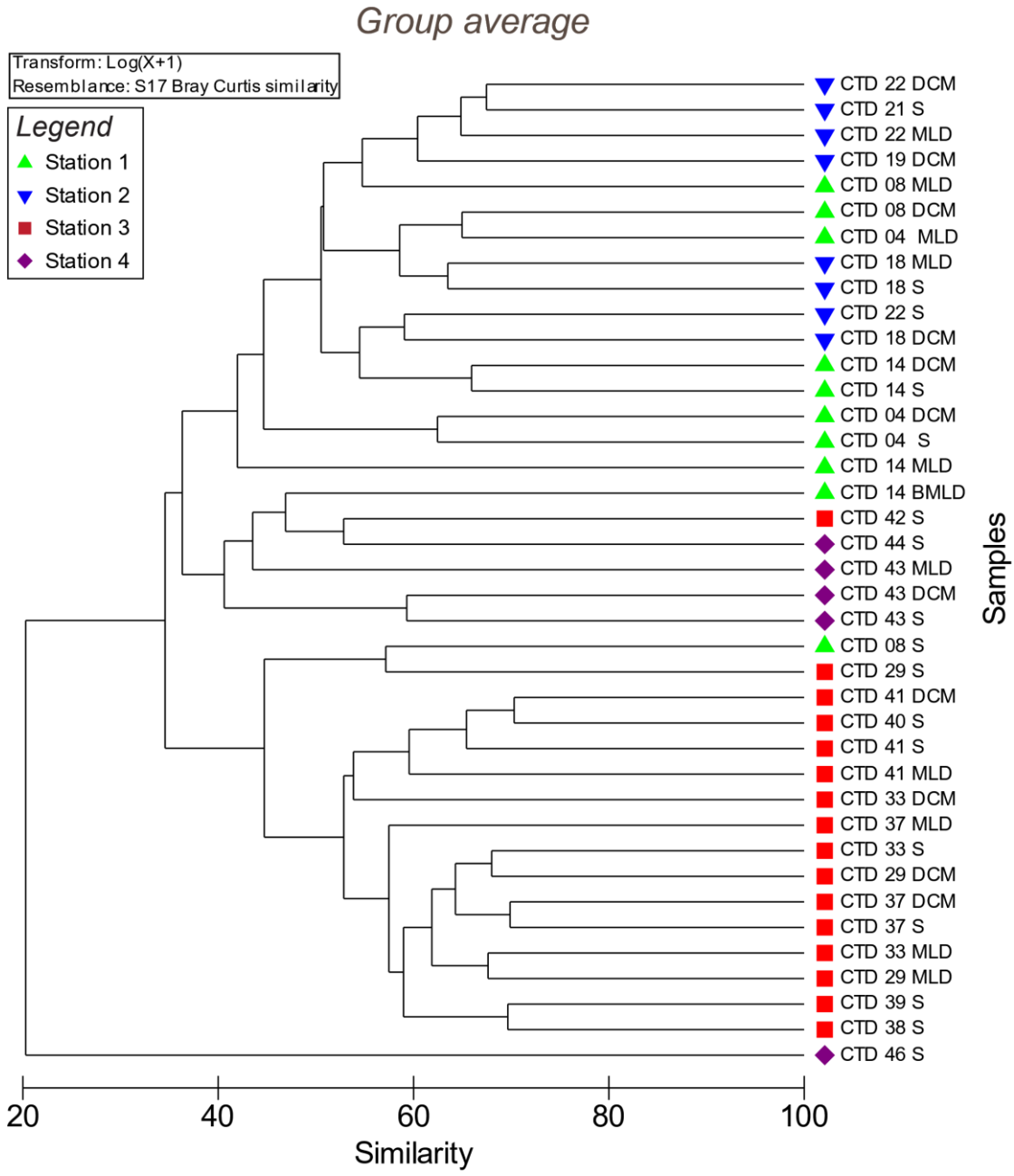

Fig. 18. The similarity of stations based on phytoplankton abundance using hierarchical cluster analysis. Abbreviations: S – surface, DCM – deep chlorophyll maximum, MLD – mixed layer depth, BMLD - bellow mixed layer depth.

For additional confirmation, the non-metric dimensional scaling was used to calculate similarity and differences between the samples of phytoplankton abundance and pigment concentrations per each station (Fig. 19). Analysis of phytoplankton abundance showed four distinct environments, separated at the similarity of 40%. The green cluster represents oligotrophic waters of ST1 and ST2, while red one contains samples from California's coastal waters, the ST3. Same separation of ST4 samples in two different clusters from previous analyses is present again. Majority of ST4 samples have separated into a transitional environment marked in purple. Its similarity has been positioned between the oligotrophic and coastal stations, whereas the CTD 46 S, marked in grey, has distanced furthest from resto of the clusters.

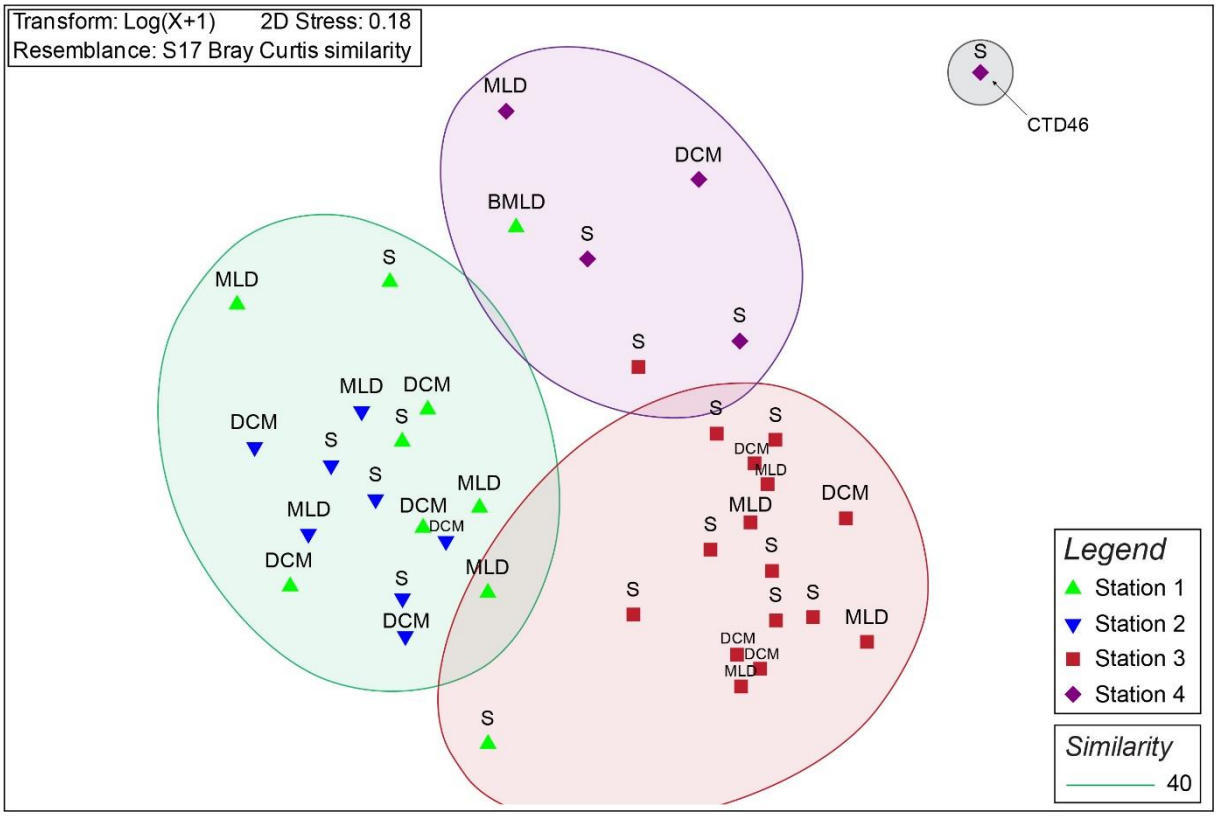

Fig. 19. Non-metric multidimensional scaling (nMDS) ordination plot of Bray–Curtis community similarities between investigated stations based on phytoplankton abundances. Abbreviations: S – surface, DCM – deep chlorophyll maximum, MLD – mixed layer depth, BMLD - bellow mixed layer depth.

To reinforce previous results, the principal component analysis has been used to correlate variables between phytoplankton samples and stations (Fig. 20). The PC analysis aims to reduce a large number of variables into a smaller number of major components, those components whose inherent values were less than 1.00 are considered trivial. The first two principal components that tend to explain the largest amount of variation between samples of phytoplankton abundance have a relatively low cumulative variation of 32.8%. The cumulative variation represents the percentage of differences between sampled stations based on main components, and by combining the axes, the cumulative variation rises, explain the higher percentage of variations. The eigenvalues of PC1 and PC2 axes are 101 and 41, respectively. Eigenvalues represent the amount of variance that refers to a particular component (Table 8).

According to the PC analysis, similar separation of the four stations present in previous multivariant analyses is also visible here with significant overlapping of the cluster. Low variability between samples of the oligotrophic ST1 and ST2 clustered them very tightly together, while coastal ST3 samples are more widely dispersed pointing to a higher variability. Once again, the station CTD 46 from the ST4 has separated into its own cluster, colored in grey. Each cluster represents similarity of 40% between the samples.

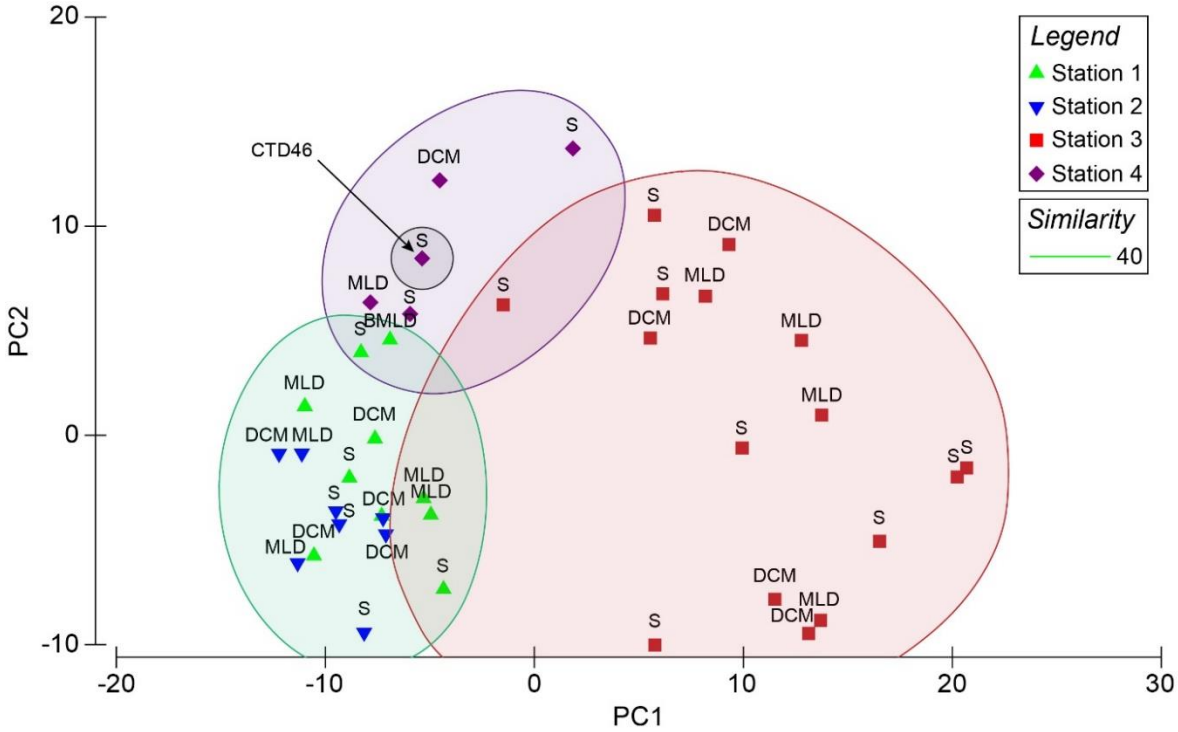

Fig. 20. Distribution of phytoplankton abundance samples per stations using PCA loadings of the first two principal components with a cumulative variation of 32.8%. Abbreviations: S – surface, DCM – deep chlorophyll maximum, MLD – mixed layer depth, BMLD - bellow mixed layer depth.

4.2. Pigment concentrations analyses

A similar pattern was recorded with pigment concentrations along the investigated transect (Fig. 21). Clear separation between the open and coastal ocean is visible between oligotrophic ST1 and ST2 where Chl *a* concentration didn't exceed 0.4 µg, and eutrophic ST3 and ST4, where Chl *a* concentrations were more variable and higher, reaching maximum at station CTD 41 (DCM layer, 1.5 µg L^{-1}). Eutrophic stations exhibited higher variability in chlorophyll *a* concentrations, both spatially and vertically.

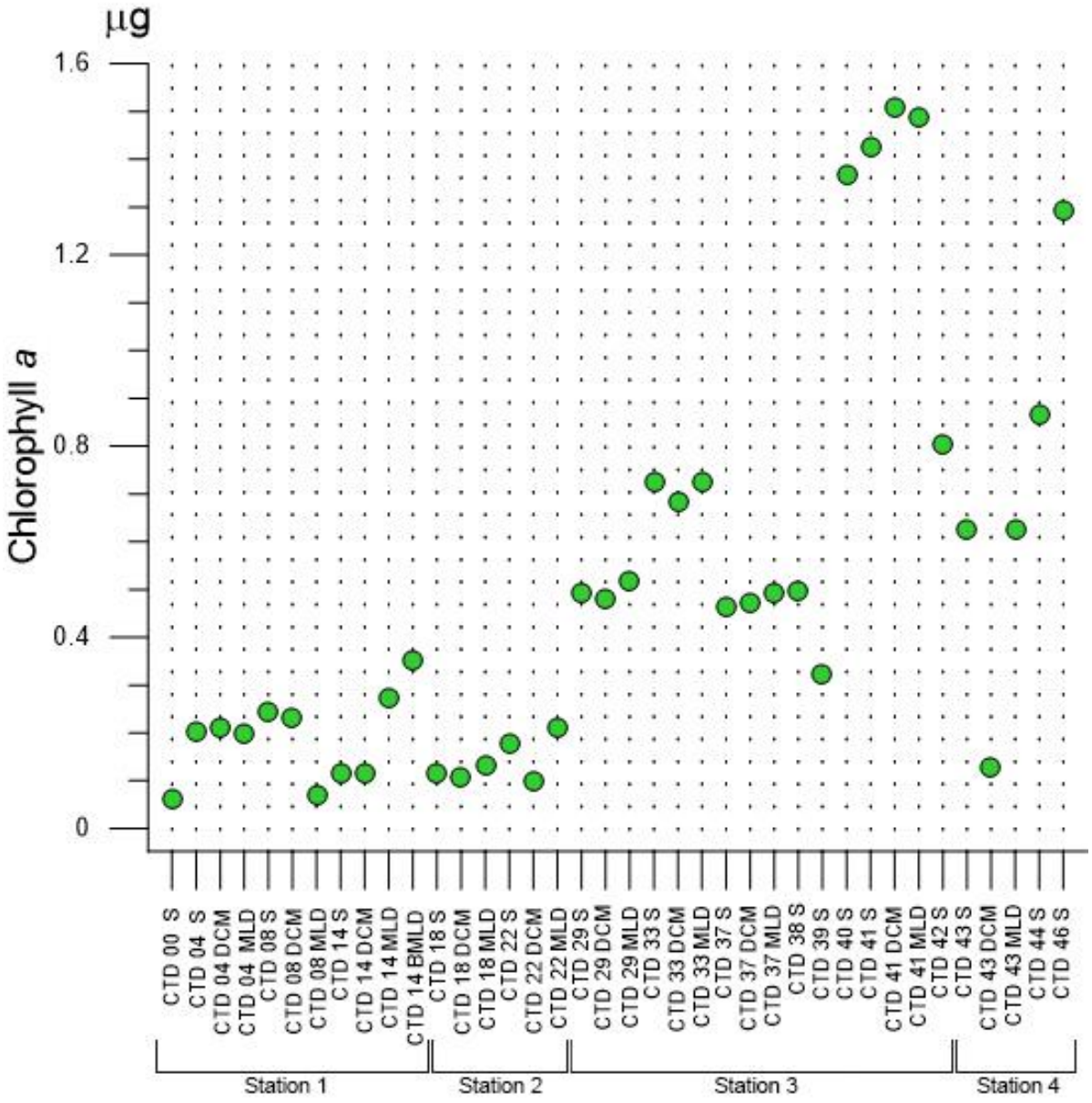

Fig. 21. Spatial distribution of chlorophyll *a* concentration along the transect for each CTD cast in the North Pacific, winter 2017.

Total Chl *a* concentration varies differently at every stations and depth with a high increase in average concentration at the eutrophic ST3 and ST4 (Fig. 20). While total Chl *a* concentration was recorded constant with depth, at the ST1, at ST2 a decrease with depth was recorded with the lowest average concentration being 0.03 µg at MLD. With ship's entrance into the eutrophic region, total Chl *a* concentrations rise and stayed constant with depth at ST3. Biggest variation in concentration was recorded at ST4, where average surface concentration was highest recorded (0.93 µg).

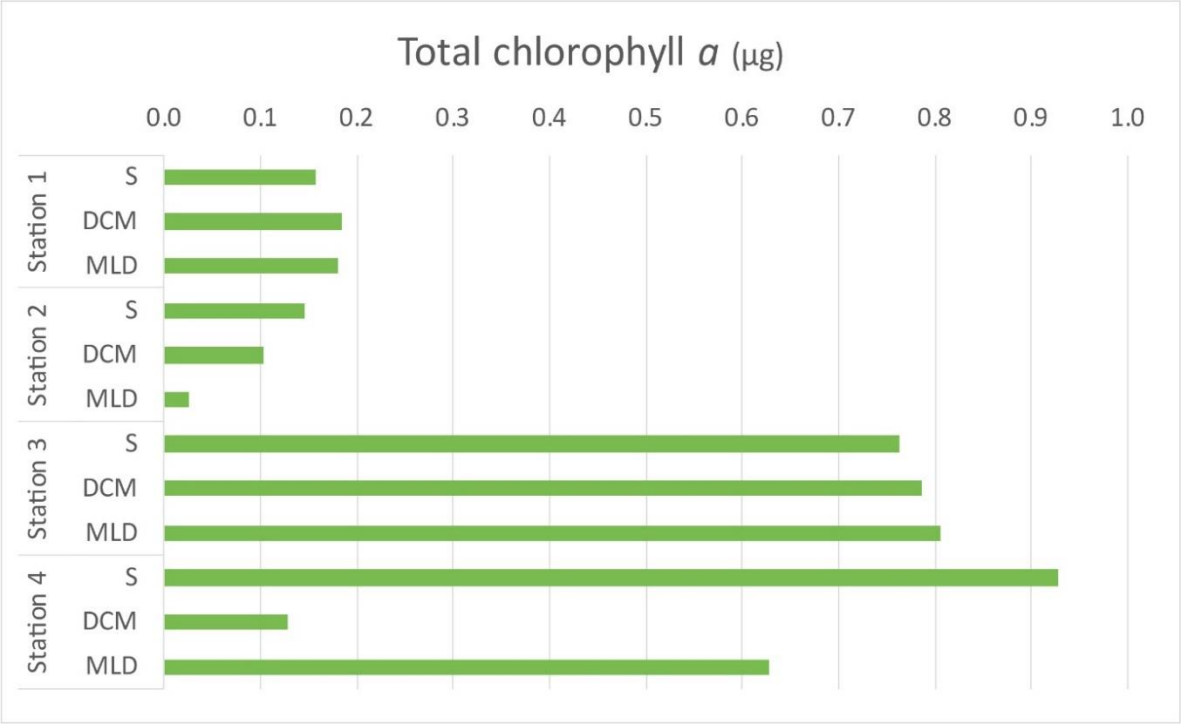

Fig. 22. Averaged Chl *a* concentrations at three investigated layers (surface, S; deep chlorophyll maximum, DCM; mixed layer depth, MLD) at four trophic regions in the North Pacific, winter 2017.

Only the change of signature pigments that can be used as biomarkers with depth has been depicted in Fig. 23. Oligotrophic stations exhibit lower general concentrations of pigments due to a lower number of cells with the differences being divinyl chlorophyll *a* and zeaxanthin, the biomarkers for *Prochlorococcus* and *Synechococcus*, respectively. DVChl *a* and zeaxanthin concentrations were highest at ST1 and ST2, implying the cyanobacteria domination I the oligotrophic region. Entering into eutrophic waters, the concentration of 19HF and fucoxanthin increase dramatically, implying the shift in the community to coccolithophores (19HF) and diatoms (fucoxanthin). The variation with depth is negligible at ST3, while concentration of all pigments drop at the DCM layer of ST4. Alloxanthin and peridinin and prasinoxanthin have a more significant contribution only in the eutrophic waters. The concentration of peridinin and prasinoxanthin varies slightly with depth change, with the exception of ST4 DCM, whereas the concentration of alloxanthin rises slightly at ST3 with the highest concentration being at the surface of ST4. The vertical distribution of all pigment concentration indicates a well-mixed euphotic layer.

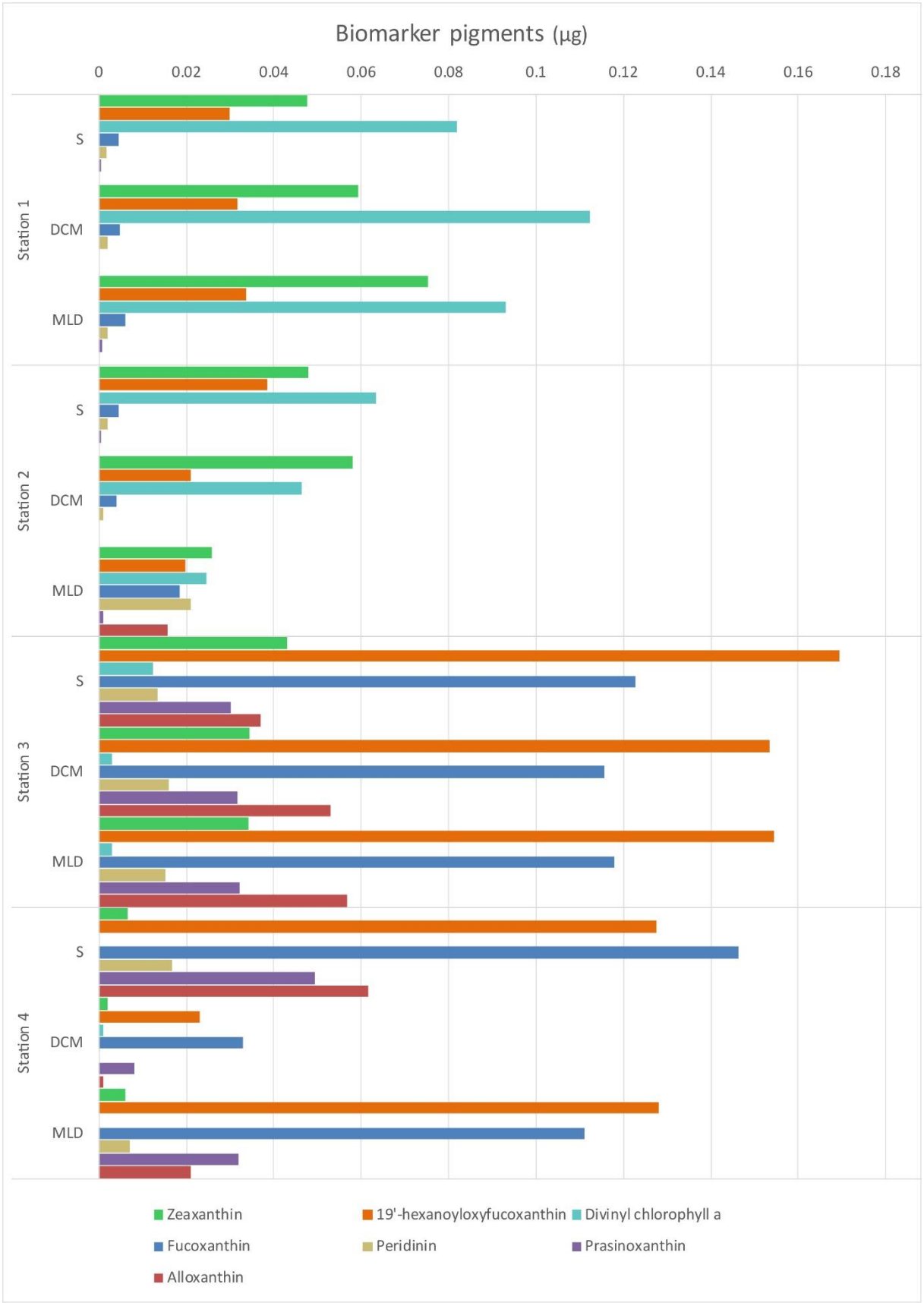

Fig. 23. Signature pigment concentrations at three investigated layers (surface, S; deep chlorophyll maximum, DCM; mixed layer depth, MLD) at four trophic regions in the North Pacific, winter 2017.

The average concentration of major pigments, for each of the stations, is shown in Table 6. Pigments derived from chlorophylls have by far largest concentrations at all stations, especially components derived from chlorophyll *a*. Oligotrophic stations have the lowest concentrations of all pigments except the zeaxanthin, and DVChl *a* and *b*. Carotenes are constant across all stations. Concentrations of all other pigments exhibit a substantial increase at two eutrophic stations. Alloxanthin has been detected only on ST3 and ST4. Lutein has not been detected at ST2. Most significant increase by a single primary pigment has fucoxanthin, from ST 1 and ST2. Lastly, tertiary pigments do not exhibit increase as large as in previous classes of pigments, but more prominent concentrations changes are those of violaxanthin and prasinoxanthin.

Table 6. Pigment concentration (in µg/L) averaged by stations.

	SAMPLE NAME	Station 1	Station 2	Station 3	Station 4
PRIMARY	Total chlorophyll *a*[1]	0.189	0.141	0.768	0.743
	Total chlorophyll *b*[2]	0.050	0.026	0.098	0.128
	Total chlorophyll *c*[3]	0.037	0.034	0.174	0.169
	Carotenes	0.023	0.013	0.034	0.029
	19'-butanoyloxyfucoxanthin	0.023	0.023	0.047	0.051
	19'-hexanoyloxyfucoxanthin	0.037	0.036	0.149	0.149
	Alloxanthin			0.047	0.038
	Diadinoxanthin	0.008	0.007	0.062	0.033
	Diatoxanthin	0.001	0.001	0.006	0.002
	Fucoxanthin	0.006	0.005	0.122	0.110
	Peridinin	0.002	0.002	0.014	0.016
	Zeaxanthin	0.064	0.045	0.037	0.010
SECONDARY	Monovinyl chlorophyll *a*	0.088	0.079	0.742	0.727
	Divinyl chlorophyll *a*	0.100	0.061	0.012	0.013
	Chlorophyllide *a*	0.001	0.001	0.020	0.011
	Monovinyl chlorophyll *b*	0.019	0.012	0.097	0.128
	Divinyl chlorophyll *b*	0.032	0.014	0.004	
	Chlorophyll c_1 + chlorophyll c_2 + MGDVP[4]	0.017	0.015	0.099	0.097
	Chlorophyll c_3	0.020	0.019	0.075	0.072
TERTIARY	Lutein	0.001		0.003	0.004
	Neoxanthin	0.001	0.001	0.011	0.014
	Violaxanthin	0.001	0.001	0.023	0.018
	Total pheophytin *a*	0.002	0.001	0.007	0.007
	Total pheophorbide *a*		0.001	0.017	0.020
	Prasinoxanthin	0.001	0.001	0.032	0.036

[1]DVChl *a* + MVChl *a* + Chlorophyllide *a* + Chl *a* allomers + Chl *a* epimers; [2]DVChl *b* + MVChl *b* + Chl *b* epimers

[3]Chl c_1 + Chl c_2 + Chl c_3 + MGDVP; [4]Mg-2,4-divinyl pheoporphyrin a_5 monomethyl ester

Along-transect variability in pigment composition and concentration is shown in Fig. 24. The variability of primary pigments was similar to that of total Chl *a* depicted in Fig. 19, with lower concentrations found on oligotrophic stations. Chl *b* and zeaxanthin, had highest concentrations at oligotrophic stations. ST3 shows two patterns of increase of concentrations. The first increase is visible from CTD 29 to CTD 39 with the first significant appearance of diadinoxanthin and alloxanthin. The second wave is peaking from CTD 40 to 42, with a significant increase of all pigments, especially total Chl *c*, fucoxanthin and 19'-hexanoyloxyfucoxanthin. The latter shows the highest peak of 0.34 µg at CTD 42 surface layer, closely followed by total Chl *c*. ST4 again exhibited a sudden drop of concentrations and gradual increase towards the end of the transect. Zeaxanthin gradually decreased towards the end of the transect.

Spatial distribution of secondary and tertiary pigment concentration showed three clearly distinct environments (Fig. 21). First one encompasses oligotrophic stations just like the previous analyses. Only divinyl chlorophylls a and b are present in higher concentrations varying from trace amounts to 0.15 µg (CTD 14 BMLD). Concentrations of both DVChl's fall substantially at ST3 and ST4 while concentrations of all other secondary and tertiary pigments rise. The highest increase was recorded in prasinoxanthin concentration followed in descending order by violaxanthin, total pheophorbide *a*, neoxanthin, total pheophytin *a* and lutein. CTD 39 S showed similar situation like oligotrophic stations, with small concentrations of all pigments except total Chl *b*.

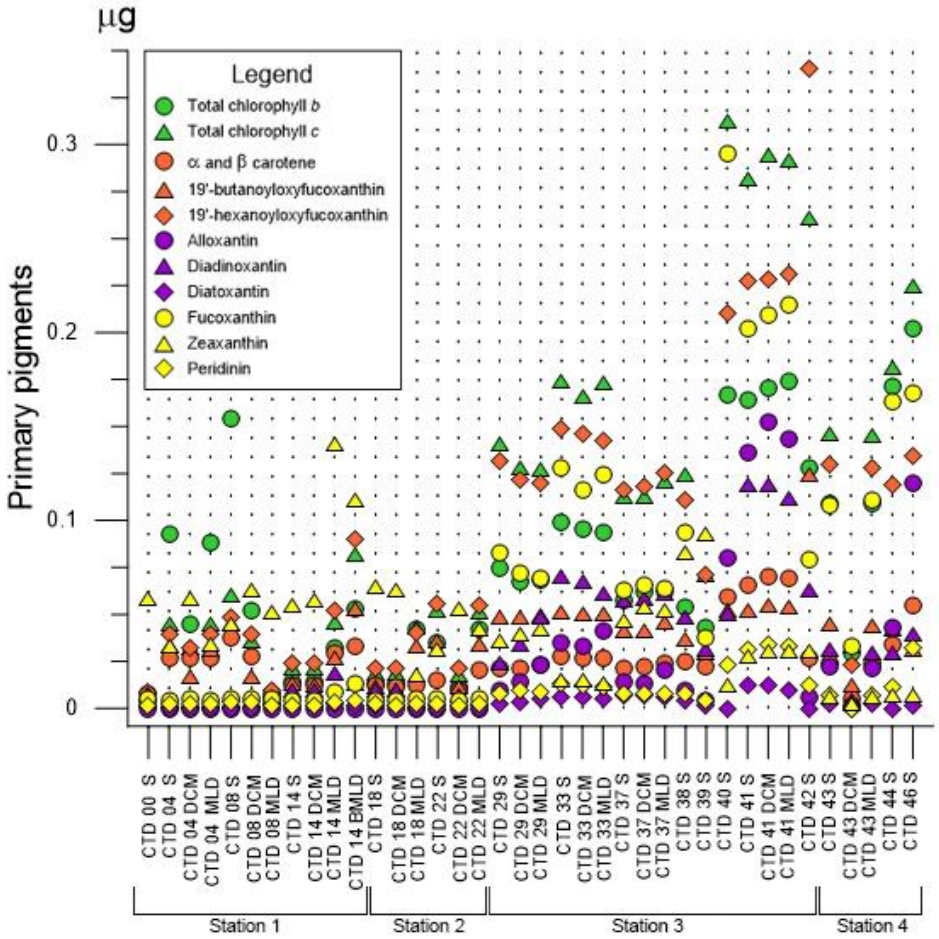

Fig. 24. Spatial primary pigment concentrations along the transect.

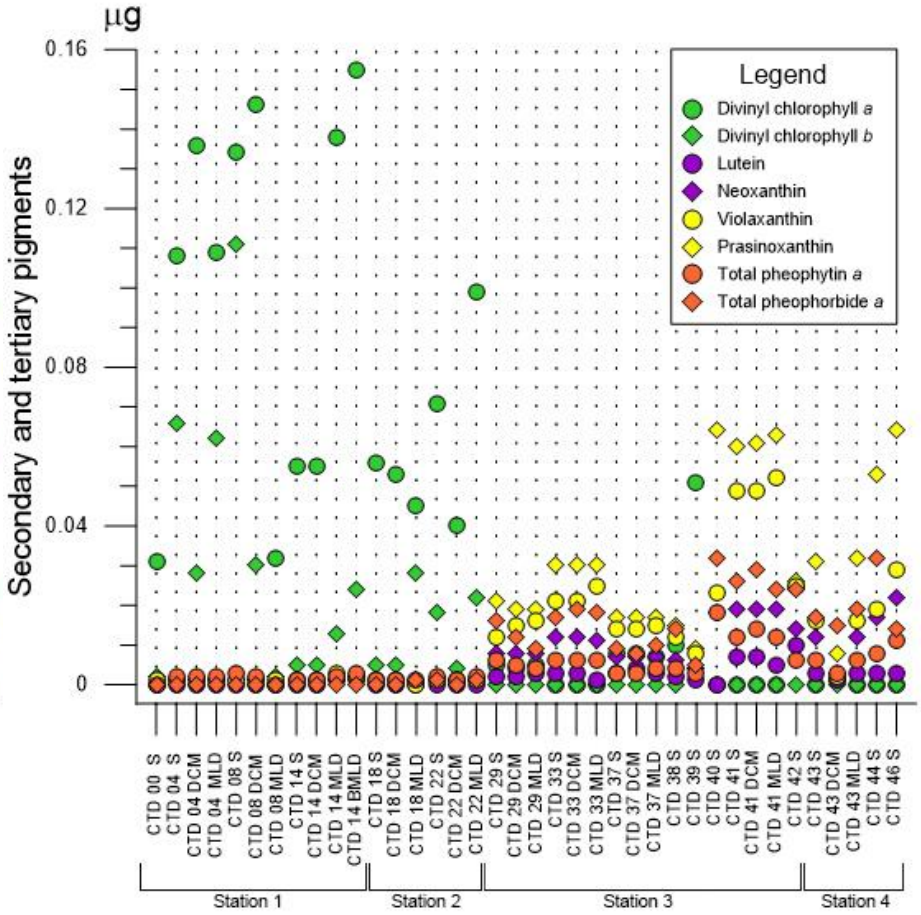

Fig. 25. Spatial secondary and tertiary pigment concentrations along the transect.

To determine the contribution of each pigment and along the transect, SIMPER analysis was calculated (Table 7). As it would be expected, total Chl *a* was the most dominant pigment at all stations. The pigment composition of ST1 and ST2 had a very similar order of contribution. The DVChl *a* had second highest contribution at ST1 (14.54%), followed by MVChl *a* with the similarity percentage 13.05%. The order of their contribution at ST2 was reversed, with MVChl *a* contributing with 15.56% and DVChl *a* 11.96%. Order of contribution for the pigments that followed was the same at the both ST1 and ST2, in the following order: zeaxanthin, 19'-hexanoyloxyfucoxanthin, total chlorophyll *c* and total chlorophyll *b*. Total Chl *a* and MVChl *a* also had the highest similarity percentage at the ST3 and ST4 (25.87% and 24.60%, 26.17% and 25.48%, respectively). The total Chl *c* followed at the both ST3 and ST4 with 7.38% and 7.44% of similarity, respectively. The order of contribution diverges afterward, with 19'-hexanoyloxyfucoxanthin and fucoxanthin following at the ST3 while at the ST4, the total Chl *b* and MVChl *b* had highest similarity percentage below the total Chl *c*. SIMPER has not taken tertiary pigments into account due to their low concentrations.

Table 7. Similarities percentage (SIMPER) analysis for each pigment by stations. Abbreviations: δ/σ = average contribution/standard deviation, Σδ% = species contribution, MGDVP = Mg-2,4-divinyl pheoporphyrin a_5 monomethyl ester.

Station 1 Pigments	**δ/σ**	**Σδ%**
Total chlorophyll *a*	3.73	27.12
Divinyl chlorophyll *a*	2.88	14.54
Monovinyl chlorophyll *a*	4.25	13.05
Zeaxanthin	2.03	11.43
19'-hexanoyloxyfucoxanthin	2.94	5.08
Total chlorophyll *c*	2.68	4.91
Total chlorophyll *b*	1.23	4.56
Carotenes	3.02	3.47
19'-butanoyloxyfucoxanthin	2.17	2.82
Chlorophyll c_3	2.48	2.57
Divinyl chlorophyll *b*	0.93	2.38

Station 2 Pigments	**δ/σ**	**Σδ%**
Total chlorophyll *a*	7.88	27.39
Monovinyl chlorophyll *a*	6.40	15.56
Divinyl chlorophyll *a*	5.98	11.96
Zeaxanthin	1.70	8.95
19'-hexanoyloxyfucoxanthin	4.07	6.30
Total chlorophyll *c*	3.32	5.81
Total chlorophyll *b*	2.30	4.11
19'-butanoyloxyfucoxanthin	2.27	3.62
Chlorophyll c_3	2.70	3.14
Carotenes	7.41	2.86
Chlorophyll c_1 + chlorophyll c_2 + MGDVP	4.47	2.69

Station 3 Pigments	**δ/σ**	**Σδ%**
Total chlorophyll *a*	5.26	25.87
Monovinyl chlorophyll *a*	4.88	24.60
Total chlorophyll *c*	4.86	7.38
19'-hexanoyloxyfucoxanthin	4.89	7.00
Fucoxanthin	3.86	4.63
Total chlorophyll *b*	4.65	4.11
Monovinyl chlorophyll *b*	4.45	4.07
Chlorophyll c_1 + chlorophyll c_2 + MGDVP	4.36	4.06
Chlorophyll *c3*	4.93	3.54
Diadinoxanthin	3.09	2.64
19'-butanoyloxyfucoxanthin	4.62	2.60

Station 4 Pigments	**δ/σ**	**Σδ%**
Total chlorophyll *a*	2.31	26.17
Monovinyl chlorophyll *a*	2.33	25.48
Total chlorophyll *c*	2.18	7.44
Total chlorophyll *b*	2.42	5.78
Monovinyl chlorophyll *b*	2.42	5.78
19'-hexanoyloxyfucoxanthin	2.05	5.56
Fucoxanthin	2.70	5.17
Chlorophyll c_1 + chlorophyll c_2 + MGDVP	1.94	4.20
Chlorophyll c_3	2.55	3.28
19'-butanoyloxyfucoxanthin	2.63	1.95

The multivariant analysis used for abundance was to distinguish environments based on pigment concentrations. The hierarchical clustering clearly separated the two major environments at 50% of similarity, corresponding to oligotrophic (ST1 and ST2) and eutrophic (ST3 and ST4) waters (Fig. 26). At higher similarity percentage the ST3 samples cluster into subgroups, with the exception of CTD 39 S and CTD 43 MLD, which have clustered into the oligotrophic group. ST4 samples clustered between the ST2 and ST3, except the CTD 46 S being less similar to them. The results correspond to the trend recorded with abundancy analysis.

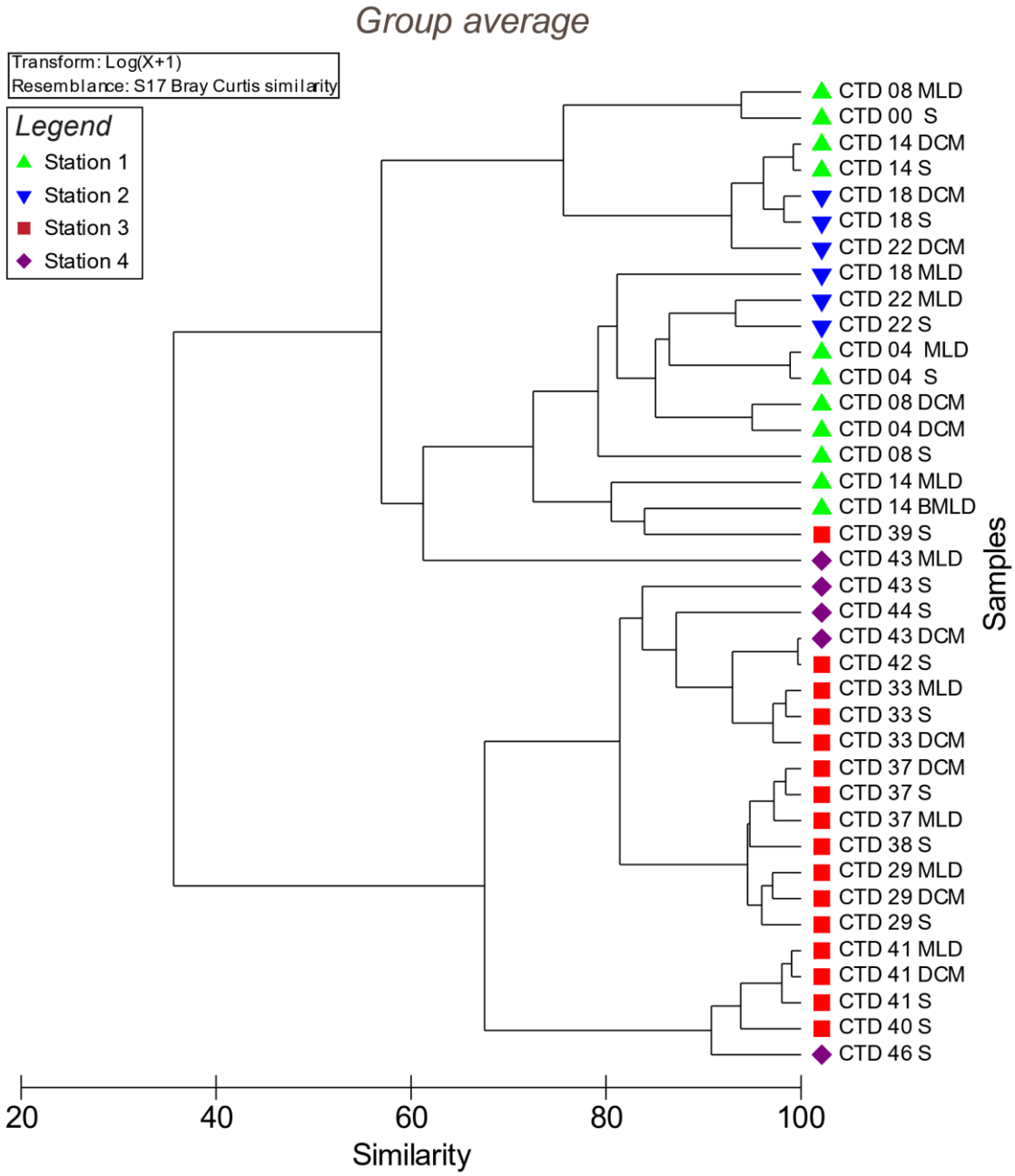

Fig. 26. The similarity of stations based on pigment concentrations using hierarchical cluster analysis. Abbreviations: S – surface, DCM – deep chlorophyll maximum, MLD – mixed layer depth, BMLD - bellow mixed layer depth.

Pigment concentrations showed a similar trend, elucidating two with only two major trophic states (Figs. 27–28). The two states correspond to oligotrophic (green cluster) and eutrophic (red cluster) waters, with the similarity of 40%. Furthermore, the CTD 39 S and CTD 43 MLD have distanced from their parent stations with a higher resemblance to the oligotrophic cluster.

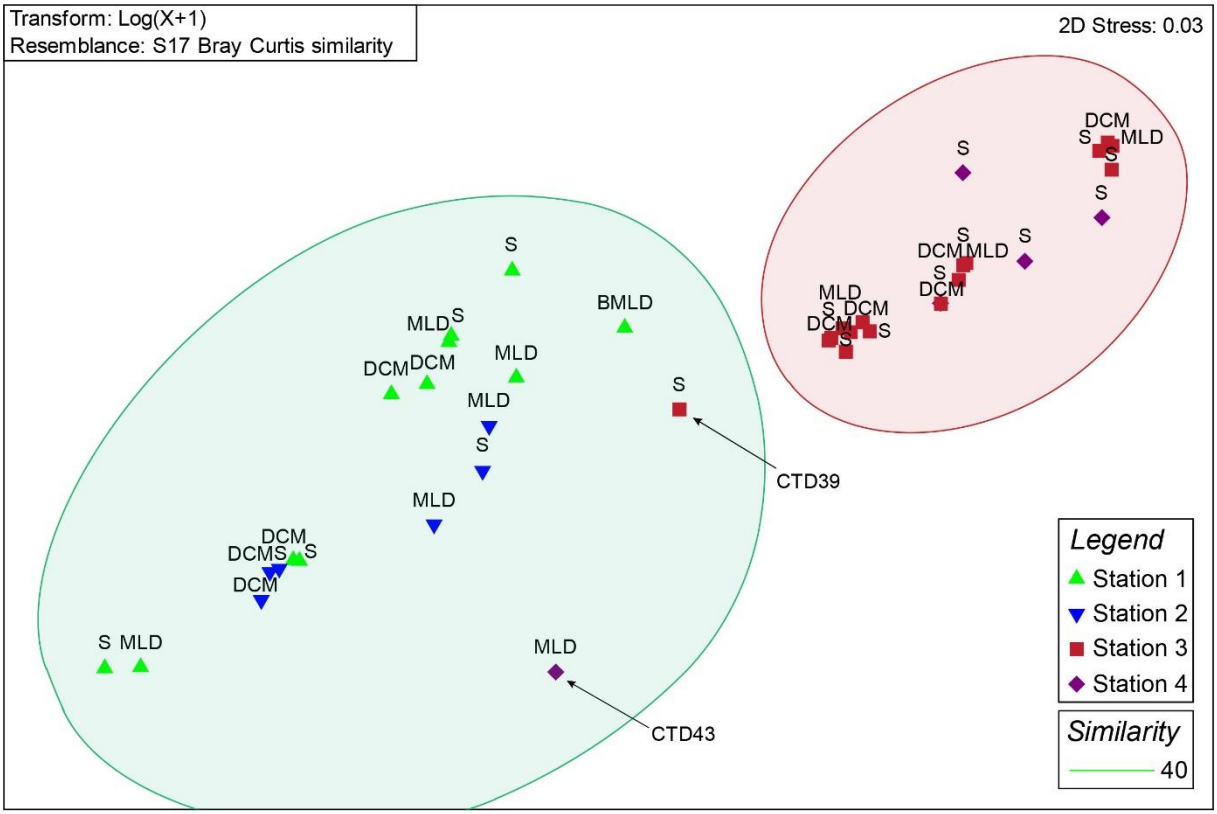

Fig. 27. Non-metric multidimensional scaling (nMDS) ordination plot of Bray–Curtis community similarities between investigated stations based on phytoplankton abundances. Abbreviations: S – surface, DCM – deep chlorophyll maximum, MLD – mixed layer depth, BMLD - bellow mixed layer depth.

For the pigment analysis, first two principal component axes have been used for the PCA loading, with a high cumulative variation of 93.4% (Fig. 28). It is apparent that these two axes tend to explain the much large amount of variation that the PCA of phytoplankton abundance. The eigenvalues of PC1 and PC2 axes are 128 and 25.2, respectively (Table 8). The oligotrophic samples from ST1 and ST2 are more widely dispersed, with cluster overlapping more than half of eutrophic sample from ST3 and ST4. The ST3 and ST4 samples are clustered very tightly inside a cluster, except the CTD 39 surface layer having least resemblance to the rest of ST3 samples. Still, two main environmental states are present as in previous analyses.

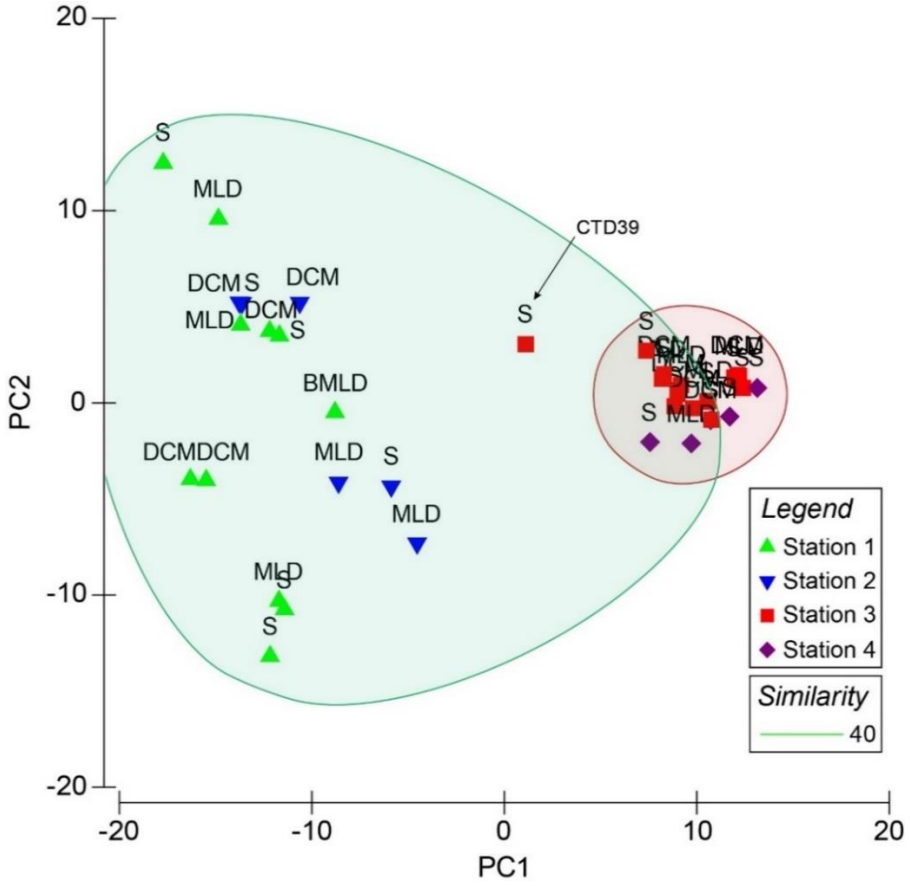

Fig. 28. Distribution of pigment concentrations per stations using PCA loadings of the first two principal components accounting for 93.4% of the variance.

Table 8. Eigenvalues, variations and cumulative variations of 5 axes for phytoplankton abundance and pigments concentration.

	Eigenvalues								
	PC	Eigenvalues	% Variation	Σ% Variation		PC	Eigenvalues	% Variation	Σ% Variation
Phyto. abund.	1	101	23.3	23.3	Pigment conc.	1	128	78	78
	2	41	9.4	32.8		2	25.2	15.3	93.4
	3	28.8	6.6	39.4		3	5.2	3.2	96.5
	4	26.6	6.1	45.5		4	3.53	2.2	98.7
	5	22.5	5.2	50.7		5	1.05	0.6	99.3

4.3. Underway system

Ship's underway sampler took 12 different samples during the transect from the surface including both the phytoplankton and pigments. Multivariant analyses were performed but they didn't show any correlation at all between the phytoplankton samples (Fig. 29). Samples are completely intermixed without any significant resemblance for both analyses. Pigments' multivariant analyses clustered samples UW 1–11 together, only sample UW 12 is most dissimilar among the samples (Fig 30).

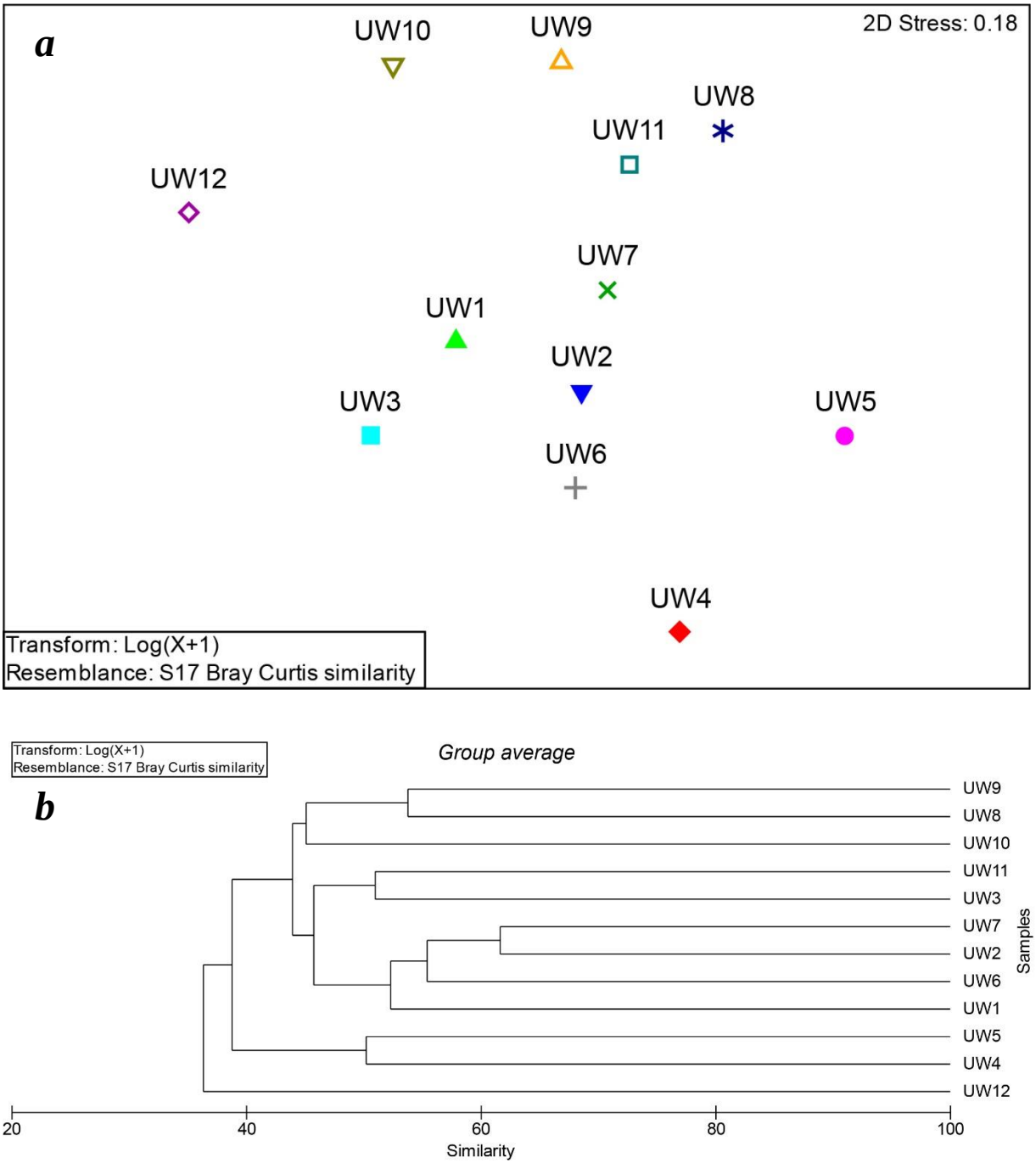

Fig. 29. Multivariant analyses of underway samples of phytoplankton: a) nMDS; b) hierarchical clustering.

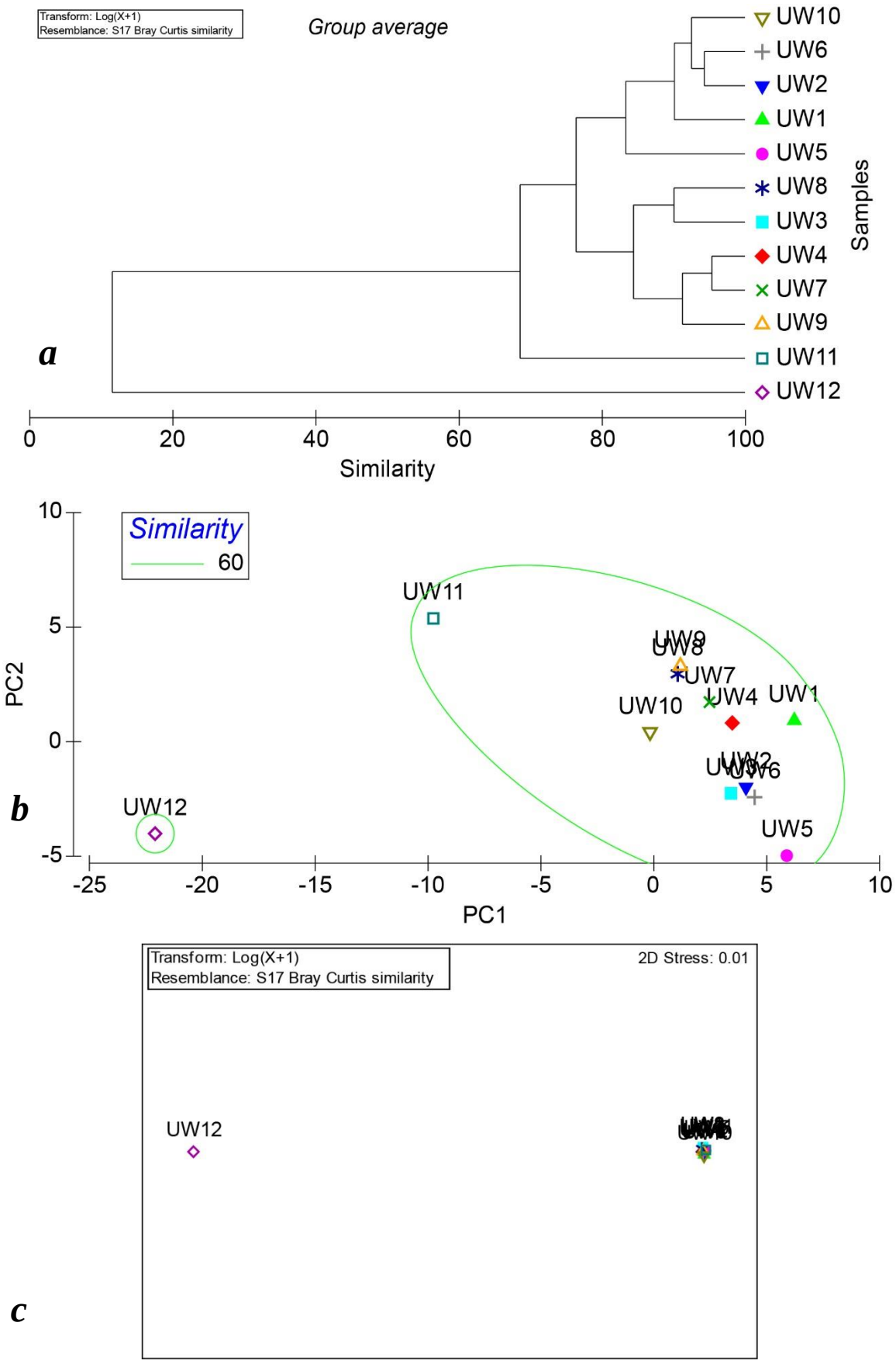

Fig. 30. Multivariant analyses of pigments from the UW system: a) HCA; b) PCA; c) nMDS.

5. DISCUSSION

In this master thesis, the analyzed data showed distinct environments characterized by differences between phytoplankton abundances and concentrations of pigments along with a transect that comprises an open ocean and coast with river plume. ST1 and ST2 are located inside of North Pacific Subtropical Gyre (NPSG) which is a High-Nutrient, Low-Chlorophyll (HNLC) part of North Pacific. This designates them as oligotrophic marine environments with lower production rates, higher concentrations of macronutrients at the surface, low phytoplankton pigment biomass and the dominance of small producer species (Martin *et al*., 1989; Latasa *et al*., 1997). On the other hand, the ST3 and ST4 are a part of the California Current System (CCS) which has more complex circulation patterns which influence the spatial distribution of phytoplankton differently than the open ocean. Also, the Columbia River substantially contributes terrigenous sediments, especially iron ("iron fertilization"), and total organic matter to the CCS, raising the trophic state of the region and stimulating the growth of planktonic organisms (Kammerer, 1987; Morgan *et al*., 2005; Kudela *et al*., 2010). Recorded phytoplankton abundance was lower at oligotrophic stations and higher at eutrophic stations. Generally, higher production is attributed to seasonal upwelling characteristic with eastern boundary current systems (Hill *et al*., 1998). In the case of the CCS, its northern part has much higher chlorophyll concentrations which are reflected in higher trophic levels of in the Washington/British Columbia region (Ware and Thomson, 2005). Furthermore, the Columbia River influences the CCS with an increased input of freshwater affecting circulation, stratification and light penetrance. Nutrient supply is significantly enriched with terrigenous contribution raising the trophic state and altering the composition of the phytoplankton community. Because of its considerable amount of iron, the plume of Columbia River deposits it in sediment along the Washington and Oregon coasts which can then be mixed with bottom water and amplify the effect of already nitrate-rich water (Hickey and Banas, 2008).

The sunlit portion of the ocean is up to 200 m deep on average, depending on the suspended particles. Most of the primary production in the oligotrophic ocean is limited to the layers of deep chlorophyll maxima (DCM) that may correspond to enhanced phytoplankton production or physiological adaptation of photosynthetic apparatus on the limited photosynthetic active radiation (PAR). In this research, DCM layer was recorded as higher fluorescence signal (ST1 and ST2, ~110 m; ST3 and ST4, ~30 m). The mixed layer depth (MLD), the depth of the ocean or a lake where turbulence caused by wind, currents, and heat-exchange have homogenized water column and nutrients contained within, was up to 130 m at ST1 and ST2 and up to 90 m depth at ST3 and ST4. Bellow the MLD, the stratification occurs, and phytoplankton cannot sustain photosynthesis anymore. As previously stated, the DCM should have the highest abundance of phytoplankton but, due to the intense storms that were present during that winter season, the whole column was thoroughly mixed with little vertical variation

in both phytoplankton abundance and pigment concentrations. Data presented in this thesis are highly valuable due to the lack of studies that used detailed microscopic analysis of phytoplankton performed here on such a wide transect in the Pacific Ocean are very scarce. The *Tara* Oceans expeditions gave general metagenomics data of numerous planktonic organisms in photic zones of world's oceans, including the picophytoplankton of NPSG which can be discussed with here presented results. Upwelling region at the southern Patagonian zone in the Southern Ocean where Humboldt current flows has a pico-nanophytoplankton (0.8–5 μm) community ratio with the subequal contribution of diatoms, coccolithophores, and dinoflagellates (De Vargas *et al*., 2015) similar to our data from the Californian upwelling zone. Furthermore, lesser richness at the oligotrophic NPSG has the somewhat similar composition to the metagenomic analysis by De Vargas *et al*. (2015) with a very low abundance of nano-diatoms and a larger number of dinoflagellates. Still, the nano-coccolithophorid contribution is larger at ST1 and ST2 than the T*ara* oceans samples. In this way, metagenomic studies coupled with taxonomic and chemotaxonomic analyses confirm and support the oligotrophic state of ST1 and ST2 at the edge of NPSG and the eutrophic state of ST3 along the Californian coast.

The geography has an important role in phytoplankton community structuring (the β diversity) due to dispersal limitations, at least for the tropical and subtropical open ocean. Villarino *et al*. (2018) found that more abundant pico- and nanophytoplankton can be passive dispersed farther with ocean currents than less abundant microphytoplankton. The central Pacific Ocean is a biogeographic region with low species connectivity due to limited mixing between neighboring communities. The larger similarity and homogeneity of smaller phytoplankton fraction at the ST1 and ST2 stations could be explained by this spatial species-turnover. Nano-coccolithophores are present in higher abundance on all stations, while much larger micro-diatom community stays less unchanged at the coastal ST3 and ST4 stations. Bigger *Pseudo-nitzschia pseudodelicatissima* can be dispersed harder northward along the coast as it is visible in results, with the highest abundance at ST3 and no presence northward. Also, Villarino *et al*. (2018) detected that Hawaiian archipelago may act as an oceanographic barrier, separating plankton communities into two different groups at either side of the islands. Because only one test sample, MOBY, was taken at the other side of Hawaiian Islands before departing towards the West Coast it was not possible to distinguish and statistically prove differences in community composition between the two sides of the archipelago.

While the ST1 and ST2 are intermixed, falling both under the same similarity cluster, there are bigger differences in taxa and abundance between ST3 and ST4. Because of the ship's crisscross sampling route along the coast, the samples may vary due to differences in the currents' flow dynamics. The CTD closest to the Columbia River plume, the CTD 46, has separated itself from the rest of ST4 samples, which would be regarded as the only true CRP station. Other CTDs under the ST4 would be transitional environment between the coastal ST3 and CRP, with a gradual increase of riverine system influence and community composition.

Similar situation with the increase of cryptophytes at the CRP, and in the extension the West Coast, was observed by Šupraha *et al*. (2014) in the Krka River Estuary which is one of the most productive zones along the eastern Adriatic Sea (Ujević *et al*., 2010). High cryptophyte abundance and high concentration of biomarker pigment alloxanthin were detected in the surface layer and at halocline of the highly stratified estuary. The phytoplankton community in the estuary is otherwise dominated by diatoms, whereas during the bloom 40 to 49% of total phytoplankton were cryptophytes. The cryptophytes dominated bloom was supported by the slower river flow rate and the increased temperature as well as higher nutrient concentration, primarily orthophosphates. The Šibenik harbor is situated at the mouth of the estuary, where a higher concentration of orthophosphate originates from the anthropogenic eutrophication and bacterial regeneration of the organic matter (Fuks *et al*., 1991, Legović *et al*., 1994). The same trend of slower river flow rate and temperature increase due to damming of Columbia River was observed by Sullivan *et al*. (2001). Combining latter effects with an anthropogenic increase of nutrient input (probably from the city of Portland) would likely explain higher amount of cryptophytes in the phytoplankton community along with the higher concentration of alloxanthin. Prasinoxanthin followed a similar trend with higher but constant concentrations at ST 3 and ST4 implying larger prasinophyte contribution to the community (Latasa *et al*., 2004).

The number of diatoms has increased with the lower discharge and slower river flow, which is similar to the non-bloom community at the Krka River noted by Šupraha *et al*. (2014). Even in some shallow and unstratified estuarine systems, the dominant groups throughout the year were diatoms and cryptophytes (Gameiro *et al*., 2004). This may explain the presence of both the higher abundance of cryptophytes at the surface of ST4 and the domination of micro-diatoms at both coastal stations. Also, Frame and Lessard (2009) reported that diatom community usually made over 65% of the total photosynthetic biomass in all samples at Columbia River plume, and was the same community found along the coast. The most abundant genera in terms of biomass, on average, was *Thalassiosira*. Size category of *Thalassiosira* taxon in Frame and Lessard (2009) was <20 mm for over 80% of cells and 50% of the biomass in the samples. Finally, cryptophytes were also present in their plume sample while they were virtually absent from the non-plume sample. This coincides with here presented results where (i) diatoms made a significant contribution to community composition at ST3 and ST4, (ii) *Thalassiosira* being third most abundant and most abundant diatom at ST3 and ST4, respectively, and (iii) cryptophytes were most abundant in surfaces samples of the CRP.

ST3 had the highest abundance of the *Pseudo-nitzschia pseudodelicatissima,* even though it was absent from other stations. Parsons and Dortch (2002) have reported high abundance of *Pseudo-nitzschia* genus, primarily dominated by *Pseudo-nitzschia pseudodelicatissima,* in the sediment cores of the Mississippi River. Furthermore, high concentrations of neurotoxic domoic acid, associated with the *Pseudo-nitzschia* genus, have been repeatedly detected in the plume of Mississippi River during heightened nutrient input (especially nitrate), and stronger river flow (Pan *et al*., 2001). The possible

correlation of *Pseudo-nitzschia* taxa with domoic acid and higher productivity was noted in the northern Adriatic Sea (Marić *et al*., 2011) and in the Krka River Estuary (Ujević *et al*., 2010). Different phenomena have been tied to the increase in abundance of *Pseudo-nitzschia,* both natural and anthropogenic. Trainer *et al*. (2000) found that two *Pseudo-nitzschia* species were causing sea lion die-off due to domoic acid poisoning along the central California coast. They observed that appearance of *Pseudo-nitzschia* species coincided with upwelling zones near coastal headlands. Others point to increased fertilizer use and agricultural run-off causing eutrophication (Smith *et al*., 1990). A diatom species *Lennoxia faveolata* had second highest abundance among diatoms at ST3 and wasn't detected in other stations. Thomsen *et al*. (1993), who first described it, found high numbers from in samples from Californian waters during winter, but not much more is known about it.

None cyanobacterial cell has been detected due to their picoplanktonic size preventing them from being filtered and analyzed like large cell phytoplankton. Nevertheless, presence of the most common cyanobacterial taxa in the marine environments, the *Prochlorococcus* and the *Synechococcus*, can be observed indirectly through the concentrations of their signature pigments, the DVChl *a* for the *Prochlorococcus* and zeaxanthin for the *Synechococcus* (Guillard *et al*., 1985; Stockner and Antia, 1986; Morel *et al*., 1993). Both taxa generally prefer the warm and euphotic, oligotrophic waters of open oceans, even though the *Synechococcus* dominates more in the colder and nutrient-richer coastal waters or more temperate, mesotrophic open ocean waters (due to the adaptation properties of its photosynthetic apparatus, Biller *et al*., 2014), whereas *Prochlorococcus* prefers warm oligotrophic waters with temperatures >15 °C (Partensky *et al*., 1999b). Partensky *et al*., (1999a) also observed *Prochlorococcus* often being much more abundant than *Synechococcus* in co-occurring areas, except seasonally or permanently nutrient-enriched regions with strong upwellings and/or coastal inputs. They also noted that, even though *Synechococcus* has the highest abundance in coastal and upwelling regions (Partensky *et al.,* 1996) it is always present, albeit in low abundance, in central gyres of Atlantic and Pacific oceans that are nutrient-depleted (Olson *et al.,* 1990; Campbell and Vaulot, 1993; Li, 1995; Blanchot and Rodier, 1996). Campbell *et al*. (1997) found that *Synechococcus* abundance peaked in winter off Hawaii where sea temperature was >19°C, but Hall and Vincent (1990) detected of New Zealand's South Island its increase in concentration moving from colder coastal (10°C) to warmer offshore waters (>13°C) where nitrates concentration were higher than 3μM. On the other hand, *Prochlorococcus* is limited by low temperature with a sudden drop in abundance above 50°N (Partensky *et al*., 1999a). Also, *Prochlorococcus* has been observed in substantial concentrations in the western equatorial Pacific, slightly above 5 the nitracline (Partensky *et al*., 1999a according to Blanchot unpublished data), and even though it prefers oligotrophic waters, it was present with similar abundance in the warm mesotrophic, stratified area of equatorial Pacific (Partensky *et al*., 1999a). Data in this thesis supports this statement because DVChl *a* and zeaxanthin have both been detected in very high concentrations in oligotrophic samples of the ST1 and ST2, implying high abundance and domination of the

Prochlorococcus and *Synechococcus.* The concentration of the same pigments falls substantially at the more eutrophic ST3 and ST4 samples, as it would be expected for *Prochlorococcus* but not necessarily for *Synechococcus*. Babić *et al*. (2017) suggest that temperature and environmental hydrodynamics may influence variation in the abundances, structure, and distribution of both *Prochlorococcus* and *Synechococcus* populations making them ideal indicator organism for predicting future changes in the ecosystems caused by the climatological changes - the global warming.

Synechococcus may also be indirectly observed using the abundance of diatom *Leptocylindrus mediterraneus* which itself has a symbiont colonial protozoan *Solenicola setigera* Pavillard inside which the *Synechococcus* may reside. This indirect three-partner associated symbiosis was detected by Buck and Bentham (1998) in the open, oligotrophic waters of the Pacific Ocean. Gomez (2007) found a higher abundance of *Solenicola–Leptocylindrus* consortia both at the DCM in nutrient-rich oligotrophic waters 1300 km off the coast of Chile and in eutrophic slope waters near Japan. *Leptocylindrus mediterraneus* has been detected on both the ST1 and ST2, albeit with low abundance. Nevertheless, the number of cyanobacterial cells should be much higher than the number of symbionts they inhabit.

Coccolithophorid contribution to community composition is significant on all stations, with nano-coccolithophores being dominant on all stations, especially at greater depths. While micro-coccolithophores have more significant abundancy at oligotrophic ST1 and ST2, they are virtually absent at eutrophic ST3 and ST4. Their pigment proxy, 19'-hexanoyloxyfucoxanthin, has the relatively high ratio on all stations compared to other pigments. Its presence may point to the higher contribution of pico-fraction coccolithophores in bigger depths at eutrophic stations. Domination of coccolithophores at ST1 and ST2 point to species more adapted to oligotrophic conditions, while indirect observation of 19HF at ST3 and ST4 implies a shift to the more eutrophic-adapted, smaller coccolithophores species. Li *et al*. (2013) observed concentrations of 19HF in Pacific, a coccolithophorid biomarker pigment. It was generally low in the upper euphotic zone but increasing with depth, making the concentration of 19HF usually highest at DCM and c. This would suggest that the coccolithophores are physiologically adapted to low light, nutrient-enriched regions of the water or the 19HF came from other lineages contain the coccolithophorid-indicative marker pigment (Carreto *et al*., 2001; Landry *et al*., 2003). Interestingly, the concentrations of 19HF in this study have stayed relatively constant with depth. The contrary exception was at the DCM of ST4 where all pigments had much lower concentrations probably due to influence from Columbia River. Li *et al*. (2013) have also noted 19'-butanoyloxyfucoxanthin (19BF) which is indicative of pelagophytes to have a similar trend to 19HF. This coincided with the higher concentration trend of 19BF at ST3 and ST4 pointing to the presence of pelagophytes.

6. CONCLUSION

Detailed analysis of phytoplankton community and pigment composition of the North Pacific Ocean were quantitatively and qualitatively analyzed using microscopy. The results of this study showed that the phytoplankton community of North Pacific was mostly comprised of coccolithophores (35.5%), diatoms (25.2%) and dinoflagellates (19.5%) while cryptophytes, phytoflagellates, silicoflagellates, haptophytes, etc. were included in group "other" that makes 19.8%. A total of 207 taxa have been determined from both CTD probes and net samples of which: 106 diatoms, 48 coccolithophores, 41 dinoflagellates, 7 other autotrophs, 4 heterotrophs and 1 cyanobacteria. The area of ST1 and ST2 is oligotrophic, confirming generally lower phytoplankton composition and community structure, while coastal ST3 and Columbia River plume ST4 had higher diversity, with a higher abundance of phytoplankton and pigment concentrations. Furthermore, signature biomarker pigments have been noted to correlate with characteristic species for each trophic environment. Generally, on most stations diatoms dominated microphytoplankton while coccolithophores were most abundant in nanophytoplankton. *Prochlorococcus* and *Synechococcus* characteristic pigments, divinyl chlorophyll *a* and zeaxanthin, respectively, were present in higher concentrations at the oligotrophic stations. Cryptophytes and their signature pigment alloxanthin were found in high amount in the Columbia River plume, while toxic *Pseudo-nitzschia pseudodelicatissima* has been found along the Californian coast.

This research has great potential that could result in valuable knowledge with application in different fields essential for better understanding of the marine ecosystems' response to climate changes, anthropogenic pressure and its impact on the oceans. Based on the analysed result I conclude it should be possible in the future to use this information and correlate the data in conjunction with radiometry to develop algorithms and calibration of sensor technology of orbital satellites for better observation of the subtle color differences of the oceans. Only a few trophic environments have been studied in this research, and it is, therefore, necessary to increase research efforts and collect data of many other trophic systems around the oceans.

LITERATURE

Aakermann, T. and Skulberg, O.M., 1992. A comparison of the carotenoids of strains of *Oscillatoria* and *Spirulina* (cyanobacteria). *Biochemical systematics and ecology*, *20*, 761–769.

Airs, R. L. and Llewellyn, C. A., 2006. Improved detection and characterization of fucoxanthin-type carotenoids: Novel pigments in *Emiliana huxleyi* (Prymnesiophyceae). *Journal of Phycology*, 42, 391–99.

Alvain, S., Moulin, C., Dandonneau, Y. and Bréon, F.M., 2005. Remote sensing of phytoplankton groups in case 1 waters from global SeaWiFS imagery. *Deep Sea Research Part I: Oceanographic Research Papers*, *52*, 1989–2004.

Babić, I., Petrić, I., Bosak, S., Mihanović, H., Radić, I.D. and Ljubešić, Z., 2017. Distribution and diversity of marine picocyanobacteria community: Targeting of *Prochlorococcus* ecotypes in winter conditions (southern Adriatic Sea). *Marine Genomics*, *36*, 3–11.

Blanchot, J. and Rodier, M., 1996. Picophytoplankton abundance and biomass in the western tropical Pacific Ocean during the 1992 El Niño year: results from flow cytometry. *Deep Sea Research Part I: Oceanographic Research Papers*, *43*, 877–895.

Booth, B.C., Lewin, J. and Postel, J.R., 1993. Temporal variation in the structure of autotrophic and heterotrophic communities in the subarctic Pacific. *Progress in Oceanography*, *32*, 57–99.

Boyd, P. W., Newton P.P., 1999. Does planktonic community structure determine downward particulate organic carbon flux in different oceanic provinces? *Deep-Sea Research Part I: Oceanographic Research* Papers, 46, 63–91.

Bray, J.R. and Curtis, J.T., 1957. An ordination of the upland forest communities of southern Wisconsin. *Ecological monographs*, *27*, 325–349.

Bricaud, A., Claustre, H., Ras, J. and Oubelkheir, K., 2004. Natural variability of phytoplanktonic absorption in oceanic waters: Influence of the size structure of algal populations. *Journal of Geophysical Research: Oceans*, *109*.

Buck, K.R. and Bentham, W.N., 1998. A novel symbiosis between a cyanobacterium, *Synechococcus* sp., an aplastidic protist, *Solenicola setigera*, and a diatom, *Leptocylindrus mediterraneus*, in the open ocean. *Marine Biology*, *132*, 349–355.

Burger-Wiersma, T., Veenhuis, M., Korthals, H. J., Van de Wiel, C. C. M. and Muir, L. R., 1986. A new prokaryote containing chlorophylls *a* and *b*. *Nature*, 320, 262–63.

Campbell, L., Liu, H., Nolla, H.A. and Vaulot, D., 1997. Annual variability of phytoplankton and bacteria in the subtropical North Pacific Ocean at Station ALOHA during the 1991–1994 ENSO event. *Deep Sea Research Part I: Oceanographic Research Papers*, *44*, 167–192.

Campbell, L. and Vaulot, D., 1993. Photosynthetic picoplankton community structure in the subtropical North Pacific Ocean near Hawaii (station ALOHA). *Deep Sea Research Part I: Oceanographic Research Papers*, *40*, 2043–2060.

Carpenter, E.J., O'Neil, J.M., Dawson, R., Capone, D.G., Siddiqui, P.J., Roenneberg, T. and Bergman, B., 1993. The tropical diazotrophic phytoplankter *Trichodesmium*: biological characteristics of two common species. *Marine Ecology Progress Series*, 295–304.

Carreto, J.I., Seguel, M., Montoya, N.G., Clément, A. and Carignan, M.O., 2001. Pigment profile of the ichthyotoxic dinoflagellate *Gymnodinium* sp. from a massive bloom in southern Chile. *Journal of plankton research*, *23*, 1171–1175.

Chase, Z., Hales, B., Cowles, T., Schwartz, R. and Van Geen, A., 2005. Distribution and variability of iron input to Oregon coastal waters during the upwelling season. *Journal of Geophysical Research: Oceans*, *110*.

Chavez, F.P., Buck, K.R. and Barber, R.T., 1990. Phytoplankton taxa in relation to primary production in the equatorial Pacific. *Deep Sea Research Part A. Oceanographic Research Papers*, *37*, 1733–1752.

Clarke, K.R., 1993. Non-parametric multivariate analyses of changes in community structure. *Austral Ecology*, *18*, 117–143.

Clarke, K. R. and Warwick, R. M., 2001. Change in Marine Communities: An Approach to Statistical Analysis and Interpretation. PRIMER-E Limited.

Coale, K.H., Johnson, K.S., Fitzwater, S.E., Gordon, R.M., Tanner, S., Chavez, F.P., Ferioli, L., Sakamoto, C., Rogers, P., Millero, F. and Steinberg, P., 1996. A massive phytoplankton bloom induced by an ecosystem-scale iron fertilization experiment in the equatorial Pacific Ocean. *Nature*, *383*, 495–501.

Coble, P.G., 2007. Marine optical biogeochemistry: the chemistry of ocean color, *Chemical reviews*, *107*, 402–418.

Cushman-Roisin, B., Gačić, M., Poulain, P.M., Artegiani, A., 2001. Physical oceanography of the Adriatic Sea. Kluwer Academic Publishers, Dordrecht

De Vargas, C., Audic, S., Henry, N., Decelle, J., Mahé, F., Logares, R., Lara, E., Berney, C., Le Bescot, N., Probert, I., Carmichael, M., Poulain, J., Romac, S., Colin, S., Aury, J.M., Bittner, L., Chaffron, S, Dunthorn, M., Engelen, S., Flegontova, O., Guidi, L., Horák, A., Jaillon, O., Lima-Mendez, G., Lukeš, J., Malviya, S., Morard, R.,, Mulot M., Scalco, E., Siano, R., Vincent, F., Zingone, A., Dimier, C., Picheral, M., Searson, S., Kandels-Lewis, S., *Tara* Oceans Coordinators, Acinas, S.G., Bork, P., Bowler, C., Gorsky, G., Grimsley, N., Hingamp, P., Iudicone, D., Not, F., Ogata, H., Pesant, S., Raes, J., Sieracki, M.E., Speich, S., Stemmann, L., Sunagawa, S., Weissenbach, J., Wincker, P., Karsenti, E., 2015. Eukaryotic plankton diversity in the sunlit ocean. *Science*, 348, 1261605.

DiTullio, G.R., Hutchins, D.A. and Bruland, K.W., 1993. Interaction of iron and major nutrients controls phytoplankton growth and species composition in the tropical North Pacific Ocean. *Limnology and Oceanography*, *38*, 495–508.

Dore, J.E., Letelier, R.M., Church, M.J., Lukas, R. and Karl, D.M., 2008. Summer phytoplankton blooms in the oligotrophic North Pacific Subtropical Gyre: Historical perspective and recent observations. *Progress in Oceanography*, *76*, 2–38.

Eakins, B.W. and Sharman, G.F., 2010. Volumes of the World's Oceans from ETOPO1, NOAA National Geophysical Data Center, Boulder, CO.

Edwards, D., Morris, J.L., Richardson, J.B. and Kenrick, P., 2014. Cryptospores and cryptophytes reveal hidden diversity in early land floras. *New Phytologist*, *202*, 50–78.

Everitt, D.A., Wright, S.W., Volkman, J.K., Thomas, D.P. and Lindstrom, E.J., 1990. Phytoplankton community compositions in the western equatorial Pacific determined from chlorophyll and carotenoid pigment distributions. *Deep Sea Research Part A. Oceanographic Research Papers*, *37*, 975–997.

Fahey, D., Doherty, S., Hibbard, K., Romanou, A. and Taylor, P., 2017. Physical drivers of climate change. In: *Climate Science Special Report: Fourth National Climate Assessment*, Volume I [Wuebbles, D.J., D.W. Fahey, K.A. Hibbard, D.J. Dokken, B.C. Stewart, and T.K. Maycock (eds.)]. U.S. Global Change Research Program, Washington, DC, USA, 73–113

Falkowski, P.G., Barber, R.T. Smetacek, V., 1998. Biogeochemical controls and feedbacks on ocean primary production. *Science*, 281, 200–206.

Field, C.B., Behrenfeld, M.J., Randerson, J.T., Falkowski, P., 1998. Primary Production of the Biosphere: Integrating Terrestrial and Oceanic Components. *Science*. 281, 237–240.

Finlay, B.J., 2002. Global dispersal of free-living microbial eukaryote species. *Science*, *296*, 1061–1063.

Flombaum, P., Gallegos, J.L.,. Gordillo, R.A, Rincón, J., Zabala, L.L, Jiao, N., Karl, D., MLi, W. K., Lomas, M.W., Veneziano, D., Vera, C.S., Vrugt, J.A., Martiny, A.C., 2013. Present and future global distributions of the marine Cyanobacteria *Prochlorococcus* and *Synechococcus*. *Proceedings of the National Academy of Sciences U.S.A.* 110, 9824–9829.

Foss, P., Lewin, R. A. and Liaaen-Jensen, S., 1987. The carotenoids of *Prochloron* sp. (Prochlorophyta). *Phycologia* 26, 142–44.

Frame, E.R. and Lessard, E.J., 2009. Does the Columbia River plume influence phytoplankton community structure along the Washington and Oregon coasts?. *Journal of Geophysical Research: Oceans*, *114*.

Fuks, D., Devescovi, M., Precali, R., Krstulović, N. and Šolić, M., 1991. Bacterial abundance and activity in the highly stratified estuary of the Krka River. *Marine chemistry*, *32*, 333–346.

Gameiro, C., Cartaxana, P., Cabrita, M.T. and Brotas, V., 2004. Variability in chlorophyll and phytoplankton composition in an estuarine system. *Hydrobiologia*, *525*, 113–124.

Gersonde, R. and Harwood, D.M., 1990. 25. Lower Cretaceous diatoms from ODP LEG 113 Site 693 (Weddel sea). Part 1: Vegetative cells. *Proceedings of the Ocean Drilling Program, Scientific Results*, 113, 365–402.

Goericke, R., Olson, R.J. and Shalapyonok, A., 2000. A novel niche for *Prochlorococcus* sp. in low-light suboxic environments in the Arabian Sea and the Eastern Tropical North Pacific. *Deep Sea Research Part I: Oceanographic Research Papers*, *47*, 1183–1205.

Gomez, F., 2007. The consortium of the protozoan *Solenicola setigera* and the diatom *Leptocylindrus mediterraneus* in the Pacific Ocean. *Acta Protozoologica*, *46*, 15–24.

Guillard, R.R.L., Murphy, L.S., Foss, P. and Liaaen-Jensen, S., 1985. Synechococcus spp. as likely zeaxanthin-dominant ultraphytoplankton in the North Atlantic. *Limnology and Oceanography*, *30*, 412–414.

Hall, J.A. and Vincent, W.F., 1990. Vertical and horizontal structure in the picoplankton communities of a coastal upwelling system. *Marine biology*, *106*, 465–471.

Hamilton, T. L., Bryant, D. A., and Macalady, J. L., 2016. The role of biology in planetary evolution: cyanobacterial primary production in low-oxygen Proterozoic oceans. *Environmental Microbiology*, *18*, 325–340.

Hertzberg, S., Liaaen-Jensen, S. and Siegelman, H. W., 1971. The carotenoids of blue-green algae. *Phytochemistry*, 10, 3121–27.

Hewes, C. D., Mitchell, B. G., Moisan, T. A., Vernet, M. and Reid, F. M., 1998. The phycobilin signatures of chloroplasts from three dinoflagellate species: a microanalytical study of *Dinophysis cordata*, *D. fortii*, and *D. acuminate* (Dinophysiales, Dinophyceae). *Journal of Phycology*, 34, 945–51.

Hickey, B.M. and Banas, N.S., 2008. Why is the northern end of the California Current System so productive?. *Oceanography*, *21*, 90–107.

Hill, E.D., Hickey, B.M., Shillington, F.A., Strub, P.T., Barton, E.D., and Brink, K., 1998. Eastern Boundary Current Systems of the World. *The Sea*, *12*, 21–62.

Hooker, S. B., Clementson, L., Thomas, C.S., Schlüter, L., Allerup, M., Ras, J., Claustre, H., Normandeau, C., Cullen, J., Kienast, M., Kozlowski, W., Vernet, M., Chakraborty, S., Lohrenz, S., Tuel, M., Redalje, D., Cartaxana, P., Mendes, C.R., Brotas, V., Matondkar, S.G.P., Parab, S.G., Neeley, A. and Egeland, E.S., 2012. The Fifth SeaWiFS HPLC Analysis Round-Robin Experiment (SeaHARRE-5), NASA Tech. Memo. 2012- 217503, NASA Goddard Space Flight Center, Greenbelt, MD, 108 pp.

Jeffrey, S. W. and Wright, S. W., 2006. Photosynthetic pigments in marine microalgae: insights from cultures and the sea. In Algal Cultures, Analogues of Blooms and Applications, ed. D. V. Subba Rao. Enfield: Science Publishers, 33–90.

Jeffrey, S.W. and Hallegraeff, G.M., 1990. Phytoplankton ecology of Australasian waters. *Biology of marine plants*, 310–348.

Jenkins, D.G., Brescacin, C.R., Duxbury, C.V., Elliott, J.A., Evans, J.A., Grablow, K.R., Hillegass, M., Lyon, B.N., Metzger, G.A., Olandese, M.L. and Pepe, D., 2007. Does size matter for dispersal distance?. *Global Ecology and Biogeography*, *16*, 415–425.

Kammerer, J.C., 1987. Largest rivers in the United States (water fact sheet) (No. 87–242), US Geological Survey.

Karl, D.M. and Church, M.J., 2017. Ecosystem structure and dynamics in the North Pacific Subtropical Gyre: new views of an old ocean, *Ecosystems*, *20*, 433–457.

Karl, D.M. Church, M.J., Dore, J.E., Letelier, R.M., Mahaffey, M.C., 2012. Predictable and efficient carbon sequestration in the North Pacific Ocean supported by symbiotic nitrogen fixation. *Proceedings of the National Academy of Sciences U.S.A.* 109, 1842–1849.

Karsenti, E., Acinas, S.G., Bork, P., Bowler, C., De Vargas, C., Raes, J., Sullivan, M., Arendt, D., Benzoni, F., Claverie, J.M., Follows, M., Gorsky, G., Hingamp, P., Iudicone, D., Jaillon, O., Kandels-Lewis, S., Krzic, U., Not, F., Ogata, H., Pesant, S., Reynaud, E.G., Sardet, C., Sieracki, M.E., Speich, S., Velayoudon, D., Weissenbach, J., Wincker, P., the Tara Oceans Consortium. 2011. A Holistic Approach to Marine Eco-Systems Biology. *PLoS Biology*, 9: e1001177

Kirchman, D.L., 2000. Microbial ecology of the oceans. Wiley-Liss, New York.

Kudela, R.M., Horner-Devine, A.R., Banas, N.S., Hickey, B.M., Peterson, T.D., McCabe, R.M., Lessard, E.J., Frame, E., Bruland, K.W., Jay, D.A. and Peterson, J.O., 2010. Multiple trophic levels fueled by recirculation in the Columbia River plume. *Geophysical Research Letters*, *37*.

Landry, M.R., Brown, S.L., Neveux, J., Dupouy, C., Blanchot, J., Christensen, S. and Bidigare, R.R., 2003. Phytoplankton growth and microzooplankton grazing in high-nutrient, low-chlorophyll waters of the equatorial Pacific: Community and taxon-specific rate assessments from pigment and flow cytometric analyses. *Journal of Geophysical Research: Oceans*, *108*.

Latasa, M., Landry, M.R., Louise, S. and Bidigare, R.R., 1997. Pigment specific growth and grazing rates of phytoplankton in the central equatorial Pacific. *Limnology and Oceanography*, *42*, 289–298.

Latasa, M., Scharek, R., Gall, F.L. and Guillou, L., 2004. Pigment suites and taxonomic groups in Prasinophyceae. *Journal of Phycology*, *40*, 1149–1155.

Legović, T., Žutić, V., Gržetić, Z., Cauwet, G., Precali, R. and Viličić, D., 1994. Eutrophication in the Krka estuary. *Marine chemistry*, *46*, 203–215.

Li, B., Karl, D.M., Letelier, R.M., Bidigare, R.R. and Church, M.J., 2013. Variability of chromophytic phytoplankton in the North Pacific Subtropical Gyre. *Deep Sea Research Part II: Topical Studies in Oceanography*, *93*, 84–95.

Li, W.K.W., 1995. Composition of ultraphytoplankton in the central North Atlantic. *Marine Ecology Progress Series*, 1–8.

Lohr, M. and Wilhelm, C., 1999. Algae displaying the diadinoxanthin cycle also possess a violaxanthin cycle. *Proceedings of the National Academy of Sciences U.S.A.*, 96, 8784–89.

Longhurst, A.R., 2010. *Ecological geography of the sea*. 2nd edn 51–70. Academic Press.

MacRae, R.A., Fensome, R.A. and Williams, G.L., 1996. Fossil dinoflagellate diversity, originations, and extinctions and their significance. *Canadian Journal of Botany, 74*, 1687–1694.

Marić, D., Ljubešić, Z., Godrijan, J., Viličić, D., Ujević, I. and Precali, R., 2011. Blooms of the potentially toxic diatom *Pseudo-nitzschia calliantha* Lundholm, Moestrup & Hasle in coastal waters of the northern Adriatic Sea (Croatia). *Estuarine, coastal and shelf science, 92*, 323–331.

Martin, J.H., Gordon, R.M., Fitzwater, S. and Broenkow, W.W., 1989. VERTEX: phytoplankton/iron studies in the Gulf of Alaska. Deep Sea Research Part A. *Oceanographic Research Papers, 36*, 649–680.

Martiny, J.B.H., Bohannan, B.J., Brown, J.H., Colwell, R.K., Fuhrman, J.A., Green, J.L., Horner-Devine, M.C., Kane, M., Krumins, J.A., Kuske, C.R. and Morin, P.J., 2006. Microbial biogeography: putting microorganisms on the map. *Nature Reviews Microbiology*, *4*, 102–112.

Medlin, L.K., Williams, D.M. and Sims, P.A., 1993. The evolution of the diatoms (Bacillariophyta). I. Origin of the group and assessment of the monophyly of its major divisions. *European Journal of Phycology*, *28*, 261–275.

Meyer-Harms, B. and Pollehne, F., 1998. Alloxanthin in *Dinophysis norvegica* (Dinophysiales, Dinophyceae) from the Baltic Sea. *Journal of Phycology*, 34, 280–85.

Miyashita, H., Adachi, K., Kurano, N., Ikemoto, H., Chihara, M. and Miyachi, S., 1997. Pigment composition of a novel oxygenic photosynthetic prokaryote containing chlorophyll *d* as the major chlorophyll. *Plant Cell Physiology*, 38, 274–81.

Miyashita, H., Ikemoto, H. Kurano, N, Miyachi, S. and Chihara M., 2003. *Acaryochloris marina* gen. et. sp. nov. (Cyanobacteria) an oxygenic photosynthetic prokaryote containing Chl *d* as a major pigment. *Journal of Phycology*, 39, 1247–53.

Miyashita, H., Ikemoto, H., Kurano, N., Adachi, K., Chihara, M. and Miyachi, S., 1996. Chlorophyll *d* as a major pigment. *Nature*, 383, 402–03.

Morel, A., Ahn, Y.H., Partensky, F., Vaulot, D. and Claustre, H., 1993. Prochlorococcus and Synechococcus: a comparative study of their optical properties in relation to their size and pigmentation. *Journal of Marine Research, 51*, 617–649.

Morgan, C. A., De Robertis, A., and Zabel, R. W., 2005. Columbia River Plume Fronts: I. Hydrography, Zooplankton Distribution, and Community Composition, *Marine Ecology Progress Series, 299*, 19–31.

Mousing, E.A., Richardson, K., Bendtsen, J., Cetinić, I., Perry, M.J. 2016. Evidence of small-scale spatial structuring of phytoplankton alpha-and beta-diversity in the open ocean. *Journal of Ecology*, 104, 1682–1695.

Olson, R.J., Chisholm, S.W., Zettler, E.R. and Armbrust, E., 1990. Pigments, size, and distributions of Synechococcus in the North Atlantic and Pacific Oceans. *Limnology and Oceanography*, *35*, 45–58.

Pal, R. and Choudhury, A.K., 2014. An Introduction to Phytoplanktons: Diversity and Ecology. Springer.

Pan, Y., Parsons, M.L., Busman, M., Moeller, P.D., Dortch, Q., Powell, C.L. and Doucette, G.J., 2001. *Pseudo-nitzschia* sp. cf. *pseudodelicatissima*—a confirmed producer of domoic acid from the northern Gulf of Mexico. *Marine ecology progress series*, *220*, 83–92.

Parsons, M.L. and Dortch, Q., 2002. Sedimentological evidence of an increase in *Pseudo-nitzschia* (Bacillariophyceae) abundance in response to coastal eutrophication. *Limnology and Oceanography*, *47*, 551–558.

Partensky, F., Blanchot, J. and Vaulot, D., 1999a. Differential distribution and ecology of *Prochlorococcus* and *Synechococcus* in oceanic waters: a review. *Bulletin de l'Institut Océanographique, Monaco. Numero special*, 457–476.

Partensky, F., Hess, W.R. and Vaulot, D., 1999b. Prochlorococcus, a marine photosynthetic prokaryote of global significance. *Microbiology and molecular biology reviews*, *63*, 106–127.

Ralf, G. and Repeta, D.J., 1992. The pigments of *Prochlorococcus marinus*: the presence of divinylchlorophyll *a* and *b* in a marine procaryote. *Limnology and Oceanography*, *37*, 425–433.

Richardson, T.L. and Jackson, G.A., 2007. Small phytoplankton and carbon export from the surface ocean. *Science*, 315, 838–840.

Robinson, I.S., 2010. Discovering the ocean from space: The unique applications of satellite oceanography, Springer Science & Business Media.

Rowan, K. S., 1989. Photosynthetic Pigments of Algae. Cambridge: Cambridge University Press.

Roy, S., Llewellyn, C.A., Egeland, E.S. and Johnsen, G. eds., 2011. Phytoplankton pigments: characterization, chemotaxonomy and applications in oceanography. Cambridge University Press.

Smith, J.C., Cormier, R., Worms, J., Bird, C.J., Quilliam, M.A., Pocklington, R., Angus, R. and Hanic, L.A., 1990. Toxic Blooms of the Domoic Acid Containing Diatom *Nitzschia-Pungens* in the Cardigan River Prince Edward Island Canada in 1988. In *Toxic Marine Phytoplankton; proceedings of the Fourth International Conference on Marine Phytoplankton, held June 26–30 in Lund, Sweden* (227–232).

Steele, J.H., Turekian, K.K. and Thorpe, S.A., 2009. Encyclopedia of ocean sciences – 2nd edition, Academic Press.

Stockner, J.G. and Antia, N.J., 1986. Algal picoplankton from marine and freshwater ecosystems: a multidisciplinary perspective. *Canadian journal of fisheries and aquatic sciences, 43*, 2472–2503.

Takano, Y., Hansen, G., Fujita, D. and Horiguchi, T., 2008. Serial replacement of diatom endosymbionts in two freshwater dinoflagellates, *Peridiniopsis* spp. (Peridiniales, Dinophyceae). *Phycologia* 47, 41–53.

Tappan, H. 1980. Haptophyta, coccolithophores, and other calcareous nannoplankton. *The Paleobiology of Plant Protists*, 678–803. W. H. Freeman, San Francisco.

Thomas, M. K., Kremer, C. T., Klausmeier, C. A., Litchman, E., 2012. A global pattern of thermal adaptation in marine phytoplankton. *Science*, 338, 1085–1088.

Thomsen, H.A., Buck, K.R., Marino, D., Sarno, D., Hansen, L.E., Østergaard, J.B. and Krupp, J., 1993. *Lennoxia faveolata* gen. et sp. nov. (Diatomophyceae) from South America, California, West Greenland and Denmark. *Phycologia, 32*, 278–283.

Tomas, C.R. ed., 1997. Identifying marine phytoplankton. Academic press.

Trainer, V.L., Adams, N.G., Bill, B.D., Stehr, C.M., Wekell, J.C., Moeller, P., Busman, M. and Woodruff, D., 2000. Domoic acid production near California coastal upwelling zones, June 1998. *Limnology and oceanography, 45*, 1818–1833.

Ujević, I., Ninčević-Gladan, Ž., Roje, R., Skejić, S., Arapov, J. and Marasović, I., 2010. Domoic acid-a new toxin in the Croatian Adriatic shellfish toxin profile. *Molecules, 15*, 6835–6849.

Utermöhl, H., 1958. Zur Vervollkommnung der quantitativen Phytoplankton-Methodik (Towards a perfection of quantitative phytoplankton methodology): Mit 1 Tabelle und 15 abbildungen im Text und auf 1 Tafel. *Internationale Vereinigung für Theoretische und Angewandte Limnologie: Mitteilungen, 9*, 1–38.

Vesk, M., Dibbayawan, T. P. and Vesk, P. A., 1996. Immunogold localization of phycoerythrin in chloroplasts of *Dinophysis acuminata* and D. *fortii* (Dinophysiales, Dinophyta). *Phycologia* 35, 234–38.

Villarino, E., Watson, J. R., Jönsson, B., Gasol, J. M., Salazar, G., Acinas, S. G., Estrada, M., Massana, R., Logares, R., Giner, C. R., Pernice, M. C., Olivar, M. P., Citores, L., Corell, J., Rodríguez-Ezpeleta, N., Acuña, J. L., Molina-Ramírez, A., González-Gordillo, J. I., Cózar, A., Martí, E., Cuesta, J. A., Agustí, S., Fraile-Nuez, E., Duarte, C. M., Irigoien, X., and Chust, G., 2018. Large-scale ocean connectivity and planktonic body size. *Nature Communications, 9*, 142.

Ware, D.M. and Thomson, R.E., 2005. Bottom-up ecosystem trophic dynamics determine fish production in the Northeast Pacific. S*cience, 308*, 1280–1284.

Watson, J.R., Hays, C.G., Raimondi, P.T., Mitarai, S., Dong, C., McWilliams, J.C., Blanchette, C.A., Caselle, J.E. and Siegel, D.A., 2011. Currents connecting communities: nearshore community similarity and ocean circulation. *Ecology*, *92*, 1193–1200.

Whittaker, R.H., 1960. Vegetation of the Siskiyou mountains, Oregon and California. *Ecological monographs, 30*, 279–338.

Zapata, M., Jeffrey, S. W., Wright, S. W., Rodriguez, F., Garrido, J. L. and Clementson, L., 2004. Photosynthetic pigments in 37 species (65 strains) of Haptophyta: implications for oceanography and chemotaxonomy. *Marine Ecology Progress Series*, 270, 83–102.

Zeidner, G., Preston, C.M., Delong, E.F., Massana, R., Post, A.F., Scanlan, D.J., Béjà, O. and Zeidner, G., 2003. Molecular diversity among marine picophytoplankton as revealed by psbA analyses. *Environmental Microbiology*, 5, 212–216.

Web sources:

URL 1: NASA PACE: pace.oceansciences.org

URL 2: NASA OCEAN COLOR: oceancolor.gsfc.nasa.gov

CURRICULUM VITAE

HRVOJE VIŠIĆ **Date of birth:** December 19th, 1993 in Šibenik, Croatia

Email: hrvoje.visic@gmail.com, hvisic@stud.biol.pmf.hr

EDUCATION

2015 – 2018 Master of Science in Environmental Sciences, Department of Biology, Faculty of Science, University of Zagreb

2012 – 2015 Bachelor of Science in Environmental Sciences, Department of Biology, Faculty of Science, University of Zagreb

Thesis: Geological evidence of previous habitability on the surface of Mars

2008 – 2012 Antun Vrančić High School, Šibenik, Croatia

2000 – 2008 Juraj Šižgorić Primary School, Šibenik, Croatia

ACHIEVEMENTS AND AWARDS

2017 Rector's award for research: Višić, H. Toxicity of contaminated sediment from the Sava River on zebrafish embryos (*Danio rerio*) -original in Croatian.

ACTIVITIES IN THE FACULTY OF SCIENCE DURING STUDY

2015 Volunteer in science–popularization event *Science Picnic*

2015 Volunteer in the scientific – educational project Papuk 2015, Biology students' association – BIUS

2015 Volunteered as a guide at the *Open days of Institute Ruđer Bošković (IRB)*, Zagreb

2014 – 2017 Volunteer in popularization event *the Night of Biology* manifestation

2013 – **2018** Student representative in the Council of the Department of Biology, Faculty of Science, University of Zagreb

2013 – **2017** Demonstrator in courses *Protists* (45h) and *Invertebrates* (165h) in Department of Biology

SCIENTIFIC ACTIVITY AND PROJECTS

2017 LoLADRIA 2017 interdisciplinary research workshop on submerged paleoenvironments. Nature park "Telašćica", Sali, Dugi otok, Croatia.

2016 Research internship - Characterisation of Poly(ADP-ribosyl)ation signalling enzymes at Sir William Dunn School of Pathology, University of Oxford, United Kingdom.

2016 Cres: Education on the developmental potentials of the Croatian islands in the organization of The Geography Students' Club Zagreb (KSG) and Association for environment protection and sustainable development RIO Zagreb.

2015 Designed and acquired financing for a student project – "Study of the endemic species of *Marifugia cavatica* and *Eunapius subterraneus* in the Tounj cave system and related ecological conditions with the aim of understanding the adaptations, threats, and education." -original in Croatian.

2014 DIG – 2nd Workshop on Dinaric Glaciation: Early/Middle Pleistocene glaciations of NE Mediterranean–filling the gaps in reconstructing its geological history and climate change. Focus on glacial-interglacial transitions (sediments and processes), Starigrad - Paklenica, Croatia.

SCIENTIFIC PUBLICATIONS AND POSTERS

Babić, S., Barišić, J., **Višić, H.**, Klobučar, R.S., Popović, N.T., Strunjak-Perović, I., Čož-Rakovac, R., Klobučar, G., 2017. Embryotoxic and genotoxic effects of sewage effluents in zebrafish embryo using multiple endpoint testing. *Water research,* 115, 9–21.

Babić S., Sauerborn Klobučar R., Barišić J., Klobučar G., Kepec S., **Višić H.**, Barišić J., Topić Popović N., Strunjak-Perović I., Čož-Rakovac R., 2015. Evaluation of toxic potential of municipal waste waters from wastewater treatment plant by zebrafish embryo toxicity test. Book of abstracts of the *12th Croatian biological congress with international participation. Sveti Martin na Muri, Croatia (poster, domestic peer-review).*

Franjević, M., Hrašovec, B., Blašković, P., **Višić, H.**, Franjević, D., 2017. Brza nova metoda genetske identifikacije štetnika u zaštiti šuma. *61. Seminar biljne zaštite*, Zagreb.

Višić H., Babić S., Barišić J., Klobučar G., 2017. Impact of wastewater effluents and contaminated sediments on zebrafish embryos using multiple endpoint testing. Book of abstracts of the *20th Symposium of Biology Students in Europe (oral presentation)*, 52–53.

CONGRESS AND SYMPOSIA LECTURES

2017 20th Symposium of Biology Students in Europe, Lund, Sweden

2015 2nd International Conference on Evolution and Behaviour ICEB, Zagreb, Croatia

2015 1st International Student Conference on Environmental Sciences '15, Zagreb, Croatia

SOCIETIES, ASSOCIATIONS AND ORGANIZATIONS

- Association for environment protection and sustainable development RIO Zagreb
- Biology student association – BIUS, Zagreb, Croatia
- Speleological club "Ozren Lukić", Zagreb, Croatia